FLOOD MODELING AND RISK MAPPING:
(CASE OF KULFO RIVER IN SOUTHERN ETHIOPIA REGION)

M.Sc. THESIS

CHALACHEW SHENKUTE

HAWASSA UNIVERSITY, HAWASSA, ETHIOPIA

JUNE, 2024

FLOOD MODELING AND RISK MAPPING:

(CASE OF KULFO RIVER IN SOUTHERN ETHIOPIA REGION)

CHALACHEW SHENKUTE MEKONNEN

A THESIS SUBMITTED TO THE

DEPARTMENT OF HYDRAULIC AND WATER RESOURCES ENGINEERING,

HAWASSA INSTITUTE OF TECHNOLOGY, SCHOOL OF

GRADUATE STUDIES

HAWASSA UNIVERSITY

HAWASSA, ETHIOPIA

IN PARTIAL FULFILLMENT OF THE

REQUIREMENTS FOR THE

DEGREE OF

MASTER OF SCIENCE IN HYDRAULIC ENGINEERING

JUNE, 2024

ADVISORS’ APPROVAL SHEET

SCHOOL OF GRADUATE STUDIES

HAWASSA UNIVERSITY ADVISORS’ APPROVAL SHEET

This is to certify that the thesis entitled “FLOOD MODELING AND RISK MAPPING: (CASE OF KULFO RIVER IN SOUTHERN ETHIOPIA REGION)” submitted in partial fulfillment of the requirements for the degree of Master’s with specialization of Hydraulic Engineering the Graduate program of the Department of HYDRAULIC AND WATER RESOURCES ENGINEERING, and has been carried by CHALACHEW SHENKUTE ID. No GPHYDRW /0005/14, under our supervision. Therefore, we recommend that the student has fulfilled the requirements and hence hereby can submit his thesis to the department.

Dr. Abebe Tadesse____

Name of Major advisor Signature Date

Mr. Sisu Biru (M.Sc.) ____

Name of Co-advisor Signature Date

EXAMINERS' APPROVAL SHEET

SCHOOL OF GRADUATE STUDIES

HAWASSA UNIVERSITY EXAMINERS' APPROVAL SHEET

We, the undersigned, members of the Board of Examiners of the final open defense by CHALACHEW SHENKUTE have read and evaluated his thesis entitled "FLOOD MODELING AND RISK MAPPING: (CASE OF KULFO RIVER IN SOUTHERN ETHIOPIA REGION)", and examined the candidate. This is, therefore, to certify that the thesis has been accepted in partial fulfillment of the requirements for the degree of Master of Science in Hydraulic Engineering.

___________________________	_________________	____________________
Name of Major advisor	Signature	Date
___________________________	_________________	____________________
Name of Internal Examiner-I	Signature	Date
___________________________	_________________	____________________
Name of Internal Examiner-II	Signature	Date
___________________________	_________________	____________________
Name of External Examiner	Signature	Date
___________________________	_________________	____________________
SGS Approval	Signature	Date

DECLARATION

I hereby declare that this M.Sc. thesis is my original work and has not been presented for a degree in any other university, and all sources of material used for this thesis have been duly acknowledged.

Chalachew Shenkute

Signature:

ACKNOWLEDGMENT

First of all, I would like to thank my almighty God for helping accomplish the study. Also I would like to express my deepest gratitude to my advisor, Abebe Tadesse (PhD),) for his kind guidance, constructive approach and encourage me throughout my research and also recognize my Co-advisor Sisu Biru (M.Sc.) for his commitment and willingness to share his knowledge and time from the beginning to till the end of the work.

I would like to acknowledge my sister & brother especially my mother Fantaye Amejo, for unlimited Encouragements & Support.

For last not least I would like to appreciate the Ministry of Water and Energy, former SNNPRS Irrigation Development Administration Agency and National Metrological Agency that provided me with the data and information needed for this work.

Finally, I like to thank all my friends, who helped me in one way or another, in carrying out my research through remarkable encouragement, advice and material support.

Table of Contents

LIST OF TABLES

LIST OF FIGURES

LIST OF ABBREVIATIONS

CN	Curve Number
DEM	Digital Elevation Model
ESRI	Environmental System Research Centre
EM-DAT	Emergency Events Database
GIS	Geographic Information System
Geo-HMS	Geospatial Hydrological Modeling System
GPS	Global Positioning System
HEC-HMS	Hydraulic Engineering Centre –Hydrological Modeling System
HEC-RAS	Hydraulic Engineering Centre –River Analysis System
HSG	Hydraulic Soil Group
ISDAA	Irrigation Development Administration Agency
ITCZ	Inter Tropical Convergence Zone
LULC	Land use land cover
MASL	Mean above sea level
MOWE	Ministry of Water & Energy
NMSA	National Metrological Services Agencies
SDCSE	South Design Construction & Supervision Enterprise
SNNPRS	South Nation Nationalities People Regional State
TIN	Triangulation Irregular Network
USACE	United States Army Corps of Engineers

ABSTRACT

Floods pose significant threats globally, causing immense damage to lives, societies, and economies. This study aimed to assess flood hazards, evaluate vulnerabilities, and determine flood risk along the Kulifo River floodplain. To achieve the objectives of a study, advanced hydrological and hydraulic modeling techniques were analyzed, using data from various sources, including rainfall from the National Meteorological Agency, stream flow data from the Ministry of Water Resources, and land use/land cover data from USGS. The HEC-HMS model accurately calibrated and validated using observed stream flow data, the result of model calibration gives Nash Sutcliffe efficiency (NSE) of 0.81, Percent Bias (PBIAS) of 1.77, coefficient of determination (R^2) of 0.77, and Relative Mean Square Error (RMSE) of 4.28. During the validation period, the model gives (R^2) of 0.79, NSE of 0.78, PBIAS of 1.09, and RMSE of 2.13. After model calibration and validation, flood hydrographs for different return periods were generated. These hydrographs served as inputs for the HEC-RAS hydraulic model, integrated with GIS software to map flood inundation areas. The resulting flood inundation maps revealed extensive flood-prone areas along the Kulifo River, with maximum flood depths of 15.2 meters and maximum velocities of 6.9 m/s during a 100-year flood event. Flood hazard maps classified areas into different hazard categories from low to extreme hazard, and 59% of inundated area falling under extreme, very high, and high hazard levels, 41% of inundated area falling under medium, and low hazard levels. Vulnerability analysis considered indicators such as flood depth, velocity, duration, slope, land use, and population density, highlighting 25% of the flooded area as very high and high vulnerability, 20% of the flooded area as moderate vulnerability and 55% of the flooded area as low and very low vulnerability. Combining flood hazard and vulnerability information, a comprehensive flood risk map was developed, identifying 32% of the flooded area as very high and high risk, 15% of the flooded area as moderate risk and 55% of the flooded area as low and very low risk. These high-risk zones were concentrated in the Limat area of Arba Minch city, emphasizing the need for mitigation measures and emergency response plans. The flood risk map provided valuable insights for decision-making processes, guiding the implementation of structural and non-structural measures, floodplain zoning, and population relocation. This study's findings contribute to effective flood management, land-use planning, and disaster risk reduction strategies along the Kulifo River.

Keywords: Flood hazard, Flood Vulnerability, Flood risk, Kulifo River, HEC-HMS, HEC-RAS

1. INTRODUCTION

1.1 Background

Flood is one of the leading natural hazards worldwide both in terms of the frequency of occurrence and the resulting damages to human lives, the environment, and economic assets (Jonkman 2005; Doocy et al. 2013).

Topographically, Ethiopia is both a highland/mountainous and lowland country. It is composed of nine major river basins, the drainage system of which originate from the centrally situate highlands and make their way down to the peripheral or outlying lowlands. Especially during the rainy season, the major perennial rivers as well as their numerous tributaries forming the country's drainage systems carry their peak discharges.

Ethiopia is one of the natural hazard-prone (drought, flood, etc.) countries in Sub Saharan Africa. The impact of drought and flood combined with poverty and high population growth let several peoples become sufferers of various disasters. It is indicated by the significantly increased number of people and areas affected; several deaths; and infrastructure and property loss. The manifestation of climate change in the form of unpredictable rainfall, frequent and severe floods; and droughts have serious consequences on the livelihood, the security of smallholder farming communities, and making them more vulnerable in countries like Ethiopia. Many countries are frightened by the quite extraordinary and unusual magnitude of flooding. The problems are more
acute in the river basin as well as urban areas (Niguse and Adhanom, 2019).

The occurrence of flood depends on meteorology, topography, land use, soil type, and antecedent moisture conditions (Funk 2006; Youssef et al. 2016; Agbola et al. 2012). The multi-dimensional causes of flood made it less predictable and aggravated its impacts worldwide. In the coming decades, the effect of climate change and urbanization is expected to exacerbate flood induced risks.

Flooding affected millions of people in the first six months of the year, with significant humanitarian and economic consequence across the world. There were nearly 100 major flood events recorded across all populated continents in the first six months of the 2023. The floods that had the largest Socio-economic impacts are highlighted. Many of which were the result of heavy rainfall over whelming rivers and urban drainage systems,

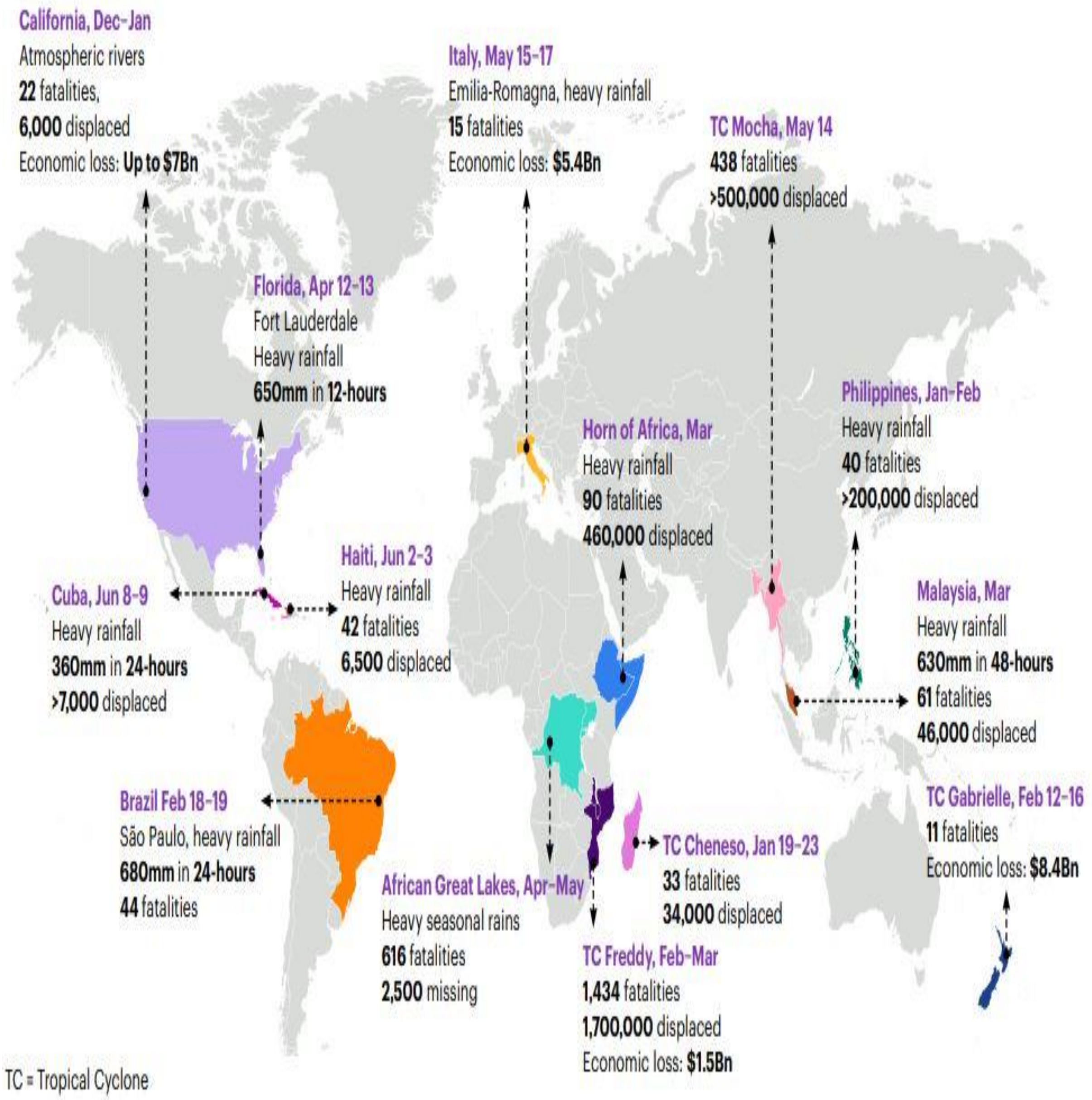

Figure 1. Global flood events with the largest Socio-Economic Impact that Occurred between January and June 2023. Source:-WTW Research Network Newsletter 2024

1.2 Statement of the Problem

Kulfo River is one of the rivers which cause flooding at irrigation user's community farm land, Arba-minch Agricultural research Centers, Crocodile Ranching Camp, Irrigation Schemes, Homes & Airport field. The river builds up from continuous rainfall on the catchments and local rainfall on the flood plain to result in flooding problems. The Kulfo River Catchment has been subjected to repetitive flooding during its history. Most of the severe floods occurred during with its peak in May and October, which brought large volume of runoff to the relatively large Catchment of Kulfo River. Part of Kulfo community farm land is affected by flood that drained from the Kulfo River catchment.

Floods at different time have destroyed crops in the field of Kulfo River irrigation user's community. Flooding is the major problem in the downstream reach of the catchment. Severe flooding occurred on the year 2013, 2016, 2017 and 2021 are among the most events. During June 2016, July 2017 and Oct 2021 floods, it has been associated to the series of floods that hit Kulfo River irrigation user's community farm land. The irrigation user's community lost their irrigable land about more than 100 ha of their farm land and extreme flooding affected Arba-Minch Agricultural research Centers, Crocodile Ranching, Irrigation Schemes, Homes & in some part of Airport field.

Therefore, this necessitates the development of hydraulic modeling and flood mapping of the study area in order to take mitigation measures to avoid the risk. Thus, the specific problem for this thesis paper is the problem of flooding on part of Kulfo River irrigation user's community farm land from the Kulfo River due to over toping of the river banks. Hence the hydraulic modeling needs to be performed to a sufficient degree of accuracy so as to identify flood inundation vulnerability for the Kulfo River irrigation user's community farm land.

1.3 Objective of the Study

1.3.1 General Objective

The general objective of the study is flood modeling and developing risk map of Kulfo River watershed Rift Valley Lakes Basin, Ethiopia.

1.3.2 Specific Objective

The specific objectives were:

- To estimate the flood Inundation area of Kulfo watershed,
- To determine flood Hazard,
- To prepare flood vulnerability map of Kulfo river basin,
- To develop flood risk map of the study.

1.4 Research Questions

- What is the estimated inundation flood areas?
- Which part of the area more Hazards?

- ❖ Which parts of Kulfo area more vulnerable related to other?
- ❖ Which parts of Kulfo areas suffer from more flood risk?

1.5 **Significance of the study**

Kulfo catchment farm land has been used for modern and traditional irrigation agricultural purposes for years. But due to the improper land use of Kulfo catchment and its steepness unexpected flood occurs. In the latest years, there is a big trend for agriculture purpose in the farm land as well as on watershed areas. The idea of this study is to identify flood risk on the Kulfo River and define the possible flood water level by applying latest hydrologic (HEC-HMS) and hydraulic modeling tools (HEC-RAS) and GIS software. So, the study may create public awareness about the causes and consequences of flood risk on flood affecting areas. Moreover, it will give some relevant information for further improvement and investment approaches for various implementing agents.

1.6 **Scope of the Study**

This study was carried out flood risk mapping in order to evaluate and identify flooded areas and the intervention plans. The hydrologic analysis will be generated by modifying watershed characteristics and geometry using HEC-HMS model. The output from HEC-HMS was then used to run the HEC-RAS mode land generates water surface flooding.

It is not possible to cover the whole aspect of the study area due to time and resource limitation. Hence, this study will not include the ground water assessment of Kulfo catchment, the impact of land use or land cover change and sedimentation of Kulfo River.

2. LITERATURE REVIEW

2.1 Over view of Flood Mapping

Flood is a temporary condition of partial or complete inundation of normally dry areas from overflow of inland or tidal waters or from unusual and rapid accumulation or runoff. Flood phenomenon is considered as one of the worst hazards in terms of magnitude, occurrence, geographical spread, loss of life and property, displacement of people and socio-economic activities (Myers and White, 1993).

Flood can be defined as any relatively high-water flow that overtops the natural or artificial banks in any portion of a river or stream. People may be washed away in a short span of time, and properties may be heavily damaged by flood. When a bank is overtopped, water spreads over the flood plains and generally becomes a hazard. Flooding is the most common environmental hazard due to the widespread geographical distribution of river valleys and coastal areas. By attraction of human beings to such areas for settlements and farming make it as a fatal obstacle to social progress both in developing and developed countries (Jayseleen, 2003).

A flood is a relatively high stage of river which is usually accompanied by overtopping of the natural banks of the river in a particular reach. The flood occurs because of heavy rains or the discharge in the river is so high that its natural cross-section is unable to contain flow consequently and over siltation or sediment deposition at channel which is to reduce the carrying capacity of river. The river banks are overtopped, and the flood water spreads over the flood plains (ARORA, 2009).

A flood may defined as an overflow coming from some river or from some other body of water. A river may get flooded due to excessive rainfall or excessive melting of snow or some other form of ice obstruction in the form of jams. Whenever the water over flows the banks of the river, the river is said to be flooded. In fact, the banks of the stream may vary in height through its course, and hence there is no definite stage at which the whole river is about to overflow. However, on important river arbitrary representative warning and danger level are generally assigned at important location (Garg, 2006).

2.2 Over View of flood Inundation Map

The most prevalent indicator for the intensity of a flood is the inundation depth (Mertzetal. et.al, 2007); the water depth identified by different studies (Penning-Row selletal., 1994) as the flood characteristics, which has the biggest influence on flood damage. Building stability against flotation and foundation failures, flood proofing, and crop survival have different degrees of tolerance to inundation. In each case, these identified and the depth established

2.3 Over View of flood Hazard Map

This map shows the extent of inundation as determined from a thorough technical study of flooding at a given location. Flood hazard maps are commonly used in floodplain information reports and require updating when changes have occurred in the channels, on the floodplains, and in upstream areas. These changes include structural modifications and channel or floodplain modifications in upstream areas. Development of new buildings on the floodplain, obstructions, or other land-use changes can affect the stream discharges, water surface elevation, and flow velocities, thereby changing the elevation profile defining the floodplain (Aliy, 2018).

2.4 Over View of flood vulnerability Map

To determine vulnerability, information on functional land use was used. It was obtained from the cadastral maps, orthophotos from the year 2011, and field research. Each area was assigned an attribute about how it is currently used. The functional areas were then categorized into the classes of functional areas according to the methodology of spatial planning and local development plan of municipality (URBION 2012).

2.5 Over View of flood Risk map

The area of inundation, in combination with land use data, reveals that elements at risk affected in case of a certain flood event Flood risk mapping model is one of the means to understand the behavior of flood in a particular area. Development of flood model comes with the development of efficient computational tools

Flood risk maps can be prepared at a high resolution with better accuracy for preparedness planning Flood risk as the probability of potentially damaging flood situations in a given area and within a specified period of time (Mertzet al., 2007). Going beyond the information on flood frequency curves, flood risk statements need to quantify the intensity of the process. There are number of indicators that represent the intensity of flood.

Flood risk management in a narrow sense is the process of managing an existing flood risk situation. In a wider sense, it includes the planning of a system, which will reduce the flood risk. The purpose of these two aspects of flood risk management is to control the flood disasters in the sense of being prepared for a flood and to minimize its impact (Erich, 2002). These include the process of risk analysis, which provides the basis for long term management decisions for the existing flood protection system. Risk analysis can be defined as “a systematic use of available information to determine how often specified events may occur and the magnitude of their likely consequences (Granger, 2002).

A good risk analysis process yields hazard or risk maps, which are drawn by means of Geographical Information Systems (GIS) based on extensive surveys of vulnerability combined with topographic maps. In order to do this, the hazards are to be combined with the vulnerability into the risk. The vulnerability of the persons or objects (the ‘elements at risk’) in an area, which is inundated if a flood of a certain magnitude occurs, is weighted with the frequency of occurrence of that flood (Kowalczak, 1999).

For this study, flood hazard and flood vulnerability will be developed, flood risk then developed by overlaying flood hazard map and food vulnerability map. According to Zimmermann, 2005) the conventional expression of risk is,

Risk=Hazard * Vulnerability

2.6 Previous Studies in the National Level

Many researches been carried out to address the impacts of flood risk on Flood risk modeling and flood mapping. The Fogera Flood plain area characterized as high flooding prone area, there are still few studies applied. The current flood problem and lack of studies in the areas show the importance of the in-depth study. Some of the studies tried to describe shortly as follows.

Belay Z. (2008) focuses on his study GIS based hydrological modeling for Woldiya watershed and hydraulic modeling of upper reach. A digital elevation model of 90 meter was used for the delineation of the basin, which has very low resolution. So, DEM which has high resolution should be used in order to improve the result. Verification and validation of model results in both cases was not done because of absence of recorded flow data. So, these two things should be done in order to reach to conclusion that whether the model is appropriate or not for the study area.

Abera Z. (2011) his study focuses on Fogera flood plain using 1D hydraulic modeling (HEC-RAS). He tries to relate flood frequency analysis results with the flow generated for different return periods using HEC-HMS. The researcher has used cross-section of the river and the flood plain extending to 4 Km from each river bank. However, he has used a DEM resolution of 30*30, which is difficult to represent the flood plain as compared to the latest DEM sizes currently used.

Gashaw & Legesse (2008) focuses on flood risk and risk assessment in Fogera woreda using GIS and remote sensing. The study results flood risk and risk maps. Although the study has produced use full input for developing strategies for decision makers, not based on the actual cause and effect relationship.

Berhane H. (2011) studied on hydraulic modeling and flood mapping of Fogera flood Plain. But he did not include, risk analysis of the flooding in the flood plain. Thus, to select the type of mitigation measure it is required to undertake further flood risk analysis study instead of the traditional way of design to protect the area from flood.

2.7 Previous Research in the Study Area

Many researches and organizations been carried out to address the impacts of Kulfo Flood risk modeling and flood mapping at various time but the problem is still affecting the river peripheries areas of farm lands & Institutions. The Kulfo river flood affected area characterized as high flooding prone area some of the studies tried to describe shortly as follows.

South Design Construction Supervision Enterprise (SDCSE-2021) unpublished document, the study focuses on to investigate the effect of flood prone and to provide medium flood mitigation measure for Kulfo watershed areas. Kulfo flood plain using 1D hydraulic modeling (HEC- RAS) document tries to relate the peak flood determined for T years return period the 100-year life time is 127.86 m^3/s. Further calculation is must be done.

3. MATERIALS AND METHODS

3.1 Description of the Study Area

3.1.1 Location

Kulfo River watershed is located near Arba Minch town which is located 524 km away from Addis Ababa, capital city of Ethiopia via Hawassa Shashemen road and 434 km Via Alaba Butajira Road. The catchment area of Kulfo watershed is about 376.4 km^2 outlet at Lake near Limat Village Bridge, and located between 6654487.18 m N and 692547.17 m N latitude and 313259.69 m E and 339159.68 m E longitude (Figure 3.1). Nearly 62.25% of land use of the catchment is covered with Built area and Grassland.

The Kulfo River begins from the junction of Titika and Gulando River at 6º 07’N latitude and 37º27’E longitude that joins the outflow to Abaya and the inflow to Lake Chamo at the 5º 55’N latitude and 37º 33’ E longitudes. The principal tributaries are Baba, Gulando and Yeremo draining to the upper part of Kulfo watershed whereas the tributaries such as Wobale and Mojale drain to the middle part of the watershed and Korzha, Ambule and Titika to the lower part of the catchment area. (South Design and Construction Supervision Enterprise, 2021)

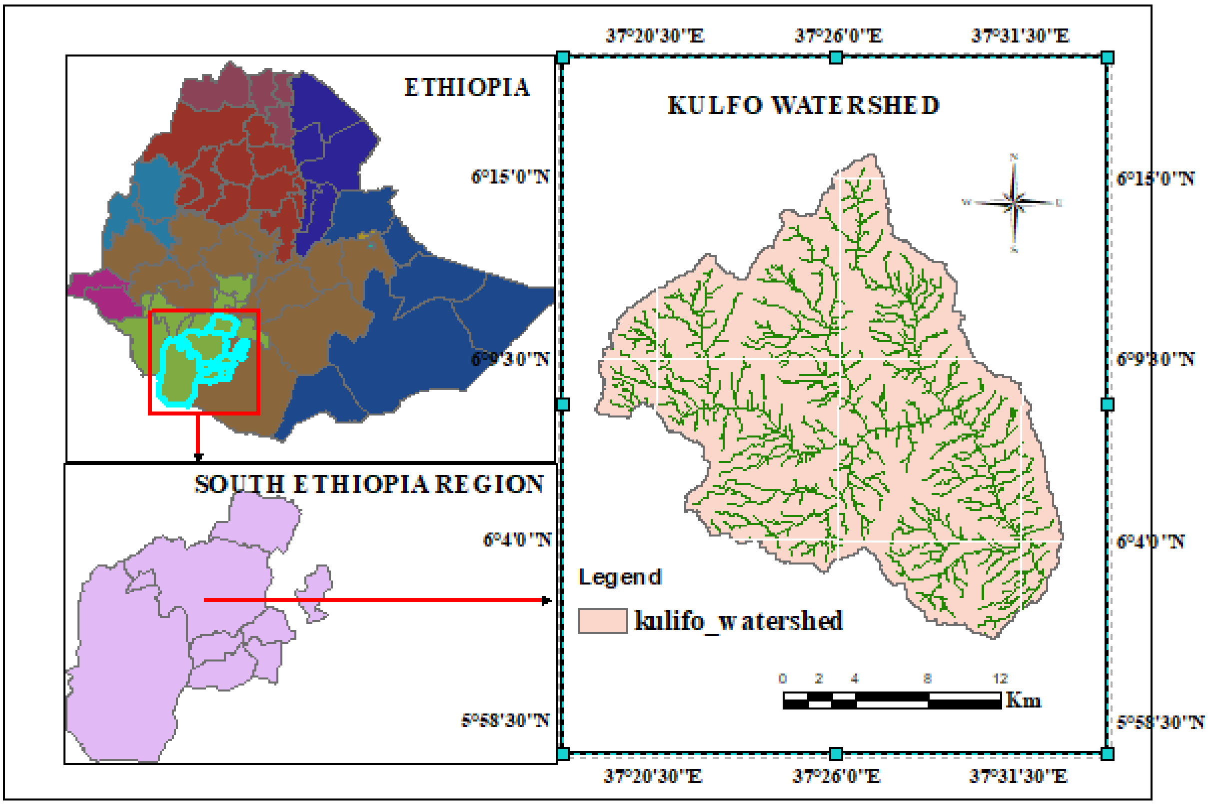

Figure 3.1: Map of Kulfo Watershed.

3.1.2 Climate

Climate of Ethiopia is characterized by tropical climate moderated by altitude with a marked wet season. The eastern lowlands (elevation less than ~ 900 m.a.s.l) are much drier with a hot semi-arid to a desert climate. In contrast the south-western Ethiopia is characterized by humid tropical climate with rainfall higher than 1,000 mm. Traditional classifications based on altitude and temperature show presence of five zones (D. Gemechu, 1977).

The hot, arid zone covers the desert lowlands below 500 m, where average annual rainfall is less than 400 mm and average annual temperatures range between 28°C and 34°C or higher, the warm to hot, semi-arid zone includes those areas with an altitude of 500 m–1,500 m, average annual rainfall generally of around 600 mm (but as high as 1,600 mm in the western lowlands of Gambella), and an average annual temperature range of 20 °C –28 °C, the warm to cool, semi-humid zone covers the temperate highlands between 1,500 m and 2,500 m. Average annual temperatures vary between 16°C and 20°C, and annual rainfall is generally around 1,200 mm, reaching 2,400 mm in the south-west, and the cool to cold humid zone includes the temperate highlands between 2,500 and 3,200 m, where average temperatures range between 10°C and 16°C, with an annual rainfall of 1,000 mm and up to 2,000 mm in higher areas, the cold, moist temperate zone covers the Afro-alpine areas on the highest plateaus between 3,200 and 3,500 m; average temperatures are below 10°C and annual rainfall averages less than 800 mm.

According to the above classification, Kulfo watershed area is situated in the range of warm to hot arid zone to cold moist temperate zone. Specific to the study area climate falls in the warm to hot arid zone.

The spatial and temporal variation of rainfall in Ethiopia is strongly controlled by inter annual movement of the position of the Inter Tropical Convergent Zone (ITCZ). During its movement to the north and south of equator, the ITCZ passes over Ethiopia twice a year and this migration causes the onset and withdrawal of winds from north and south. The ITCZ represented a low-pressure area of convergence between Tropical easterlies and Equatorial westerlies along which wave distributions take place. Based on the moisture distribution patterns, in the country three rainfall (moisture) regimes can be identified.

- The south-western and western areas of the country which are characterized by mono-modal rainfall pattern,
- The central, eastern and northeastern areas of the country experience a nearly bimodal rainfall distribution. These are the Belg rains (February to May) and Kiremit rains (June to September).
- The southern and southeastern areas of the country are dominated by a distinctly bimodal rainfall pattern.

3.1.3 Topography

The highest point in the Basin has an elevation of 3565 Meters above sea level (m.a.s.l.) and lowest point has an elevation of 1241 m.a.s.l. In general, the elevation in the basin decreases from West to East and from North to South. The basin can generally be divided into highlands, midlands and lowlands.

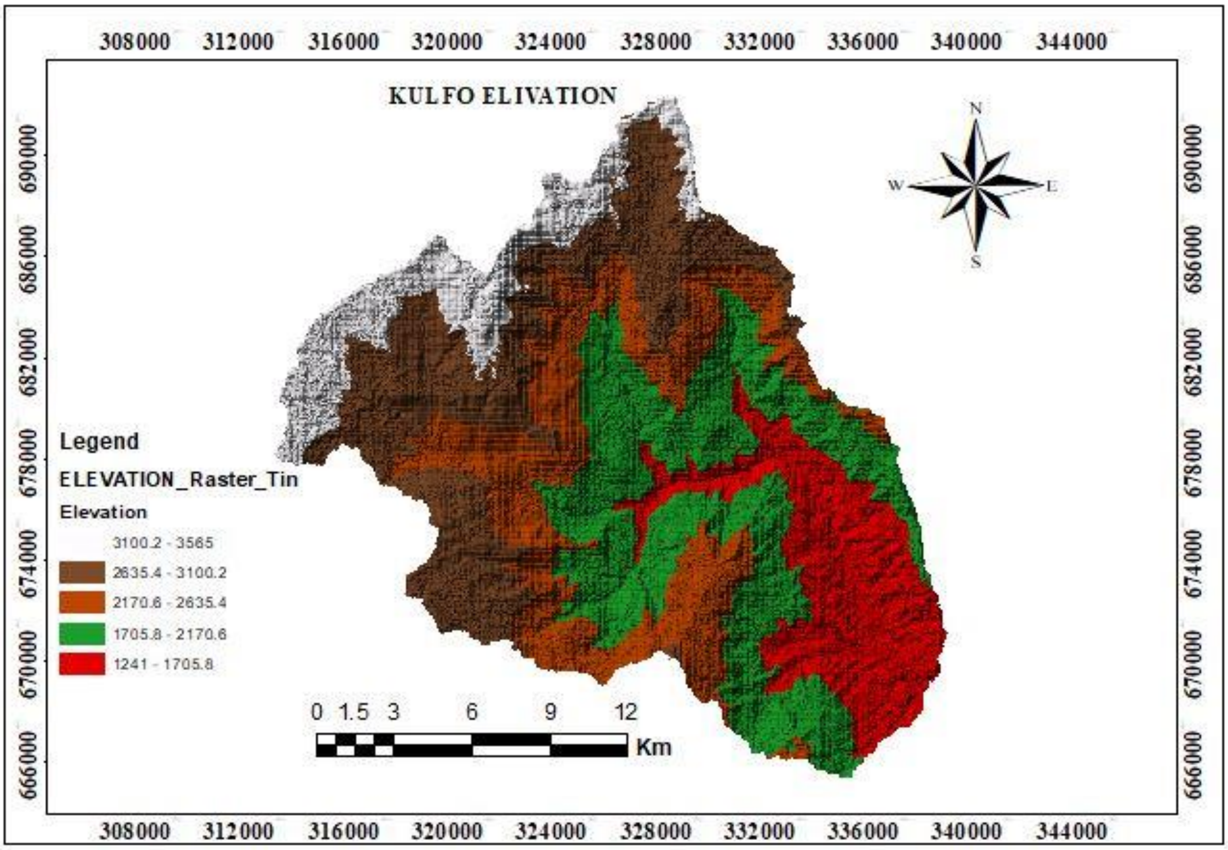

Figure 3.2: Map of Topography of Kulfo

3.1.4 Land use Land Cover

The Abaya Chamo drainage basin as a sub basin of the rift valley Lakes system has been an area of rapid population growth and settlement due partly to its water resource potential. Concomitant to this is the increasing land use and degradation of the natural ecosystem because of deforestation caused by increasing fire wood demand and clearing of lands for agriculture and burning of forests and bushes for livestock and grazing purposes. Because of the sustained dry period and lack of soil moisture, land irrigation with river waters is under a steadily increasing practice in the area. The Kulfo River is being used for irrigation and for domestic consumption by scattered settlement of the rural & urban population who also grow Banana plantation and use the Kulfo River to irrigate the plants. The flow diverted by this scheme is so high that during the dry season the river is completely diverted towards the farm leaving the downstream without any water. The downstream section is a wetland area whose ecosystem has been reportedly affected by the dry up.

Land usage and land cover significantly affect the watershed's ability to generate runoff. Therefore, it is essential to classify the land use and land cover in order to determine how changing land use and land cover may affect stream flow. Therefore, distinct LU/LC in the Kulfo catchment will be identified and defined as follows based on prior studies in the catchment (Halcrow, 2008; Damtew Fufa, 2015).

Land is defined as a delineable area of the earth's terrestrial surface, encompassing all attributes of the biosphere immediately above or below this surface including those of the near-surface climate, the soil and terrain forms, the surface hydrology (including shallow lakes, rivers, marshes, and swamps), the near-surface sedimentary layers and associated groundwater reserve, the plant and animal populations, the human settlement pattern and physical results of past and present human activity, such as terracing, water storage or drainage structures, infrastructure, buildings (UN, 1995).

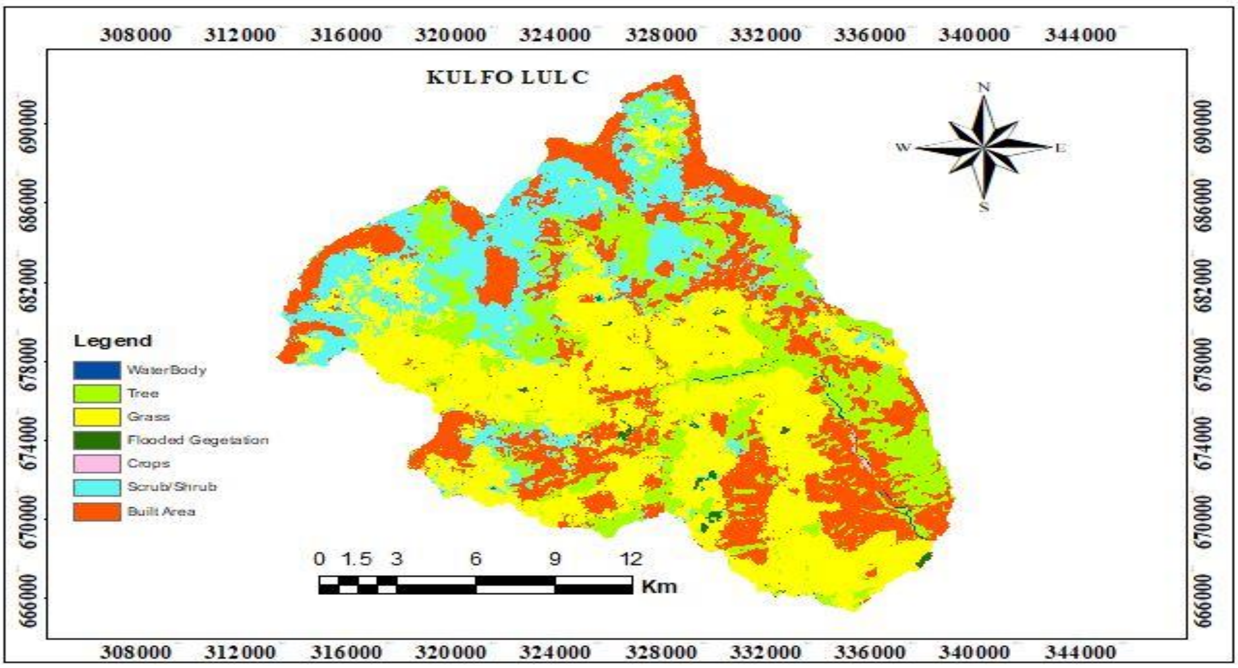

Figure 3.3: Map of Kulfo Land Use Land Cover

Land use applies to the current use of the land, whether agricultural or non-agricultural, in which the soil or command area is located (FAO, 2006). Land use has a major influence on the direction and rate of soil formation.

Table 3.1: Kulfo Land Use Land Cover

Name	Area (SQKM)	Weightage (%)
Cropland	0.62	0.08
Grassland	75.94	20.18
Shrub land	137.19	36.45
Flooded Vegetation	1.82	0.48
Tree	0.3	0.08
Water Body	63.4	16.85
Built Area	97.09	25.8

3.1.5 Soil Type

Soil types in the rift valley are closely related to soil parent materials: Basalt ignimbrite, lava, gneiss, volcanic ash and pumice, riverine, and lacustrine alluvium. Cracking clays occur locally at lower elevations on colluvial fans-characteristic feature of Abaya and Chamo basin. The fans, deltas and flood plains around Abaya and Chamo Lakes are built up from materials recently deposited by rivers and Lakes. Soil fertility, structure and drainage are generally favorable for agriculture provided that there is enough moisture (EPA, 2006).

A Soil survey as defined by Rossiter (2000) is the process of determining the pattern of the soil cover, characterizing it, and presenting it in understandable and interpretable form to various consumers.

The basic soil groups identified in the area according to FAO/UNDP classification are Vertisols, Nitosols (Alfisols), Lithosols, Andosols, Cambisols and Fluvisols. The soils around Lake Chamo are chromic vertisols and eutric nitosol with textural classification ranging between clay to clay-loam. The soil types along the eastern shore of Lakes Abaya and Chamo are vertisols, luvisols and nitosols with textural classification of clay to clay. Soil type B

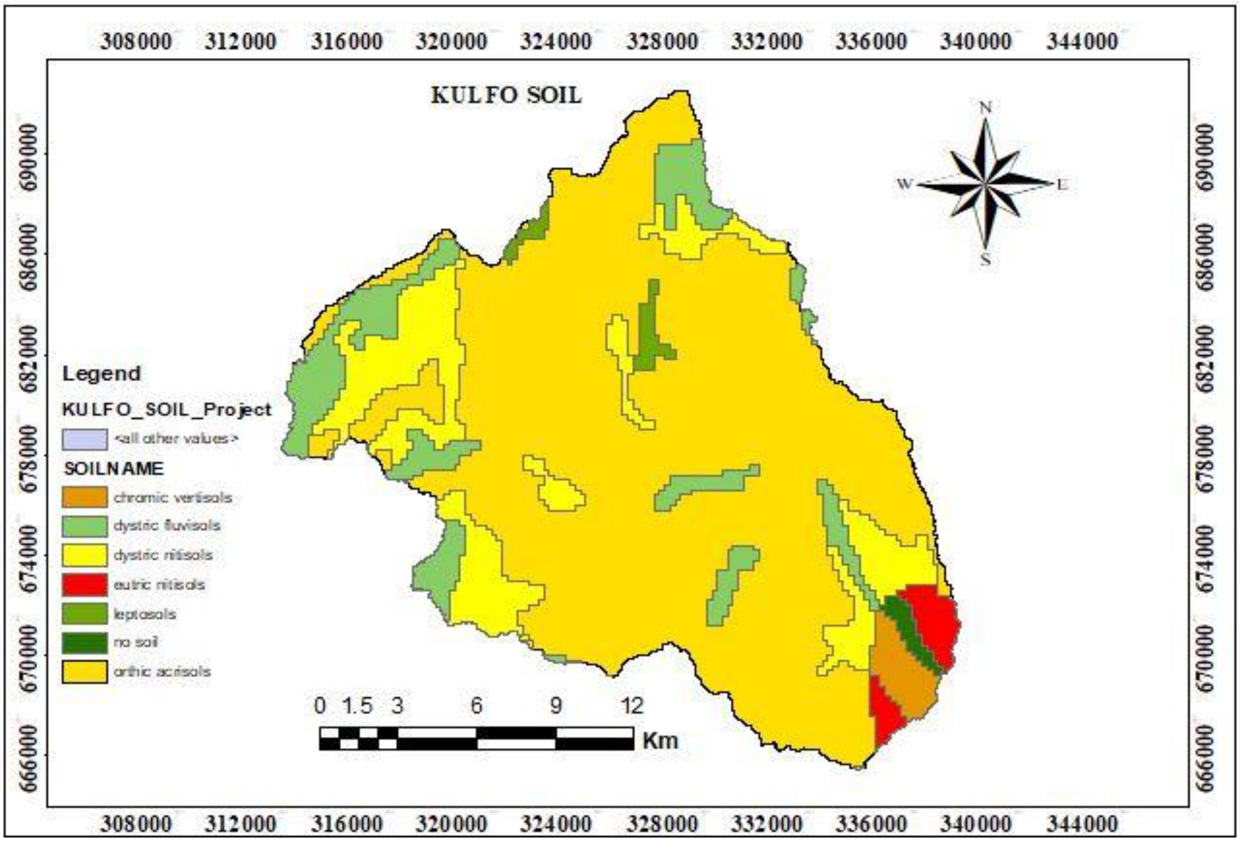

Figure 3.4: Map of Kulfo Soil Type

Table 3.2: Kulfo Soil Type

Name	HYSG	Area (SQKM)	Weightage (%)
Chromic vertisols	D	6.25	1.66
Dystric-fiuvisols	B	36.19	9.62
Eutric-nitisols	B	6.7	1.78
Leptosols	D	3.79	1.01
Dystric-nitisols	B	53.89	14.32
Orthic acrisols	B	267.18	70.99

3.1.6 Slope

The topographic component of RUSLE model was computed and suggested by Moor and Bruch (1985); Mitasova and Matias (1999); and Simms et al. (2003). As shown in the figure 3.5 below in the lower part of the watershed the slope length is high due to high flow accumulation. On the other hand, slope inclination is high in the middle parts of the watershed. Slope has major implications for land use. The speed and extent of runoff depend on slope of the land. The greater the slope, the greater the velocity of flow of the runoff water occur. The erosive capacity of runoff varies in direct proportion with the slope of a land on which the runoff occurs. According to the (FAO, 2006) slope class of the study area is categorized, described and presented below.

Table 3.3: Slope class of the watershed

No.	**Slope class**	**Area(km2)**	**Area (%)**	**Description**
1	<3.5	3.98	1.06	Plain
2	3.5-10	32.03	8.51	Gently sloping
3	10-25	118.15	31.39	Sloping
4	25-45	109.79	29.17	Moderately steep
5	>45	112.40	29.87	Very step

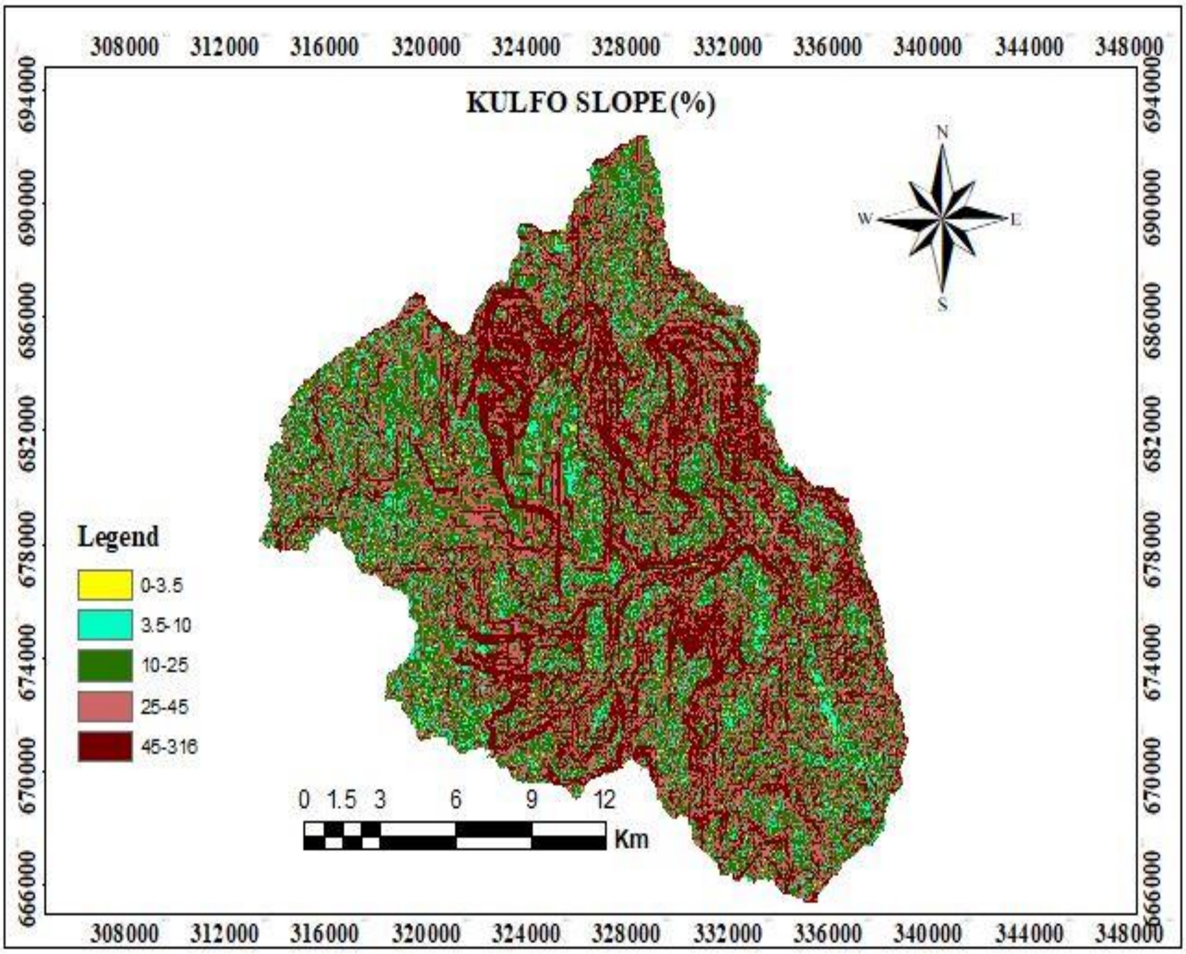

Figure 3.5: Map of Kulfo Slope

3.1.7 Topographic Data

The Digital Elevation Model (DEM), from Ethiopian mapping agency.

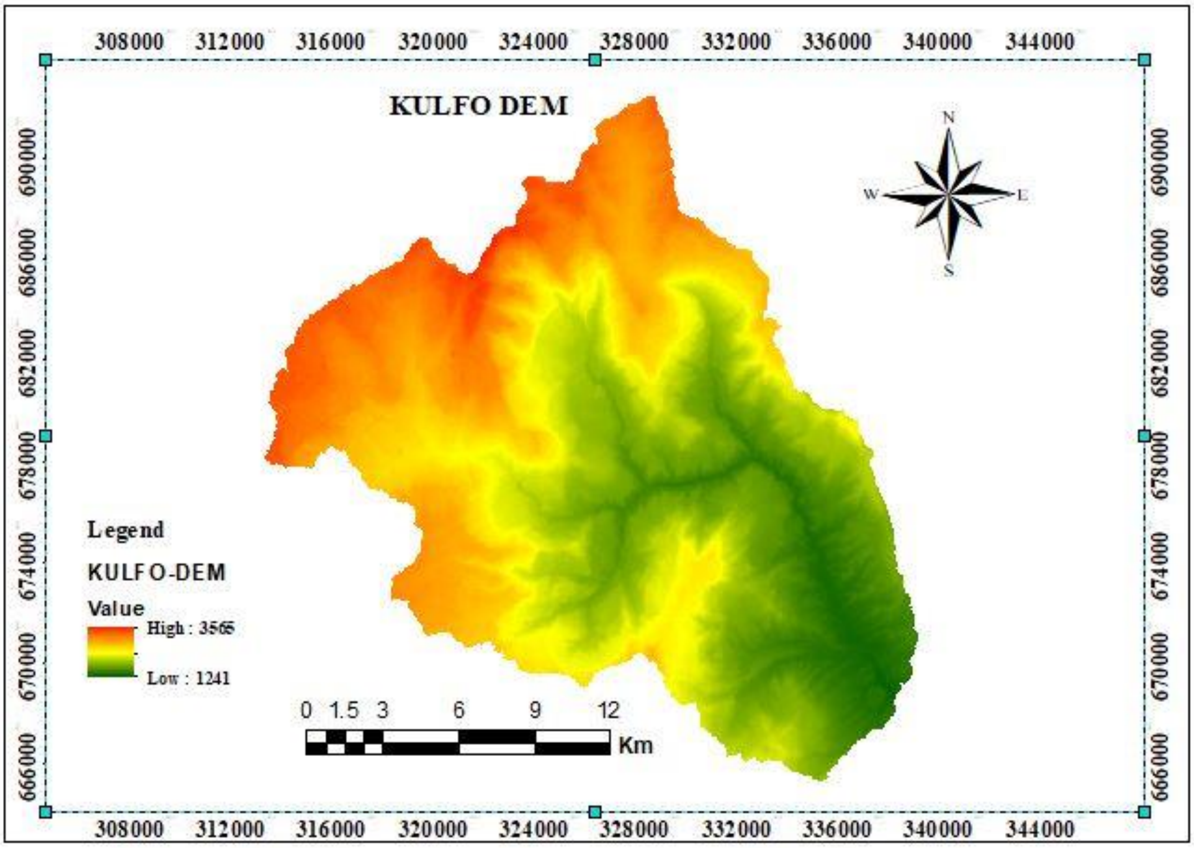

Figure 3.6: Map of Kulfo DEM

3.2. Methods

3.2.1. Conceptual research frame work

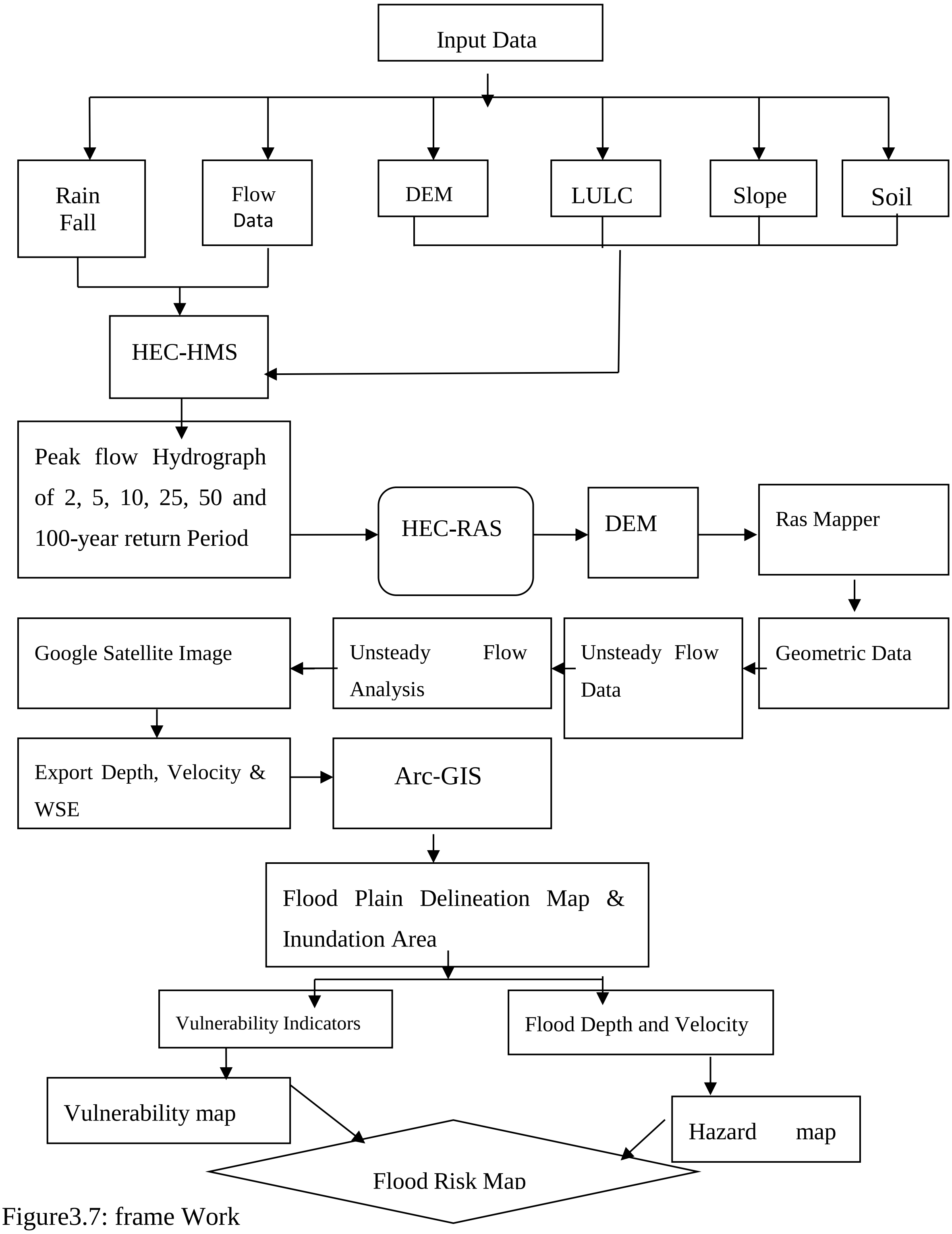

Figure3.7: frame Work

3.2.2. Materials Used

For the progress of Kulfo River, the data is collected form field, respected office, Metrological stations and executed projects near to the project. The data collected is refined before analysis. Here are the main data sources for the development of the thesis. The materials used for this thesis work include the following, but not limited to:

Collect relevant Primary and secondary data from all sources; local farmer's interview, Zonal and Town office discussion, assess previous studies conducted on the area and from the recommended source of hydrological and meteorological data

(i.e. Daily Rainfall, Temperature, Land use/cover, & Stream flow etc.…)

Data organizing, pre-processing, analysis, producing relevant maps

(i.e. DEM resolution, drainage system and sub-catchments area delineation from DEM data using Global Mapper 18, Google Earth, Arc GIS 10.8, Hydrognomon 4.1.0-, HEC-HMS 4.11 and HEC-RAS 6.1, Software's & Tools)

Spatial data:

(i.e. DEM, LULC, CN, Soil, Slope)

3.3 Data Collection and Analysis

3.3.1. Hydro-Meteorological Data Collection

3.3.1.1. Meteorological Data Collection

This includes data such as Daily Rainfall, monthly min, max and average temperatures, monthly average rainfall intensity, its distribution, and other important climatic features of the study area has been collected from National Meteorological agency (NMA)

In this regard, the study has been investigating the most representative meteorological station for the study area in order to use the representative meteorological data for the study objectives. Accordingly, the study checked the rainfall data from Arba-Minch, Mirab-Abaya, Gato, Gidole and Geresse Meteorological station which is found at near distance of the study area and temperature, humidity, sunshine hours, and other elements solely from this station.

The meteorological data was collected from five stations located in the vicinity of the study area as given on Table 3.4 below. Among the listed below stations except Arba Minch station the rest are located outside of the project area. The rainfall record length ranges from 1988 to 2020 years as depicted on Table 3.4. Out of the five stations, two of them was used for this study.

Table 3.4: Meteorological Stations

NO.	Name	Lat	Log	Elev (m)	Class	RF	Temp	Wind Speed	RH	Sunshine
1	Arba Minch	6.05	37.38	1290	II	√	√	√	√	√
2	Geresse	5.55	37.19	2300	III	√				
3	Gato	5.28	37.27	1300	III	√				
4	Gidole	5.39	37.21	2550	I	√				
5	Mirab Abaya	6.30	37.78	1240	I	√	√	√	√	√

3.3.1.2 Hydrological Data Collection

The goal of the hydrological data is the estimation of water availability and its reliability. Thirty-three years of daily flow data for the stations i.e., Kulfo, near Arba Minch was obtained from MOWRE. The name and location of hydrological stations are Kulfo at Sikela near Arba Minch, Kulfo at Abaya Flow data in the Kulfo River is measured at Sikela near Arba Minch (37^o 33’ E and 6^o 02’ N) and Kulfo at Abaya outlet (37^o 33’ E and 6^o 04’ N) are available from January 1987 to December 2015.

The monthly available river flow data was obtained from the Hydrology and water quality directorate of the MOWE for the stations in proximity to the project area.

Table 3.5: Kulfo river stream flow gage location

Gauging Station	Lat	Log	Area ($km^{2)}$	Start Date
NR. Arba-Minch	6.05	37.38	376.4	1987-2015

There was one flow gauging station within the study reach, just under the foot bridge. Currently both the gauging station and the foot bridge were removed. The gauging station had long records of daily stream flow data (1984-2015).

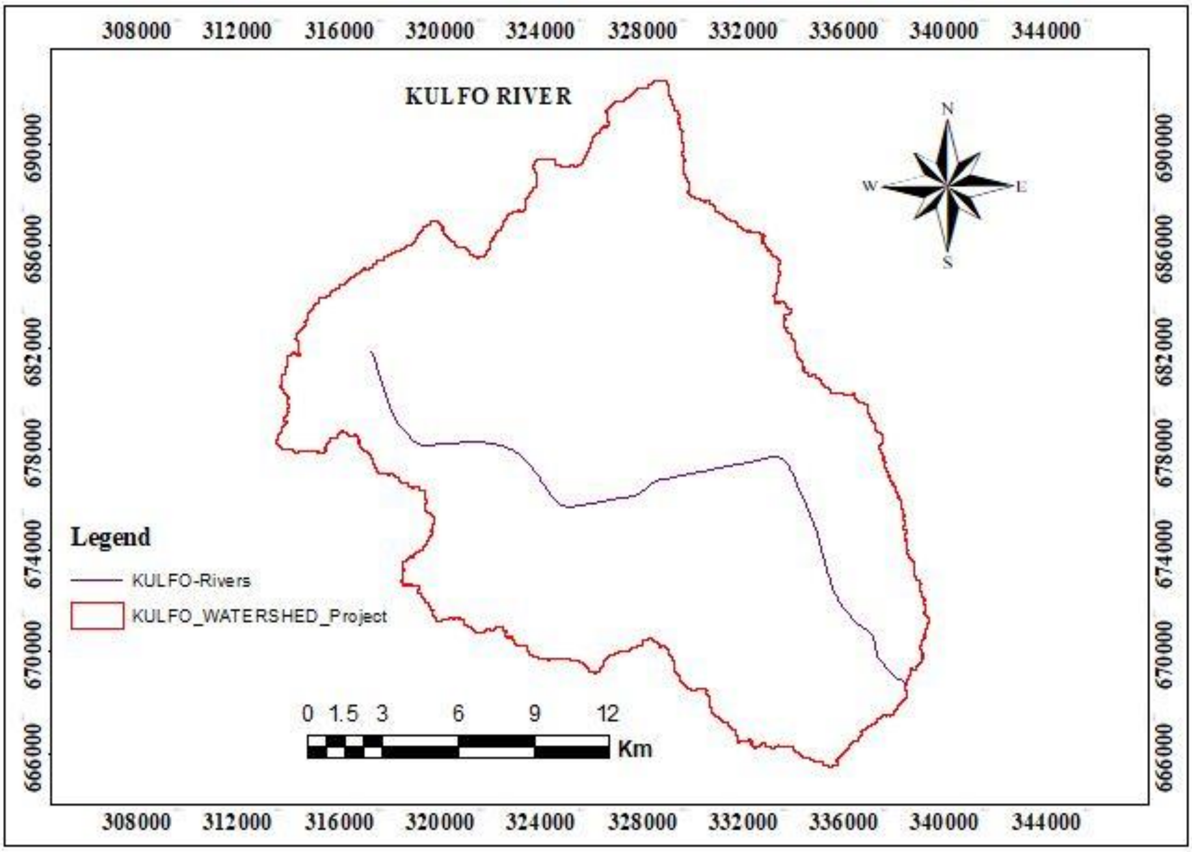

Figure3.8: Map of Kulfo River

3.3.2 Hydro-meteorological data processing

3.3.2.1 Meteorological data processing

a) Precipitation Gage weight

Estimation of Areal Rainfall There are many methods are available for computation of average precipitation over the basin. However, depending on the accuracy and objective of the analysis the followings methods are commonly used: Arithmetic average, Thiessen polygon, Isohyetal, Grid point, Orographic or isopercental method. Among those methods, Theissen polygon method is used for this study even though the method depends on a good network of the representative rain gauge. Thiessen polygon and representative station in our watershed the meteorological station which are essential to simulate catchment processes were stored in the meteorological model. Thiessen polygon precipitation of each sub catchments has been used to weight the rainfall distribution for selected stations; as a result, areal rainfall was used for each sub-basin to compute precipitation (Subramanya, 2008).

$$P_{ave} = \sum_{i=1}^{m} W_i P_i \text{ --3.1}$$

$$W_i = \frac{A_i}{A_T} \text{ ---3.2}$$

Where;

A_i = Area defined by the Thiessen polygons

A_T = Total basin or watershed area.

P_i = precipitation i stations

W_i =is the sum of all the polygons and

$W_i = A_i/A_T$ such that $W_1 + W_2 + . . . + W_n = 100$.

The closest stations located in and around the research area are shown in Figure 3-8 above. For the estimation of mean areal rainfall of the area under investigation, Thiessen polygon method was applied. The meteorological stations Geresse station is located at the upper catchment (7.07%) and Arba-Minch station represents the lower catchment (92.93%) and command area of the project. As per the Thiessen polygon and orographic nature, the Kulfo catchment could be represented by Arba-Minch station. Thus, for the estimation of rainfall in the Kulfo Catchment area proportionally the representative station's data was applied.

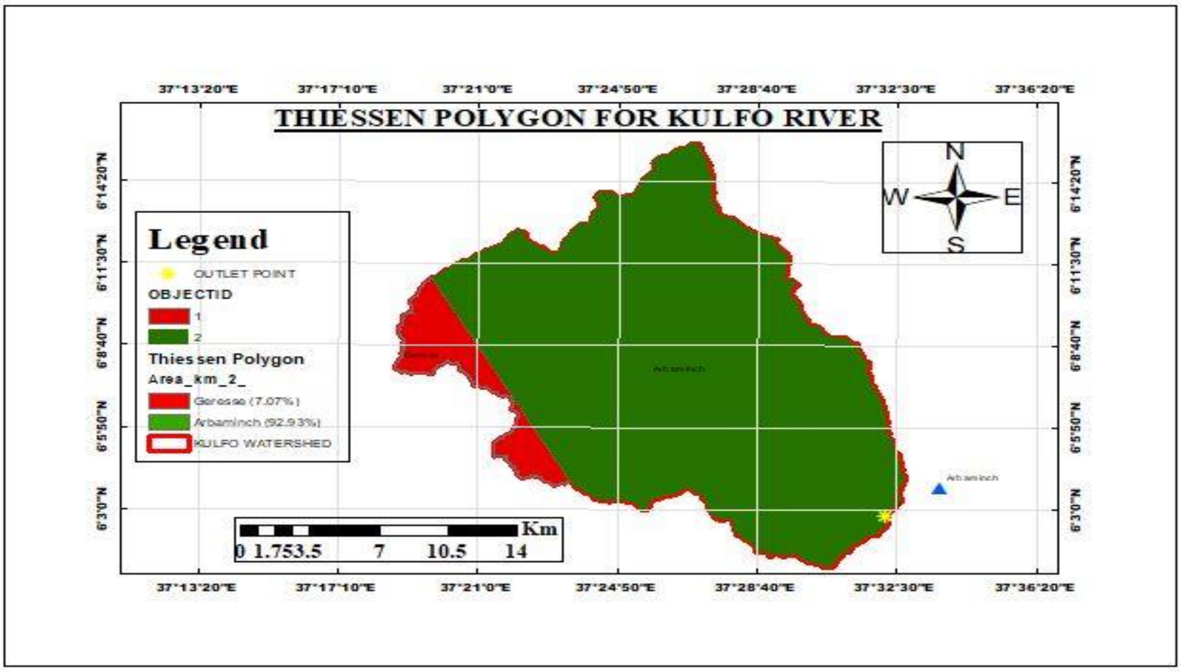

Figure 3.9: Map of Kulfo Thiessen Polygon

Table 3.6: Thiessen Polygon

S. No	St. Name	X	Y	Area(km^2)	Weight (%)	W(decimal)
1	Arba-minch	436061	868312.2	349.73	92.93%	0.93
2	Geresse	411842.2	886594.8	26.61	7.07%	0.07
Sum				376.34	100.00%	1.00

The mean annual rainfall of the study area is 1017 mm with an average temperature of 27 ^{O}C. Based on the long-term mean monthly rainfall estimated from the selected rain gauge stations, the region's rainfall pattern is bimodal that is two rainfall peaks occurred in the primary rainy season (from March to April) and the secondary rainy season (from October to November). These rainy seasons are usually controlled by the movement of the Inter-Tropical Convergence Zone (Seleshi and Zanke, 2004).

b) Consistency check

Stations in similar group were used to fill missed records. Shifting of gauge location, observational and instrumental errors are the common causes for inconsistency of rainfall record. A change due to meteorological causes would not cause inconsistency (change in slope of double mass plot), as all base stations would be similarly affected. A consistent record is one where the characteristics of the record have not changed with time. Adjusting for gauge consistency involves the estimation of an effect rather than a missing value. An inconsistent record may result due to shifting of a rain gauge station to a new location, change in the ecosystem due to calamities, such as forest fires, landslides, and occurrence of observational error from a certain date (Subramanya, 2008).

The checking for consistency of rainfall records is done by the method of double mass curve analysis as shown in the (Figure 3.10-3.14). This technique is based on the principle that when each recorded data comes from the same parent population, they are consistent. Double mass curve analysis is a graphical method for identifying and adjusting inconsistency in a station record by comparing its time trend with those of adjacent stations. For this purpose, double mass curve technique was applied using Hydrognomon version 4.1.0 (N.T. University of Athens, ITIA research team, 2012).

$$P_{CX} = P_X * \frac{M_c}{M_a} \qquad \text{3.3}$$

Where,

P_{cx} = corrected precipitation at any period time t_1 at station X

P_x = Originally recorded precipitation at period time t_1 at station X

M_c =corrected slope of the double-mass curve

M_a = original slope of the double-mass curve.

Hydrognomon is capable of performing many of the statistical procedures in hydrology. It is such a powerful tool for double mass curve analysis. In addition to plotting the double mass curve, it is capable of automatically correcting the homogeneity of the time series with respect to a user selected reference station.

The result of double mass curve analysis shows that there is no significant change in the observed time series for almost all stations tested

ii) Homogeneity test

In order to check the homogeneity of the selected gauging stations the monthly rainfall records were non–dimensional-zed and plotted to compare the stations with each other (Figure 3-15).

The non-dimensional-zing of the monthly values were carried out as per R.K Linsley, L.H, (1983),

Test Homogeneity is an important issue to detect the variability of the data. In general, when the data is homogeneous, it means that the measurements of the data are taken at a time from the same environment. The collected data said to be homogenous if the measurements have been consistently done by the same method, with the same instrumentation, at the same time and place, and in the same environment (McCuen et al.,1998).

$$Pi = (pi/ P) *100 \quad\text{--}3.4$$

Where;

Pi= non-dimensional value of precipitation for the month i

pi =Over years averaged monthly precipitation for the station i

p =the over years averaged yearly precipitation of the station

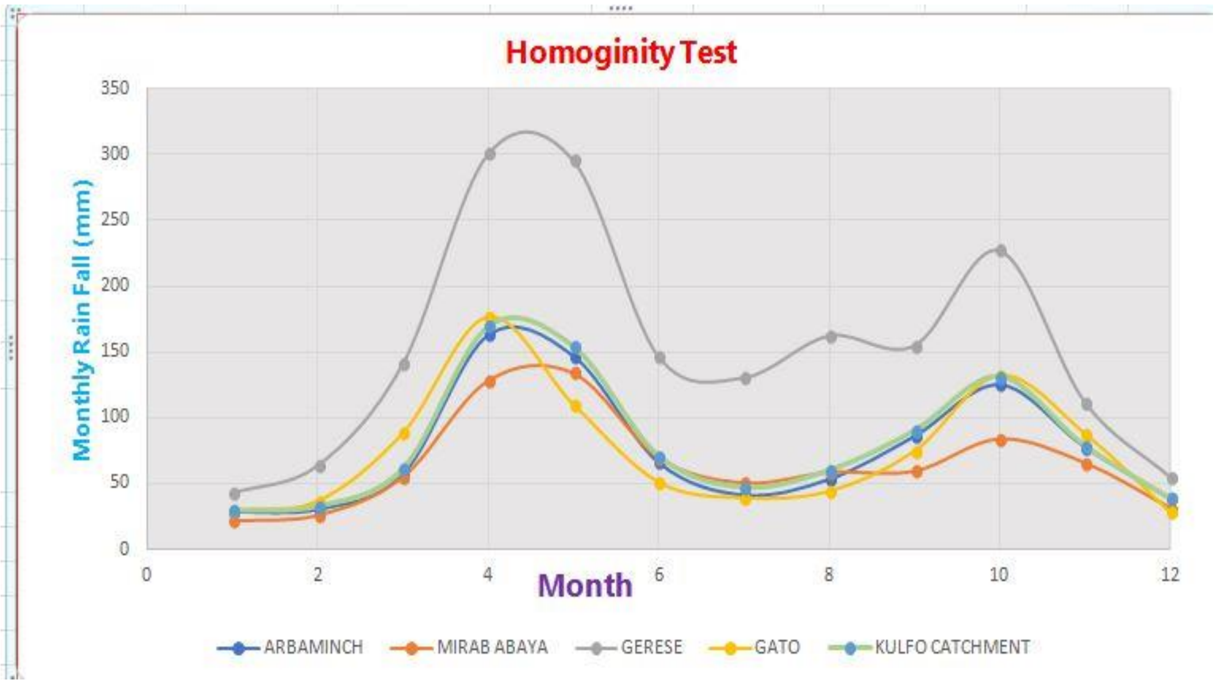

Figure 3.10: Map of Non-dimensional zed plot of selected stations nearby Kulfo

As it can be seen from the figure above all stations have bi-modal rainfall pattern

c) Missing record and filling missed data

A number of methods are available for estimating missing rainfall data. They are station average method, inverse-distance weighting method, and regression methods. For this study, the missing values of daily rainfall recorded were completed by using the Inverse Distance (US Weather Service) Method provided.

Whereas air temperature, relative humidity, sunshine hours, wind speed and hydrological data were filled with normal annual average and linear regression methods.

$$P_x = \frac{\sum_{i=1}^{n} W_i P_i}{\sum_{i=1}^{n} W_i} * 100 \quad \text{--3.5}$$

$$Wi = \frac{1}{D^2} \quad \text{--3.6}$$

$$D = \sqrt{(\Delta X^2 + \Delta Y^2)} \quad \text{--3.7}$$

Where;

Px = The missing data

Pi = the annual average precipitation of the gauge with the missing data

Δx= X Coordinate of the station

Δy= Y Coordinate of the station

This is the most acceptable method and is widely used for determining the missing rainfall for any scientific analysis. However, the limitation is that it estimates missing rainfall between the highest and lowest values of the index stations.

The mean annual rainfall of the study area is 972.34 mm with an average temperature of 27 OC. Based on the long-term mean monthly rainfall estimated from the selected rain gauge stations, the region's rainfall pattern is bimodal that is two rainfall peaks occurred in the primary rainy season (from March to April) and the secondary rainy season (from October to November).

These rainy seasons are usually controlled by the movement of the Inter-Tropical Convergence Zone (Seleshi and Zanke, 2004).

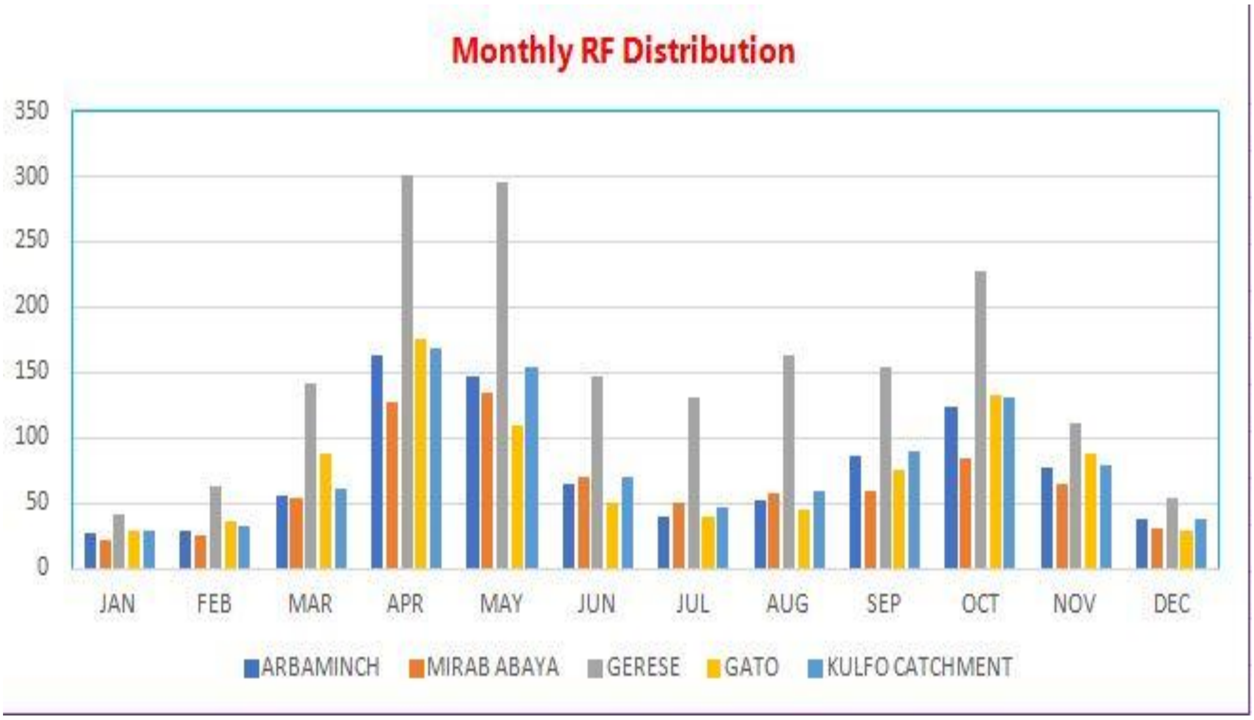

Figure 3-15 Monthly rainfall distribution of stations

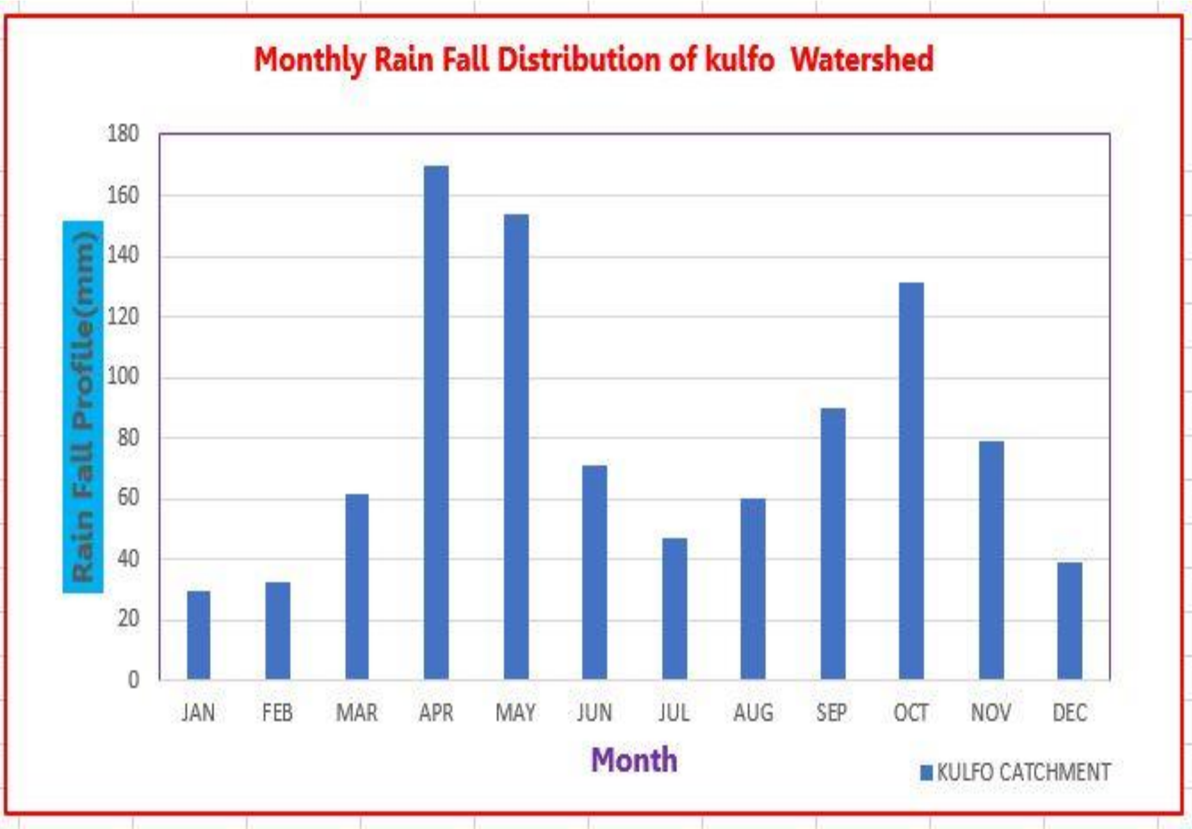

Figure 3 16 Monthly Rainfall distribution of Kulfo Watershed

From the observed rainfall of the station, it could be visualized that the rainfall extends from March to October. The rain falling in rainy seasons comprises about 81.53% of the annual total rainfall. The variability of rainfall explained by coefficient of variability.

i) Outlier test

Prior to performing frequency analysis based on the 24 hours maximum rainfall the outliers need to be checked. Errors on data may occur during recording or reporting. The quality and consistency of data is checked by outlier test as depicted below. For checking the low or high outliers the relationship given below will be applied. For coefficient of skewness (Cs) of lower than -0.4, the data should be checked first for lower outlier test otherwise the checking will be done for higher outlier.

Lower outlier

$Y_{lo}=Y_{avg}-K_n*S_y$--3.8

Where,

Y_{lo}: Low outlier,

$Y_{avg:}$ Mean of samples converted to logarithmic value,

K_n: Coefficient of frequency and

S_y: Standard deviation. Low outlier should check for lower value of less than 10^{Ylo}

Higher outlier

$Y_{ho}=Y_{avg}+K_n*S_y$--3.9

Where,

Y_{ho}: high outlier,

Y_{avg}: Mean of samples,

K_n: Coefficient of frequency and

S_y: Standard deviation. High outlier should check for higher value of greater than 10^{Yho}

Table 3.7: Annual Daily Maximum Rainfall serious

Sr.No	Year	Max Areal RF (mm/day)	Sr.No	Year	Max Areal RF (mm/day)
1	1988	56.45	20	2007	67.90
2	1989	86.78	21	2008	80.80
3	1990	47.30	22	2009	48.80
4	1991	64.99	23	2010	71.50
5	1992	85.70	24	2011	64.50
6	1993	84.25	25	2012	59.90
7	1994	45.74	26	2013	86.20
8	1995	48.99	27	2014	37.80
9	1996	46.58	28	2015	60.70
10	1997	82.09	29	2016	57.70
11	1998	56.09	30	2017	61.30
12	1999	90.63	31	2018	49.74
13	2000	65.36	32	2019	48.00
14	2001	57.77	33	2020	68.00
15	2002	48.87		**sum**	2084.43
16	2003	46.80		**mean/μ/**	63.16
17	2004	38.80		**stdv/αn-1/**	16.46
18	2005	102.40		**skew/Cs/**	0.57
19	2006	66.00		**Max**	102.40
				Min	37.80
				N	33

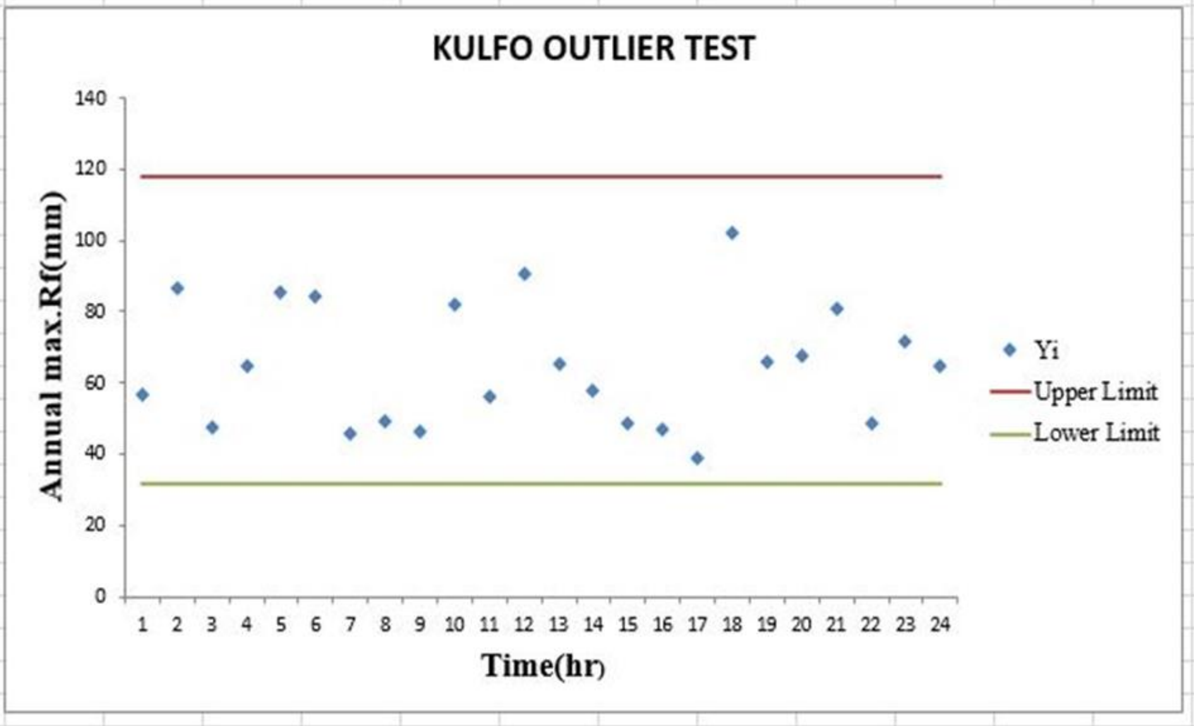

Figure 3.11: Kulfo Outlier

3.3.2 Hydrological Data Analysis

Before beginning any hydrological analysis, it is important to make sure that data are homogenous, correct, sufficient, and complete with no missing values. Errors resulting from lack of appropriate data processing are serious because they lead to bias in the final answers. Generally, data should be appropriately adjusted for inconsistency, corrected for errors, extended for insufficient, and filled for missing using different techniques. Daily rainfall and flow data of different record length for some stations were collected from National Meteorological Agency (NMA) and Ministry of Water and Energy

3.3. 2.1. Estimation of Missing Stream flow Data

Reliable information on magnitude and frequency of flood-flow is required for the economic design of flood-control structures as well as for flood plain. They're under estimation may result in disruption of service, costly maintenance, may even make the difference between life and death, while over estimates may result in excessive construction costs. For reliable estimates for extreme flood is long data series are required, this rarely exists in excess of hundred years (Singh.K.,2004).

Flood discharges are often referred to us peak discharge as they occur at the peak of stream's flood hydrograph (discharge over time). Peak discharge magnitudes are a function of their expected frequency of occurrence, which in turn relates to the magnitude of the potential damage and risk (ERA). The detail Computational steps to estimate design discharge using SCS unit hydrograph method and procedure adopted by MoWR (2002) to prepare synthetic hydrograph; to estimate the design discharge of the selected flood prone areas.

Stream flow data filling and consistency

The daily discharge has some missing values for a certain length of time and gap-filling was done using a Inverse distance method of the station with missing data and the

Steps to peak flow Estimation using SCS (graphical peak flow) method

- ❖ Determine the watershed area in km^2
- ❖ Determine the time of concentration
- ❖ Determine the soil type, soil group, land use and CN of the water shed area;

- ❖ Determine the hydrologic region, check the AMC and convert the CN value if required to wet or dry condition
- ❖ Determine the 24 hr rainfall depth and calculate the Ia/p ratio
- ❖ Calculate the unit peak flood, q_u
- ❖ Calculate the peak discharge, Q_p

3.4. Frequency Analysis

Determination of the frequency of occurrence of extreme hydrological events like floods and drought are important in water resources planning and for sizing of hydraulic structures such as spillways, culverts and bridges. There is a definite relation between the frequency of occurrences and magnitude; the ordinary events occur almost regularly than the severe storms. In general practice for rainfall frequency analysis the data series should be more than 33 years. As seen from Table 3.8 the Arba-Minch station has rainfall data series of 33 years. Therefore, the data series of the station is appropriate for the rainfall frequency analysis.

The frequency analysis was carried using the annual 24-hour maximum rainfalls of the station and fitting to the best probability distribution (PDF) as per Kolmogorov-Smirnov and x-square tests. The frequency analysis was performed using Hydrognomon 4.1.0 tool. According to the test, GEV-Min (L-Moments) distribution fits best for both distributions.

To estimate the rainfall depth for a given return period at a given site of interest, the present study used rainfall frequency analysis (RFA). The RFA, extreme value theory, uses extreme values extracted from either the annual maximum daily rainfall series (AMS) or peak over thresholds series (PoT) to estimate high-quantile extremes. The basic assumption of this theory is that the distribution of the event is identical and independent (Fisher and Tippett, 1928)

Table 3.8: Annual daily maximum rainfall distribution spastically distribution

Statics Distribution	X-Square test for All data					Kolmogorov-Smirnov test for: All data				
Probability-Distribution	**a=1 %**	**a=5 %**	**a=10 %**	**Attained (a%)**	**Pearson Param.**	**a=1 %**	**a=5 %**	**a=10%**	**Attained a(%)**	**DMax**
Normal	OK	OK	OK	10.95	4.4242	OK	OK	OK	70.89	0.1161
Normal (L-Moments)	OK	OK	OK	10.95	4.4242	OK	OK	OK	72.91	0.1140

Log Normal	OK	OK	OK	10.95	4.4242	OK	OK	OK	74.04	0.1128
Exponentia (LMoments)	OK	OK	OK	49.81	1.3939	OK	OK	OK	76.27	0.1104
Gamma	OK	OK	OK	12.74	4.1212	OK	OK	OK	76.96	0.1097
EV1-Max (Gumbel)	OK	OK	OK	10.95	4.4242	OK	OK	OK	66.09	0.12115
GEV-Min	OK	OK	OK	19.27	1.6969	OK	OK	OK	88.01	0.0964
GEV-Max (LMoments)	OK	OK	OK	12.91	2.3030	OK	OK	OK	82.16	0.1038
GEV-Min (LMoments)	OK	OK	OK	37.47	0.7878	OK	OK	OK	93.65	0.0873
EV1-Max (Gumbel, L-Moments)	OK	OK	OK	27.17	2.6060	OK	OK	OK	82.14	0.1038

As seen on table above both functions fit the data reasonably. For the estimation of the maximum rainfall, however, among these distributions GEV-Min (L-Moment) distribution is selected and presented on Table below.

Table 3.9: 24 hrs. Maximum rainfalls for different return periods

Return Period (T) years	Rainfall Intensity Duration Frequency curve for the 24 hours Rainfall (mm)
2	63.45
5	77.88
10	86.43
25	96.23
50	102.96
100	109.30

3.5. Rainfall Intensity Duration

Rainfall intensity duration frequency (IDF) analysis is carried out on the basis of 24 hours rainfall intensity of stations (Table 3.15). Maximum Intensity in mm per hour is derived for various durations and return periods for short durations of rainfall ranging from 5 minutes to 1440 minutes. Rainfall intensity is the average rainfall rate during the time of concentration. Based on this definition, it can be calculated with the equation:

$i = R_{tc} / t_{conc}$ --3.10

Where:

i = rainfall intensity (mm/hr),

R_{tc}= the amount of rain falling during the time of concentration (m),

t_{conc}= the time of concentration for the sub basin (hr).

An analysis of rainfall data by Hershfield (1961) method for different durations and frequencies showed that the amount of rain falling during the time of concentration was proportional to the amount of rain falling during the 24-hr period.

$Rtc = \alpha tc * R_{day}$ ---3.11

Where:

Rtc = the amount of rain falling during the time of concentration,

αtc = the fraction of daily rainfall that occurs during the time of concentration,

R_{day}= is the amount of rain falling during 24-hr

The Transport and Road Research Laboratory (TRRL, UK), Laboratory Report 623, Prediction of Storm Rainfall in East Africa (D. Fiddes, J.A. Forsegate and A.O. Grigg) give a valuable regional study on storm rainfalls in East Africa. The research study used the following model to fit a large number of stations data:

$I = a/ (b+t)^n$ ---3.12

Where:

I = intensity or rainfall in mm/hr

t = duration in hours a, b & n are constant

The best fit was found at b equals 0.33 hours and the index n varies from 0.78 to 1.09 and Adopting 24-hour rainfall value as I_{24}

. $I= [(b+24)^n/(b+24)^n]*I_{24}$--3.13

Therefore, in this case, the study adopts the value of "b" is 0.33 and "n" equals 0.9 (the average of n is 0.78 to 1.09 for East Africa).

Based on this formula, the rainfall intensities of the station is computed and presented on table below.

Table 3.10: Frequency Storm Depth

Minutes	hr.	Return period (year)					
		2-year	**5-year**	**10-year**	**25-year**	**50-year**	**100-year**
5	0.083	9.61	11.97	13.47	15.31	16.65	17.97
15	0.25	20.68	25.76	28.99	32.94	35.83	38.66
60	1	37.50	46.71	52.55	59.72	64.95	70.09
120	2	44.37	55.27	62.18	70.67	76.85	82.94
180	3	47.74	59.47	66.91	76.04	82.69	89.25
360	6	52.67	65.61	73.82	83.89	91.23	98.46
720	12	56.92	70.91	79.78	90.66	98.59	106.41
1440	24	60.85	75.80	85.28	96.92	105.40	113.75

Using the above frequency storm estimated for different return periods as an input, the maximum flood hydrograph for different selected return periods was obtained using the HEC-HMS model. The result indicated that the minimum peak flow for the Kulfo River occurs for a 2-year return period for 24-hour storm duration and the maximum is obtained with a 100-year frequency storm for the same duration. The value is 220.2 m^3/s and 1141.2 m^3/s for 2-year and 100-year frequency storms respectively. Figure 3.10 below shows the flood hydrographs for different return periods estimated using the HEC HMS model.

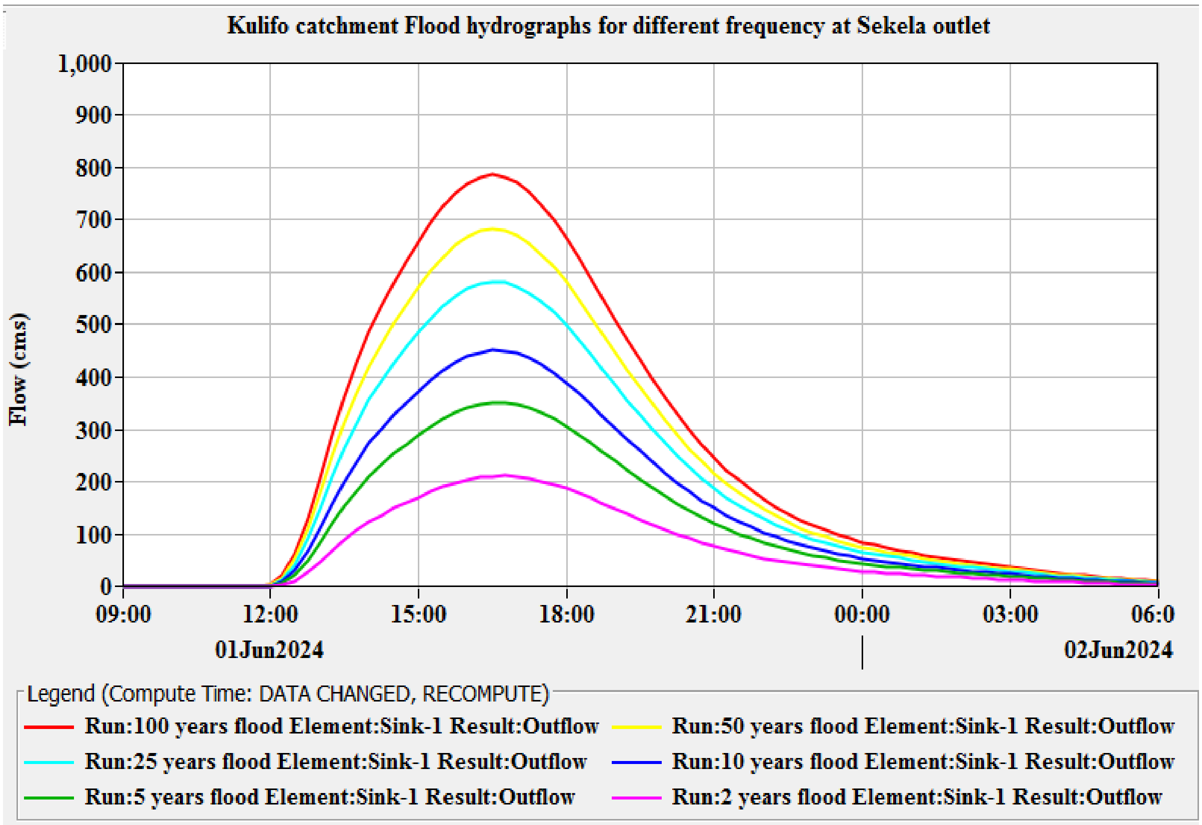

Figure 3.12: Flood hydrograph for the different return period in HEC-HMS model

3.6. Flood Modeling

Flood modeling is a simplification of the real situation event. A flood model of a particular river basin for example simulates the real flood events that have occurred using the actual hydrological input data, the basin's hydraulic characteristics and boundary conditions. These modeling are able to show effects on the results based on different boundary conditions or input data. Hence by simulation, the behavior of the flood risk or hydraulic characteristics at a certain period of time can be determined and investigated.

In the development of flood mapping, with recent advances in technology whereby computation time has been tremendously reduced, it is becoming necessary to simulate flood inundations in the flood plains caused by different magnitudes of flood events. Nowadays, different types of inundation models exist and approaches have been made by various researchers by using various hydro dynamic modeling models (Bates *et al*., 2003).

3.7. Model Selection Criteria

In addition, improvements in numerical modeling have provided engineers and hydrologists the ability to simulate hydro dynamics model with the aid of their computers. Hydrodynamic models predict outputs, such as velocities vector and water surface elevations, given specific inputs, such as stream flows. In flood models, the models represent hydrologic and hydraulic processes in the river channel and flood plain. Model simulation can provide flood depth and extent (Tarekegn et al, 2010).

The model was selected based on the recommendation enumerated in (Cunderlik 2003).

The suggested criteria are mostly project dependent, since the requirements and needs of every project is different.

- The ability of the model in predicting long-term sequence of flow series.
- Capability of the model in simulating land use/ land covers change, climate change and its representation of spatial coverage. Moreover, its ability in capturing hydrological processes.
- Availability of input data using all the required inputs by the model within the time and cost constraints of the project?
- Price (Does the investment appear to be worthwhile for the objectives of the project?) (Cunderlik 2003).

Based on the above criteria

(1) Daily rainfall-runoff model using HEC-HMS model has been implemented on that watershed having good quality of data.

(2) Predicting the stream flow from gauged watershed

The purposes and benefits of the model-output, e.g., continuous hydrograph of discharges, forecast of floods, water quality, and water resource management;

- The climatic and physiographic characteristics of the basin;
- The lengths of the records of the various types of data;
- The quality of the data both in time and space;
- The availability and size of computers for both development and operation of the model

❖ The possible need for transferring model parameters from smaller catchments to larger catchments; and

The ability of the model to be updated based on current hydro-meteorological conditions

3.8. Rainfall -runoff modeling

The use of rainfall-runoff models inevitably extends the lead time. These models relate current rainfall in a catchment to river flows or reservoir inflows. For the forecasting chain starting from the measured rainfall and using it as input to a rainfall-runoff model, forecasting lead time becomes a function of delays, mostly due to the filling of the soil storage and surface waters travel time.

Rainfall-runoff models may be either;

A. Lumped i.e. using a single rainfall input spatially averaged across the catchment
B. Distributed i.e. accounting to some extent for the distribution f rainfall.

River flows may be forecast at specific points along a river to provide warnings at these points, or used as input to flood routing models to provide warnings further downstream.

3.8.1. HEC-HMS model

Hydrologic modeling system is designed to simulate the precipitation-run off process of a dendrite watershed system. The model estimates peak discharges and runoff hydrographs for various return periods at different location of the watershed. The program computes stream flows by subtracting losses, transforming the excess precipitation and adding base flow from the precipitation.

The Hydrologic Engineering Center's Hydrologic Modelling System (HEC-HMS) is a powerful system which is deigned to simulate the rainfall-runoff processes from small urban watershed to large river basin or for the proper estimation of the quantity of the flood peak generated in a watershed. (Fatima Daide, 2021). It consists of different component processes for rainfall loss, direct runoff or develops hydrographs, and routing. The Soil Conservation Service (SCS) curve number (CN) method is one of the most popular methods for computing the runoff volume from a rainstorm.

3.8.2. HEC-RAS model

From much hydrologic software, HEC-RAS (Hydrologic Engineering Center - River Analysis System) is a good choice for 2D flood/channel/ plain modeling and sediment simulation. Its ArcGIS application companion RAS Mapper makes it easier to gather physical data required by the model from a high-resolution DEM. HEC-RAS model able to accomplish mobile bed sediment simulation with unsteady flow succession data (U.S. Army Corps of Engineers, 2021).

HEC-RAS is a modeling program developed by the US Army Corps of Engineers. It allows two different approaches to be adopted, i.e.

(i) Steady flow calculations,
(ii) Unsteady flow simulation.

The unsteady flow simulation will be used in this study to simulate the flood inundation.

One of the major purposes for using HEC-RAS is to compute water surface elevation. This is where hydrology and hydraulics come together. Hydrology allows us to calculate information such as 100-year flood flow, probable maximum flood flow (PMF), etc., then using this information in HEC-RAS the study can figure out what the possible hydraulic conditions will be for a given study area.

HEC-RAS, a hydraulic model developed by the USACE, is extensively applied in calculating the hydraulic characteristics of rivers (Carson 2006; Pappenberger et al. 2005). It is an integrated program and uses the following energy equation for calculating water surface profiles (Brunner and Bonner, 2010; Fan et al. 2009).

This program provides user to input data, data correction, to receive output display and analysis. HEC-RAS model needs details of river cross sections and upstream flow rate. The water depth and mean velocity are calculated for a given cross section using the energy conservation equation (Fan et al. 2009).

HEC-RAS calculates the water levels' variation along the channel and the water level values are overlaid on a digital elevation model (DEM) of the area to get the extent and flood depth using GIS. Spatial data like cross section, river reach, stream network, flow paths, and others have been obtained using HEC-Geo RAS (Arc-GIS extension) and these data then transferred to HEC-RAS (Baky et al. 2012).

HEC-RAS and GIS Integration

HEC-Geo RAS has been specifically designed to aid engineers with limited GIS experience in the development and display of hydraulic data for HEC-RAS. However, users must have enough experience modeling with HEC-RAS and river hydraulic to properly create and interpret GIS datasets.HEC-Geo RAS is an extension for use with Arc GIS that provides the users with a set of tools, procedures and utilities for the preparation of GIS data for import into Hydraulic Engineer Center's River Analysis System (HEC-RAS) and generation of GIS data from HEC-RAS output. This extension was developed through Cooperative Research and Development Agreements between the Hydraulic Engineer Center (HEC) and the Environmental System Research Institute, Inc (ESRI). Users must have experience modeling with HEC-RAS and river hydraulics to properly create and interpret GIS datasets. Geo RAS provides the user with environments to manage create and edit process and visualize data sets. Each environment is intended to lead the user through procedures in a clear and logical order.

3.8.3. Application of the HEC-RAS Model

In the modeling with HEC-RAS, Manning roughness coefficient (n) is one of the most input important parameters. Roughness coefficients are an indication of the relative channel roughness. Channel roughness is considered for calculating frictional energy loss between cross sections. Considering the features of this river reach, the Manning roughness coefficient for main channel and flood plain is taken as 0.02. The "n" values are found from the calibration the flood event which was happened in 1998. Since the geometry, surface and river bed is nearly same in the river, same "n" values are used for each cross-section. The resistance parameter which is known to vary with water level, decreasing with increasing water level by decreasing the effective relative roughness, and then increasing again as the flow spills over bank, since flood plain roughness is usually higher than the channel roughness (Chow, 1959). So, flood plain "n" value is taken as bigger than the river bed. Several simulations were done and tracks of previous big floods are used for the calibration. The other main input for HEC-RAS model is the river cross section. In this study, the contour map of the study areas was digitized from 1:25,000 scale topographic maps and 1:50,000 scale maps.

3.8.4. GIS Environment

A hydraulic model is intended to represents the flood physical processes over time of a river channel or flood plain as realistic as possible that able to provide acceptably accurate output for different scenarios to its user (Pullar and Springer, 2000). With GIS, a hydraulic model is presented in a spatial or geographical manner that would allow the model to analyze, predict and solve engineering problems in a more powerful and comprehensive way.

Many modeling applications uses GIS as the data base manager and visualization tools through the use of Windows Graphical User Interfaces (GUIs) making the output easier to understand by its users. The benefits of GIS integrated modeling are tremendous. With the integration of GIS in these modeling, some of the techniques or procedures from the manual flood risk mapping processes may need to be modified or changed, among others include search method, governing algorithms, data requirements and flood inundation extent and depth.(Noman *etal.,*2001).In GIS, data can be extracted, combined with others or reformatted if needed for various modeling processes and even used to generate other inputs as required by the models (Robbins and Phipps, 1996).

3.8.5. Input data for Flood Modeling

Asselman et al. (2009), highlighted the data required by any hydraulic model are in principle the boundary condition, initial condition, topography data, friction data and hydraulic data for use in model validation. Whereas, Method et al, (2007) noted the data required for flood modeling are hydraulic boundary determinations, geometric data, discharge data, roughness data and calibration and validation.

In general, modeling of flood plain flooding requires high quality input data, which should include rainfall, a digital terrain model, land use and calibration. Rainfall data should ideally be provided by a dense network of rain gauges and/or the weather radar. Both sources are important, the former is generally considered as more accurate, whilst the latter typically has higher spatial resolution, which enables advanced applications such as now casting (quick precipitation forecasting).

3.9. Hydrological Modeling

Models are central to the application of information technology because they are the means by which the real world is represented inside a computer. The model starts with data processing and acquisition of the HEC-HMS. The data required for the model is derived from different hydrological components. This hydrologic representation imported in to HEC-HMS is then combined with precipitation data and control specifications to create flow and time series data for use in a Hydrologic Data Model HEC-HMS. The flow and time series data from HEC-HMS is imported into the hydraulic model HEC-RAS along with its geometry data to develop water surface profiles.

3.9.1 HEC-HMS Model Development

The process consists of the following steps:

Data preparation: This step involves collecting and processing the required data for the model, such as rainfall, evaporation, soil, land use, topography, and stream flow. The data can be obtained from various sources, such as gauges, satellites, remote sensing, or GIS. The data can be spatially and temporally disaggregated or aggregated to match the model resolution and time step.

Model setup: This step involves defining the model structure, parameters, and options. The model structure consists of the elements that represent the physical features and processes of the catchment, such as sub-basins, reaches, reservoirs, junctions, diversions, sources, sinks, etc. The model parameters are the values that control the behavior of the elements, such as curve numbers, lag times, initial losses, base flow coefficients, routing coefficients, etc.

Model calibration: This step involves adjusting the model parameters to achieve a good fit between the simulated and observed stream flow. The model calibration can be done manually or automatically using various methods, such as trial and error, sensitivity analysis, optimization algorithms, etc.

Model validation: This step involves testing the model performance using a different set of data than the one used for calibration. The model validation can be done using the same methods and criteria as the calibration step.

Model application: This step involves using the model for various purposes, such as flood forecasting, water resources management, climate change impact assessment, etc. The model application can involve running different scenarios or simulations with different inputs or parameters to analyze the effects of different factors or interventions on the catchment hydrology.

Creating Basin Model

Basin model was created with the help of GIS, a hydrological tool in HEC-HMS

Terrain Pre-processing

The DEM was pre-processed in HEC-HMS 4.11 to derive sub-basins and drainage network of the catchment.

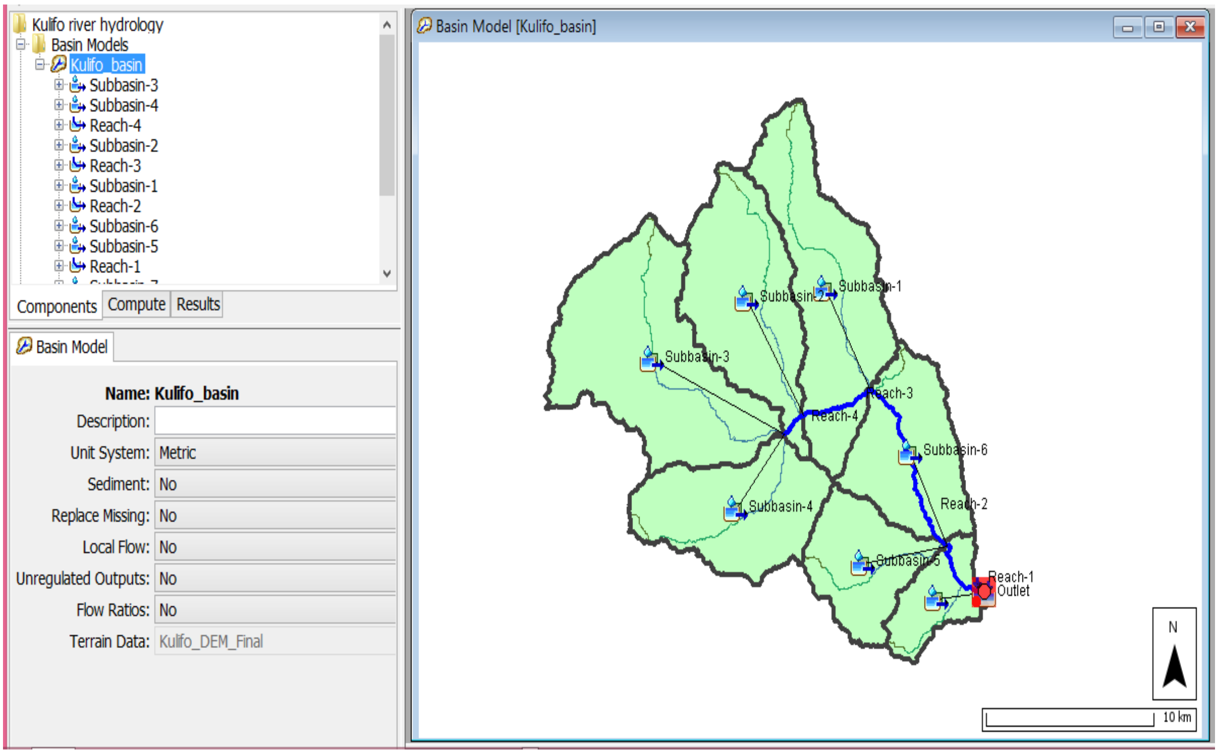

Figure 3.13: Map of Basin Processing

The delineated sub-basins and rivers were merged based on river junctions. Some major characteristics of the basin model for Kulfo watershed were tabulated in Table below:

Table 3.11: Basin Model characteristics

Sub basins	L(Km)	Basin slope	Basin Area (Km2)	CCN	Tlag(Min)	Ia(mm)
Sub basin-1	20.4	0.5	73.3	73.1	99.5	18.74
Sub basin-2	18.3	0.5	62.2	74.4	84.9	17.50
Sub basin-3	21.3	0.3	89.4	75.0	112.3	16.93
Sub basin-4	16.2	0.4	52.9	72.6	87.9	19.20
Sub basin-5	12.3	0.4	35.4	74.5	67.9	17.37
Sub basin-6	15.7	0.4	47.2	74.7	80.9	17.23
Sub basin-7	9.1	0.3	19.7	75.0	57.8	16.93

Developing hydrological parameters

The hydrological parameters were estimated by using the land and soil use data for each sub basin. The Selected methods for HEC-HMS processes for modelling loss, transform, and routing:

Table 3.12: Selected methods for HEC-HMS processes

Processes	Selected methods	Purposes
Loss	SCS Curve Number	Rainfall to Runoff/loss estimate
Transform	SCS Unit Hydrograph	Lag time or Tc
Routing	Muskingum	Routing Hydrograph

Hydrological Modeling

The initial values of loss parameters like initial abstraction were calculated using land use data and soil types of the basin.

Soil Conservation Service (SCS) curve number (CN) method

SCS and CN method was chosen for loss estimation because it was popular, easy to understand and apply, stable and accounts for most of the runoff producing watershed characteristics.

Loss Methods

This model computes the runoff volume of the catchment by calculating losses through interception, surface storage, infiltration, evaporation, transpiration and then subtracting it to the precipitation at each time step

$$Q_T = \frac{(P_T - I_a)^2}{P_T - I_a + S} \text{ ---3.16}$$

Where:

Q = accumulated direct runoff, mm

P_T = accumulated rainfall (potential maximum runoff), mm;

I_a = initial abstraction (surface storage, interception, and infiltration prior to runoff), mm;

S = potential maximum retention, mm.

The relationship between I_a and S was developed from experimental data is given as $I_a = 0.2S$. Therefore, Equation 3.16 is given as Equation 3.17 below.

$$Q = \frac{(P - 0.2S)^2}{P + 0.8S} \text{ ---3.17}$$

S is related with soil and land cover through the empirical value called Curve Number (CN), the values which ranges 0 - 100. The relationship between S and CN is expressed as in Equation 5.10

$$S = 254\left(\frac{100}{CN} - 1\right) \text{--3.18}$$

Curve number depends on land use/cover, treatment practices and the soil in the catchment. Land use/cover of the catchment area refers all the cover types, including agricultural and non-agricultural uses, vegetation, water bodies, roads, roofs, etc. The treatment practice addresses different land practice on the cultivation and non-cultivated process it includes cultivation practice as straight, contour or seeding practice as closed seeded, row and other related practices. Similarly, soil properties influence the relationship between rainfall and runoff by affecting the rate of infiltration. The SCS has divided soils into four hydrologic soil groups based on infiltration rates (Groups A, B, C, and D).

The determination of runoff curve number has also considered the effects of land-treatment measures in cultivated land use including mechanical practices such as contouring or terracing and management practices such as rotation of crops. Therefore, CN has to be selected based on the combination

$$T_c = \frac{l^{0.8}(S+1)^{0.7}}{1{,}140Y^{0.5}} \text{---} 3.19$$

Where:

T_c = time of concentration, h

l= flow length, ft;

Y = average watershed land slope, %;

S = potential maximum retention, mm

$T_{La\,g}$= 0.6* T_c--3.20

Transform method

Transform methods is an approach for computing direct runoff at the outlet of watershed area from the excess precipitation falling over it and this is done based on principles of unit hydrograph. Unit hydrograph can be defined as the runoff hydrograph produced from excess rainfall of unit depth occurring over the watershed.

The transformation method used for this study was SCS Unit Hydrograph.

$U_P=2.08*\frac{A}{P}$ &--3.21

$T_P=\frac{\Delta t}{2}+T_{Lag}$--3.22

Where:

U_P = Peak of unit hydrograph,

A = Area of watershed,

T_P = Time of peak,

Δt = Excess Precipitation Duration

T_{lag} = Basin lag.

Route Method

Flood routing is a technique of determining the flow hydrograph at the downstream point of catchment with sound information regarding hydrograph at its upstream. Flood routing along the catchment is a function of basin characteristics such as slope and length of channel, channel roughness, channel shape, downstream control and initial flow condition

Procedure to determine the flow hydrograph at a point on a watershed from a known hydrograph upstream is called routing.

Muskingum method

In this study, Muskingum method or diffusion equation which is combination of continuity equation and momentum equation has been used for river routing because of its high accuracy over other methods. Assign Muskingum=0.5 and x=0.25

3.9. 1.1. Sensitivity analysis

Sensitivity analysis is important for calibration, optimization, risk assessment and data collection. Sensitivity analysis will be conducted to identify which parameter or parameters have greater influence on the output. Parameters with high influence on model output will get the most attention in the calibration process and data collection.

Sensitivity analysis determines how much a change in an input parameter affects the model response. Prior to assessing the major impact of input variability on certain model outputs of interest, the sensitive parameter was ranked. The output response changes when the most sensitive parameter is used. As a result, sensitivity analysis was used in this study to find sensitive model parameters and link them to catchment runoff generating features (Saltelli et al, 2000).

3.9.1.2 Calibration and Validation

Calibration

The calibration of the hydrodynamic model was conducted by following a trial-and-error procedure while changing Manning's coefficients. The initial guesses for Manning's roughness coefficients were assigned based on the land use type along with visual observations.

Suggestions of Chow (1959) were further used for the justification of the values applied for the model.

Calibration involves adjusting the model parameters to match observed data, while validation involves testing the model's ability to predict future events the model was calibrated using observed water surface elevations and velocities at various points along the river.

- ❖ The model was validated by comparing its predictions to observed data from a flood event that occurred after the calibration period.

- ❖ The use of a second-order accurate numerical scheme and the Courant number method for variable time step control were found to improve the accuracy of the model predictions.

- ❖ The paper notes that calibration and validation are important steps in the modelling process to ensure that the model accurately represents the real-world system being studied.

Validation

Model Analysis and Results Comparison /Water Level Comparison the better agreement between the simulated water level in Kulfo river gauge and the observed water level was ensured with the use of the Nash–Sutcliffe efficiency coefficient (*NSE*) 's . The value 1 in the Nash–Sutcliffe efficiency coefficient denotes a perfect match. Equation presents the Nash–Sutcliffe efficiency coefficient.

Model Performance Evaluation

Three model performance evaluation methods; the Nash and Sutcliffe (1970) efficiency (E_{NS}), the coefficient of determination (r^2) and percent bias (PBIAS) were used in both calibration and validation periods (see equations 3.23-3.26).

$$E_{NS} = 1 - \frac{\sum_{i=1}^{n}(q_{oi} - q_{si})^2}{\sum_{i=1}^{n}(q_{oi} - \overline{q}_o)^2} \text{--3.23}$$

Where:

q_{si} *is* the simulated value,

q_{oi} *is* the measured value,

And $\overline{q_o}$ is the average observed flow, the E_{NS}[-] values range from 1.0 (best) to negative infinity.

$$r^2 = \frac{\left[\sum_{i=1}^{n}(q_{si}-\bar{q}_s)(q_{oi}-\bar{q}_o)\right]^2}{\sum_{i=1}^{n}(q_{si}-\bar{q}_s)^2\sum_{i=1}^{n}(q_{oi}-\bar{q}_o)^2} \quad \text{--3.24}$$

Where:

q_{si} is the simulated discharge,

q_{oi} is the measured,

$\bar{q}_s$ is the average simulated discharge and

$\bar{q}_o$ is the average measured discharge (m^3/s).

Percent bias (PBIAS): measures the average tendency of the simulated data to be larger or smaller than the observations (Gupta et al., 1999).

$$PBIAS = 100 * \left[\frac{\left(\sum_{i=1}^{n} q_{oi} - \sum_{i=1}^{n} q_{si}\right)}{\sum_{i=1}^{n} q_{oi}}\right] \quad \text{--- 3.25}$$

Where:

q_{si} *is* the simulated discharge

q_{oi} *is* the measured discharge.

A value close to 0% is best for PBAIS. A negative value indicates model over estimation and a positive value indicate model under estimation.

RMSE=$\sqrt{\sum(Pi - Oi)2/n}$……………………………..………..……………3.26

Where,

RMSE=Root means Square Error

Pi=the predicted value of the i_{th} Observation in the data set

Oi= the Observed value of the i_{th} Observation in the data set

N=Sample Size

Table 0.13: General Performance ratings for recommended statistics for a monthly time step. (Moriasi, et al. 2007)

Performance rating	For stream Flow		
	RSR	NSE	% D
Very good	0.0<=RSR<=0.5	0.75<NSE<=1	D <=±10
Good	0.5<RSR<=0.6	0.65<NSE<=0.75	±10 <=D < ±15
Satisfactory	0.6<RSR<=0.7	0.5<NSE<=0.65	±15<=D<± 25
Unsatisfactory	RSR>=0.7	NSE<=0.5	D >= ± 25

3.10. HEC-HMS model calibration

The HEC-HMS model was calibrated to optimize its parameters using the available hydro-meteorological dataset. The HEC-HMS model has a built-in self-calibration utility that employs optimization techniques. This allows the user to select different approaches for the objective function used in the calibration process. Hence, the selected gauged watershed is modeled and the results are presented. To determine the accuracy of modeled results, the simulated hydrograph at outlet is compared to the historically observed hydrograph at outlet of the watershed. Parameters of different hydrographs along with hydro-meteorological data are provided and parameters are adjusted after calibration using the optimization method. The objective function used in this study for calibration was the peak weighted RMSE method. This function was selected because it gives greater weight to matching the peak of the hydrograph. The peak weighted RMS error method focuses solely on the peak of the hydrograph. It also takes into account the volume and time of the peak as well. The univariate gradient method and was used to minimize the peak weighted RMS error-objective function. In optimization trials are done with changing the more sensitive parameters using this method. The observed and simulated flow during calibration and the scatter plot between observed and simulated flow is shown in figure 3.10 and figure 3.11 respectively.

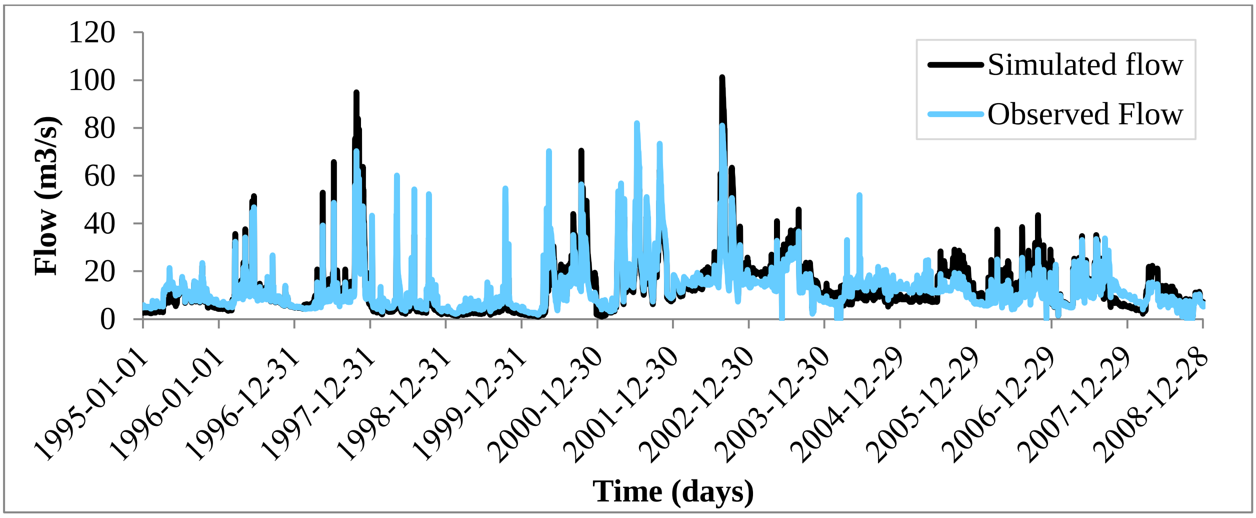

Figure 3.14: Observed and simulated flow during Calibration

The figure 3.14 above shows the comparison between observed flow and the simulated flow after calibration. The blue dotted lines denote simulated outflow and the green solid line denotes the observed flow measured at gauge stations of the outlet. This result shows a reasonable fit between the simulated and observed flow and shape and timing of peaks matched well. The calibrated model was further evaluated using scatter plot (R^2) between simulated and observed as shown in figure 3.15. The coefficient of determination is 0.79 which is classified as very good according to the performance evaluation criteria.

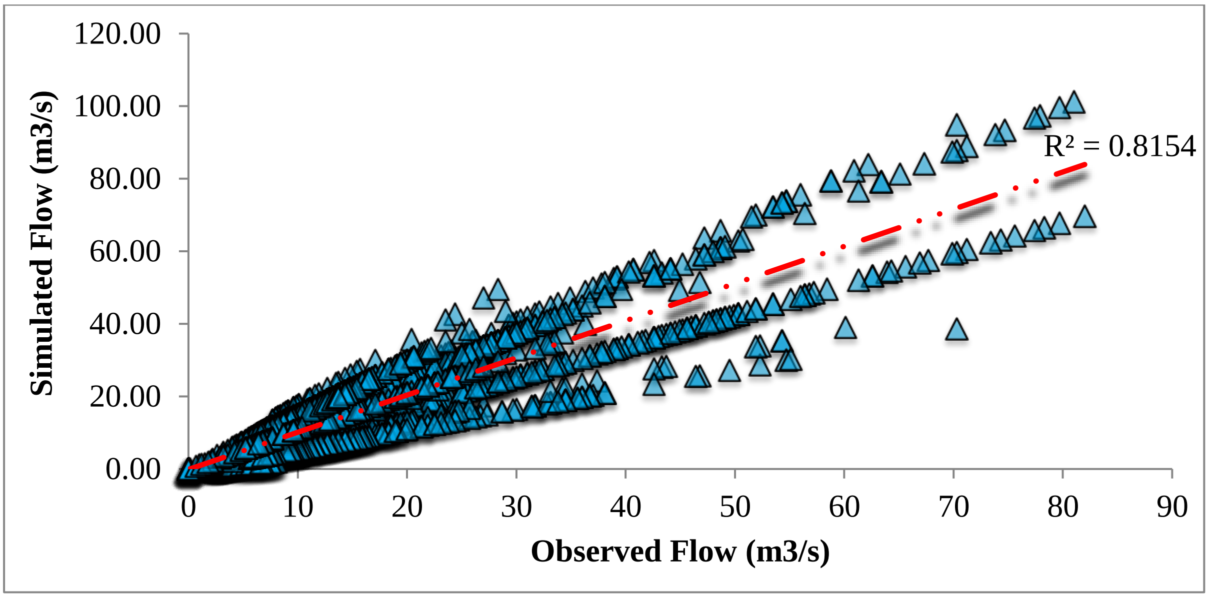

Figure 3.15: Scatter plot between Observed and Simulated Flow during calibration

3.11. HEC HMS Model validation

The purpose of validation was to demonstrate the applicability of the HEC-HMS model to predict stream flow in the watershed by comparing model prediction with observed data to evaluate if the models were able to predict the runoff at the discharge stations for the period other period. Validation was done by running the model with the respective optimized parameters for the watersheds with different input data set. The output result during validation was seen in (Figure 3.16).

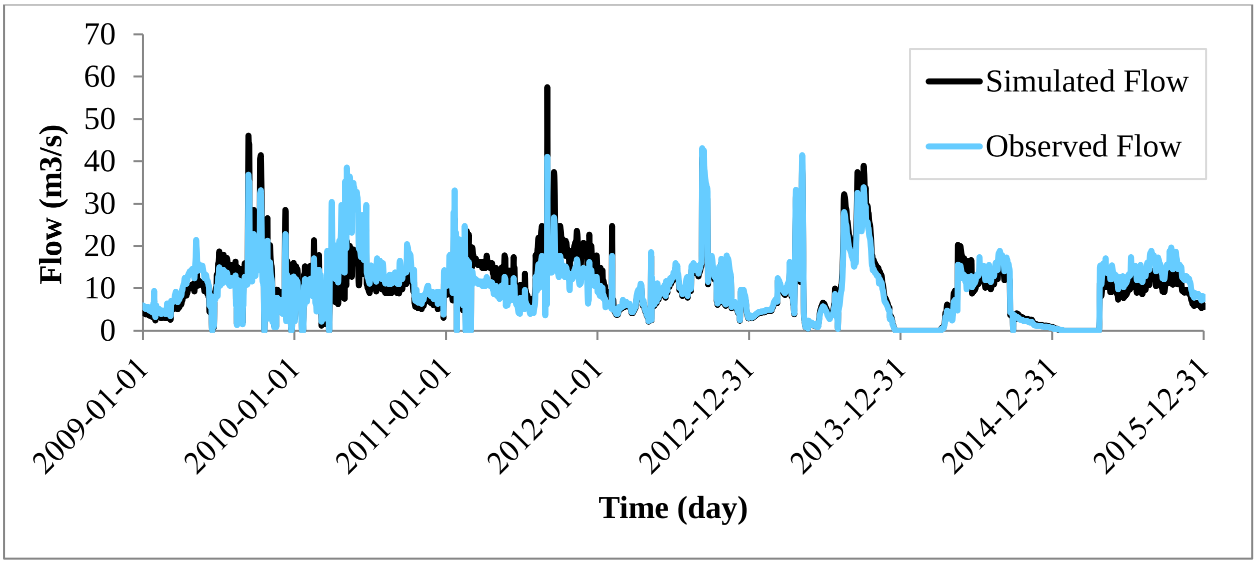

Figure 3.16: Observed and simulated flow during validation

As can be seen from the Figures 3.16, the pattern of simulated and observed flow is almost identical to each other. The validated model was further evaluated using scatter plot between simulated and observed flow and it shows that the there is strong relations between simulated and observed flow and the coefficient of determination is 0.81 which is classified as very good according to performance evaluation criteria.

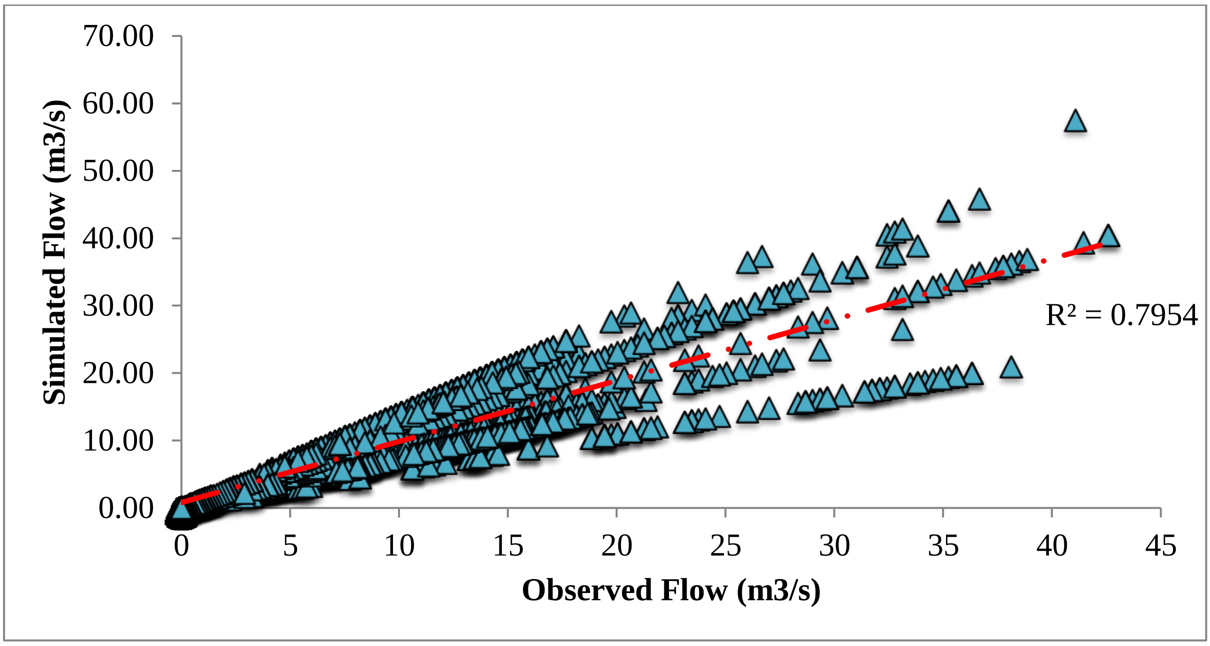

Figure 3.17: Scatter plot between Observed and Simulated Flow during Validation

The summary of the performance evaluation of HEC-HMS model during calibration and validation were presented in the Table 3.14. These performances were evaluated in terms of different performance indices such as: Coefficient of Determination (R^2), Nash Sutcliffe efficiency (NSE), root mean square error (RMSE), and percentage of bias (PBIAS)

Table 3.14: Performance Comparison of the Model by Different Performance Indicators

Methods	Performance Indicators			
	R^2	NSE	RMSE	PBIAS
Calibration	0.79	0.77	4.28	1.77
Validation	0.81	0.78	2.13	1.09

3.12. Hydraulic Modeling

3.12.1. Basic Data Requirement

Like a 1D model, a 2D model is HEC-RAS is comprised of various elements. Some of these elements are different from a 1D model. A 2D model must contain terrain data, 2D flow areas, and unsteady flow data. Unlike a 1D model, you must run the model as unsteady. There is no such thing as a steady 2D model. Like a 1D model, you can add hydraulic structures to a 2D model.

The data needed to perform these computations are divided into the following categories: Geometric data; Steady flow data, unsteady flow data and Sediment flow data. Geometric data are required for any of the analyses performed with HEC-RAS. The other data types are only required if you are going to do that specific type of analysis.

Terrain Data

The foundation of any hydraulic model is the terrain data. If your terrain data does not accurately represent the ground surface, it will not be an accurate model. You can import your terrain data using RAS Mapper. The RAS Mapper supports many different formats. However, you have to convert the terrain layer to GeoTiff file using RAS Mapper. This is because the GeoTiff file format supports compression and pyramiding of the data which allows for smaller file sizes and faster visualizations.

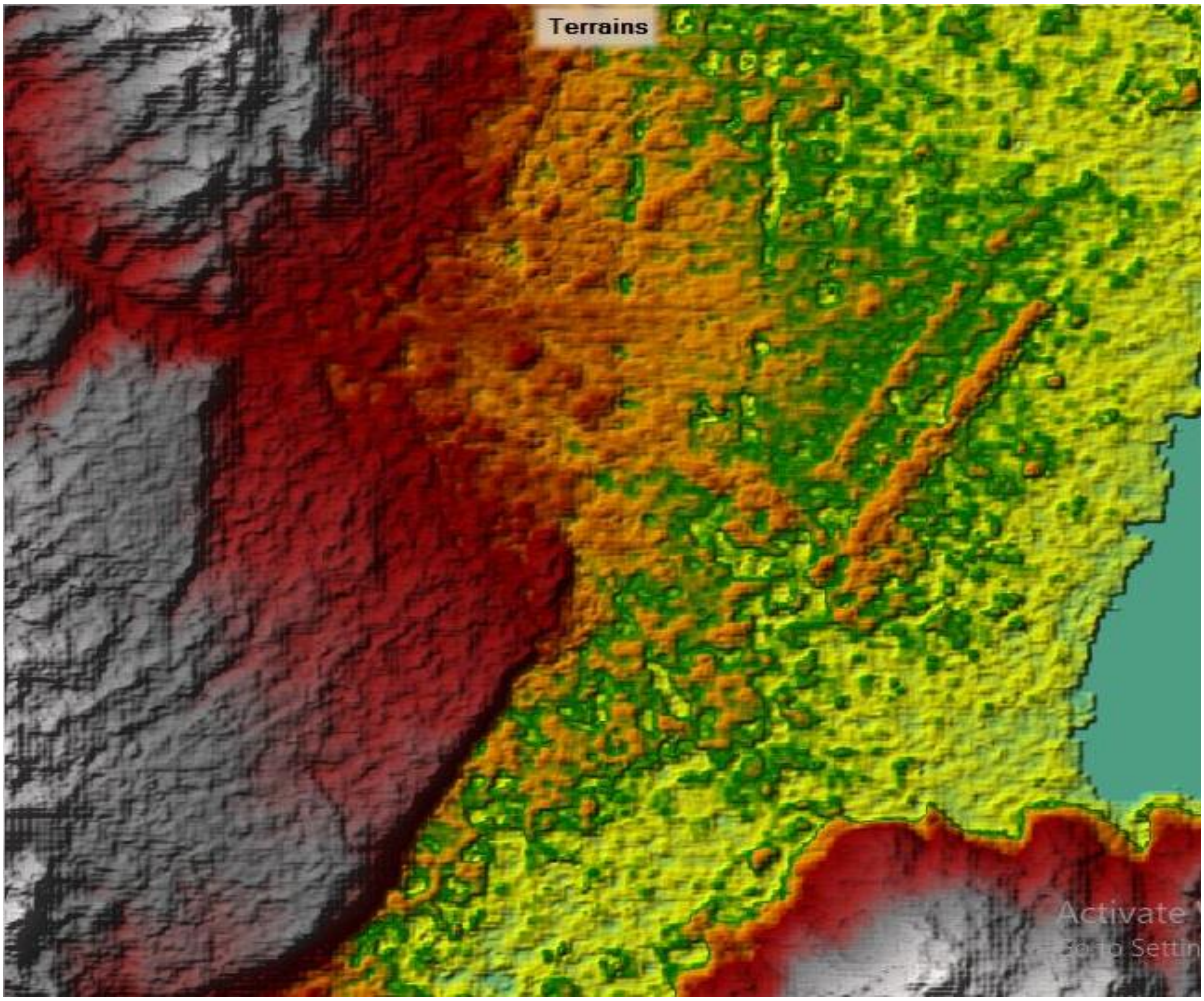

Figure 3.18: Map of Study area Terrain

2D Flow Area

A computational mesh can be structured or unstructured. The HEC-RAS program can handle a structured mesh or an unstructured mesh. A structured mesh is comprised of rectangular cells, and an unstructured mesh is comprised of cells that have an irregular shape. In HEC-RAS, the cells can be any shape, but each cell is limited to eight sides.

In HEC-RAS, the computational mesh is created using 2D Flow Areas. You define a 2D mesh by drawing a polygon to represent the outer boundary of the computational mesh. Then you specify the cell size.

Energy loss Coefficients

Manning's n selection of an appropriate value for Manning's n is very significant to the accuracy of the computed water surface profiles. The value of manning's n is highly variable and depends on a number of factors including: surface roughness; vegetation; channel irregularities; channel alignment; scour and deposition; obstructions; size and shape of the channel; stage and discharge; seasonal changes; temperature; and suspended material and bed load.

Unsteady Flow Analysis

HEC has added the ability to perform two- dimensional (2D) hydrodynamic routing within the unsteady flow analysis portion of HEC-RAS. Users can now perform two- dimensional (2D) unsteady flow modelling (Saint Venant equations of Diffusion Wave equations). A 2D flow area is added by drawing a 2D flow area polygon; developing the 2D computational mesh; then linking the 2D flow areas to directly connecting boundary conditions to the 2D areas.

Diffusion Wave Equations is used for computing the Unsteady Flow Analysis.

$$\frac{\partial H}{\partial t} + \frac{\partial (hu)}{\partial x} + \frac{\partial (hv)}{\partial y} + q = 0 \quad \text{.... 3.26}$$

$$\frac{\partial u}{\partial t} + u\frac{\partial u}{\partial x} + v\frac{\partial u}{\partial y} = -g\frac{\partial H}{\partial x} + v_t\left(\frac{\partial^2 u}{\partial x^2} + \frac{\partial^2 u}{\partial y^2}\right) - c_f u + f_v \quad \text{.... 3.27}$$

$$\frac{\partial v}{\partial t} + u\frac{\partial v}{\partial x} + v\frac{\partial v}{\partial y} = -g\frac{\partial H}{\partial y} + v_t\left(\frac{\partial^2 v}{\partial x^2} + \frac{\partial^2 v}{\partial y^2}\right) - c_f v + f_u \quad \text{.... 3.28}$$

Where,

t is time, u and v are considered as the velocity horizontal components in x and y direction, respectively, and q is a source/sink flux term. H is water surface elevation, h is water depth, g is gravitational acceleration, vt is the coefficient of horizontal eddy viscosity, cf is the coefficient of bottom friction, and f is the Coriolis parameter. A full explanation of the equations can be found in the HEC-RAS version 6.1 hydraulic reference manual (Brunner, 2016 b).

Boundary Conditions

There are several different types of boundary conditions available to the user.

Upstream Boundary Conditions

Flow Hydrograph-In HEC-RAS model Boundary conditions, including the flow values, needed for hydraulic simulations are specified in HEC-RAS using the flow data editor. You can open the flow data editor by going to edit unsteady Flow data on the HEC-RAS interface.

Downstream Boundary Conditions

For downstream boundary condition normal depth option was selected. To do this go to edit--Unsteady flow data on the HEC-RAS interface- select downstream- normal depth or friction slope.

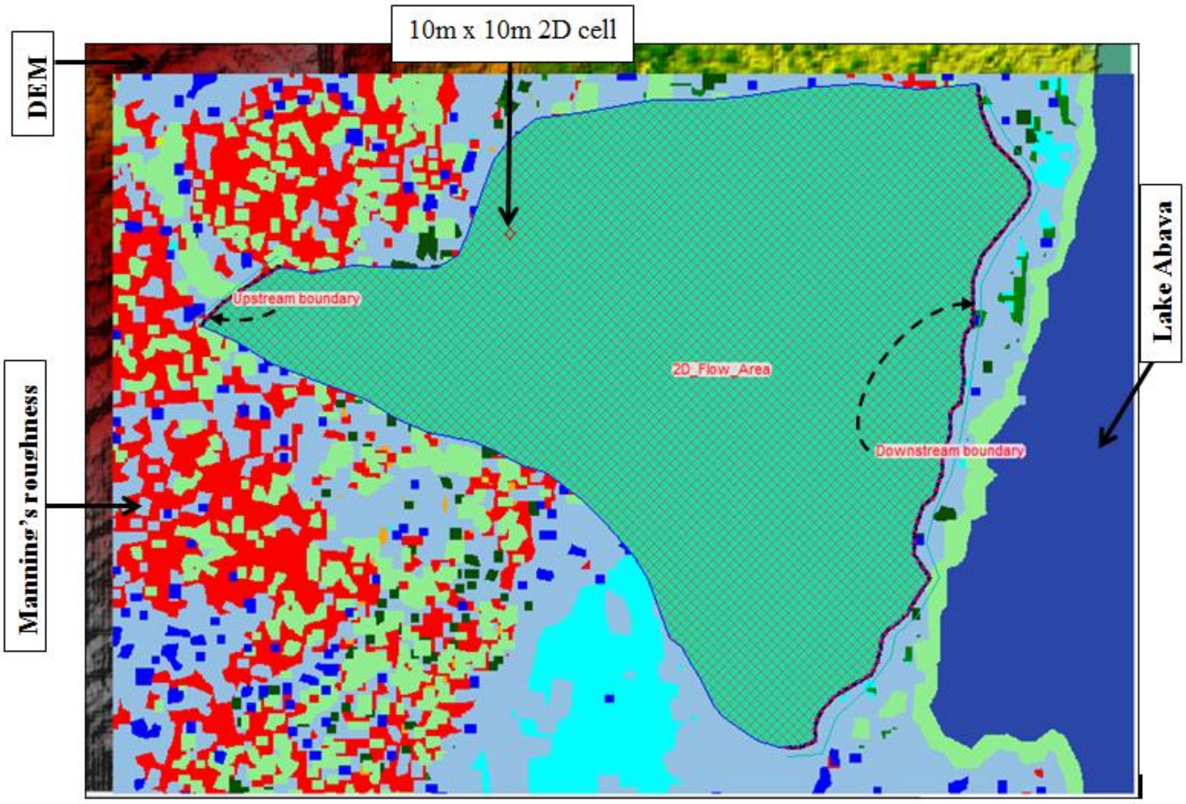

Figure 3.19 Map of HEC-RAS 2D Flow Area

3.12.2. Flood Plain Delineation

To get the actual water depth in the river channel and the floodplain, the water surface must be overlaid on the topography. This can be done using RAS Mapper.

3.13. Flood Hazard map

Flood hazards are characterized in terms of flood probability, flood depth, flow velocity, water level rise rate, and other factors. Hazard dimensions can be characterized in terms of where, when, how long-lived and how much adjustment occurs. Flood managers dealing with such dimensions should understand the location, likelihood, persistence and magnitude of prospective hazards Management options then can be evaluated besides predictions on the dimensions adjustments resulted from applying these options. Generally, in flood impact assessments, flood damage and fatalities are considered first. To identify the potential danger or hazard associated with the flood, flood hazard maps will be derived taking into account the depth and velocity of the floodwaters. The combined effect of depth and velocity of flooding will be used as Flood hazard and mapped using GIS software.

3.14. Flood vulnerability map

The vulnerability of a system to flood events can be expressed with the following general equation (Balica, 2007, p 37). This equation is used in the present study to compute Flood Vulnerability Index (FVI).

FVI = Exposure Index* Susceptibility Index- Resilience Index

Any flood vulnerability analysis requires information regarding indicators, which can be specified in terms of exposure indicators (Xi), Susceptibility indicators (Xi) and Resilience Index. The collected data were arranged in increasing order that representing indicators in order to obtain Vulnerability Index values. Depending on their functional relationship the exposure and susceptibility index (I) were obtained using the following formula:
In this study, the socio-economic indicators are considered based on the data availability. This study adopted and modified the socio-economic indicators selected by Mishra & Sinha, (2020) to suit the conditions of the study area.

The flood depth and flood velocity are considered as the key factors in vulnerability mapping because the population density is the superset of the entire vulnerability indicator drivable from population census data whereas flood depth and flood velocity are the next factor. Finally, these datasets are processed in GIS to generate spatial maps which are afterward used for the flood vulnerability analysis. The flood vulnerability map is produced by integrating these maps to a single whole using GIS analysis.

Urban areas are densely populated, which makes them vulnerable to flood impacts. These areas are vulnerable to floods because of three important reasons: exposure, susceptibility and resilience. That means the vulnerability of each area is reflective of the exposure and susceptibility and the resilience of that area to acclimate from the effects of those conditions (Meulen, 2012). Exposure is the scope that human Settlements and people lives are positioned in flood risk area (UNDP/BCPR, 2004). Susceptibility is exposed factors in the system, which affects the probabilities of being harmed during floods (UNESCO-IHE, 2013). Resilience is adaptation capacity of each community to changes in hazardous area by modifying itself to achieve an acceptable structural and functional level (Galderisi, 2005).

Many authors agree that vulnerability is a function of exposure, susceptibility and resilience (Cardona 2013; Smit and Wandel 2006; Balica et al. 2012; Balica 2007; IPCC 2001). Therefore, the general formula for computation of FVI demands categorizing the indicators as [exposure (E), susceptibility (S) and resilience (R)]. Exposure represents values that are present at the location where floods can occur. These values can be human being, properties, infrastructure, cultural heritage, agricultural fields and the like. Though there are different working definitions of exposure, the theme concept of exposure is defined as “the predisposition of a system or its elements to be affected by a food due to its location in the same area” (Balica 2007; Fuchs et al. 2011; Veenstra 2013).

Susceptibility is described as the potential of a system to be harmed by a hazardous event such as flooding, caused due to fragility, relative social or economic weaknesses or disadvantageous conditions (Cardona 2013; Balica 2007; Veenstra 2013). Resilience is the ability of a system to adjust to changes or threats, to avoid, mitigate or absorb potential damage, to cope with the consequences without loss or to even take advantage of opportunities (IPCC 2001; Pelling 2012; Veenstra 2013). Both exposure and susceptibility have a positive influence on vulnerability, and resilience has a negative influence on vulnerability

3.15. Flood Risk Analysis

Risk as a measure of danger can serve as a guideline to resolve the problem of controlling a set of circumstances that can disturb human habitats and change conditions for the functioning of society. This includes getting estimates of the levels of adversity for many different aspects. At the same time, risk also has a subjective constituent which can be measured with the help of formal methods of decision-making that take into account intuitive assessment of the situation and psychological norms of perception of the environment. Evaluation of the risk and subsequent damage requires interdisciplinary analysis of a vast amount of information. This requires the flood expert to deal with a huge, complex computer database relating to the many physical, natural, technical, economic, social and environmental aspects of flood risk. For this study, flood hazard and flood vulnerability will be developed, flood risk then developed by overlaying flood hazard map and food vulnerability map. According to Zimmermann, 2005) the conventional expression of risk is,

Risk=Hazard * Vulnerability

4. RESULT AND DISCUSSION

4.1. Flood inundation map

The flood inundation maps of the Kulifo River reveal that the river bank and floodplain areas are prone to significant flooding, especially during high return periods. One notable observation is that the 100-year flood of the Kulifo River results in an inundated area more than 1.3 times larger than that of the 10-year flood. This indicates a higher risk and severity of flooding during extreme events. The upstream floodplain of the Kulifo River exhibits steep sloped topography, which contributes to a lesser extent of inundation compared to the downstream floodplain. In contrast, the downstream parts of the floodplain, characterized by relatively flat to gentle slopes, experience more extensive inundation. The flat terrain facilitates the spreading of floodwaters, leading to larger areas being affected by flooding. Figure 4.1 illustrates that, for a 100-year return period, certain areas of Arba Minch city especially Limat area are likely to be impacted by floods. Arba Minch City serves as a focal point for floodwaters, and as a result, it is vulnerable to flooding events. Beyond Arba Minch City, the downstream areas comprise rural settlements, agricultural lands along the floodplain, and seasonal crops, which are all at risk of inundation. Finally, the floodwaters join Abaya Lake, further highlighting the interconnectedness of the river system and the potential consequences of flooding in this region.

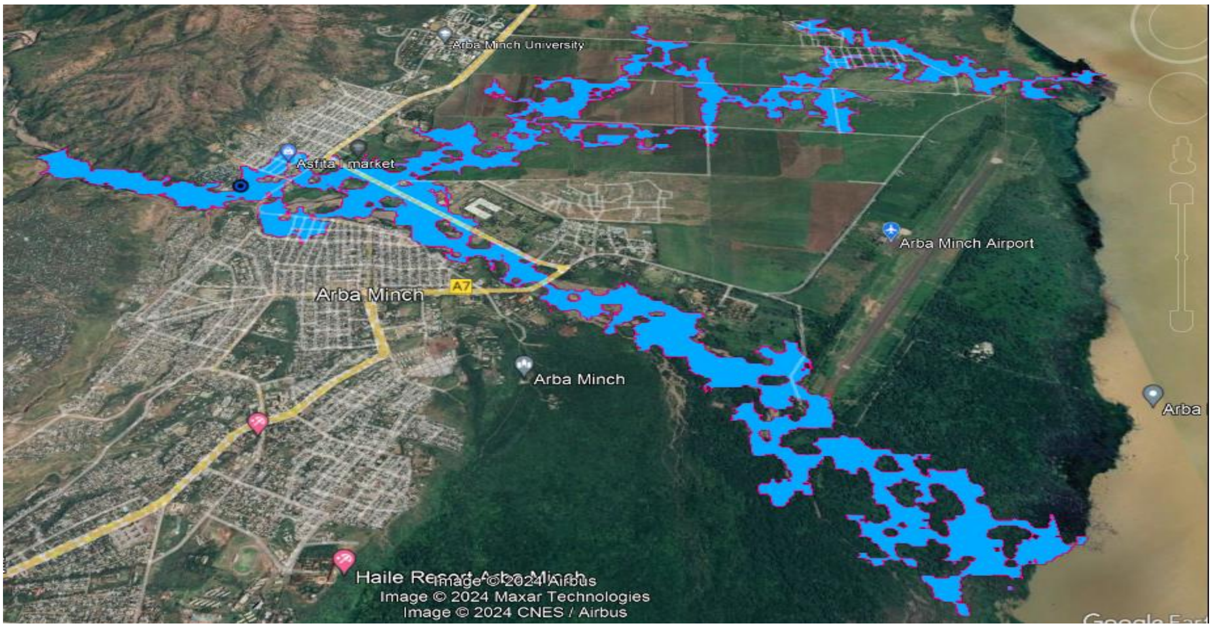

Figure 4.1: Kulifo River 100 years flood inundation area

The inundation extent map (Figure 4.2) provides a visual representation of the spatial coverage of floods for different return periods along the Kulifo River. It serves as a valuable tool for understanding the areas at risk and assists in formulating an emergency action plan. The map highlights the extent of flooding and helps in identifying the regions that are prone to inundation. Table 4.1 complements the inundation extent map by presenting the areal coverage of the flooded areas in hectares. This quantitative information allows for a more detailed analysis of the flood impact. By associating the inundation extent with specific numerical values, stakeholders can assess the magnitude of the risk and make informed decisions regarding mitigation measures and appropriate remedial actions. The inundation maps and associated data are crucial for the development of an effective emergency action plan. They provide a comprehensive understanding of the areas that are most vulnerable to flooding, enabling authorities to prioritize resource allocation and response efforts. The maps help identify critical infrastructure, residential areas, and other assets that require immediate attention and protection.

Table 3.1: Kulifo river flood inundation area for different return periods

Return period	Inundation area (ha)
10 years	346
25 years	404
50 years	435
100 years	459

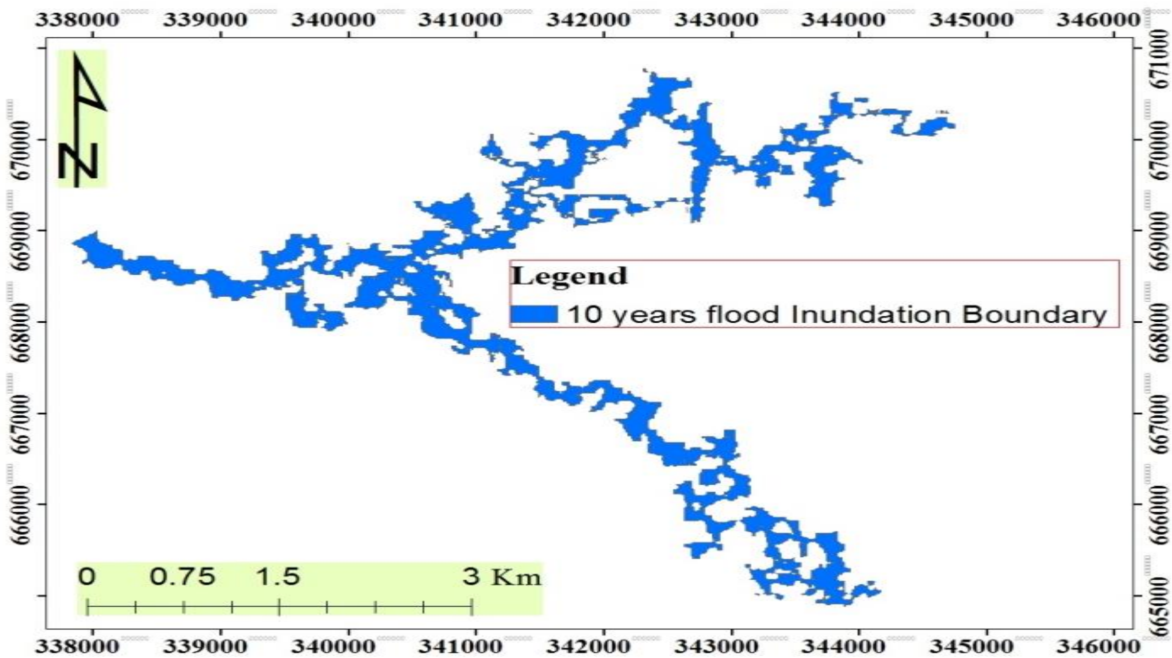
Legend
10 years flood Inundation Boundary
0 0.75 1.5 3 Km
338000 339000 340000 341000 342000 343000 344000 345000 346000
665000 666000 667000 668000 669000 670000 671000

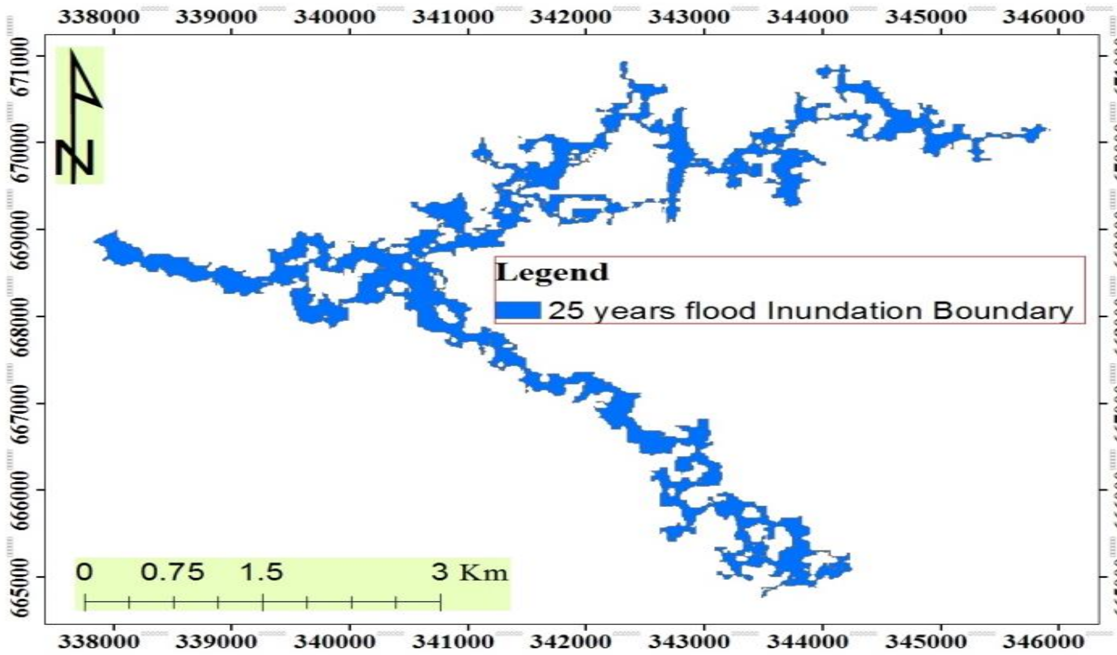
Legend
25 years flood Inundation Boundary
0 0.75 1.5 3 Km
338000 339000 340000 341000 342000 343000 344000 345000 346000
665000 666000 667000 668000 669000 670000 671000

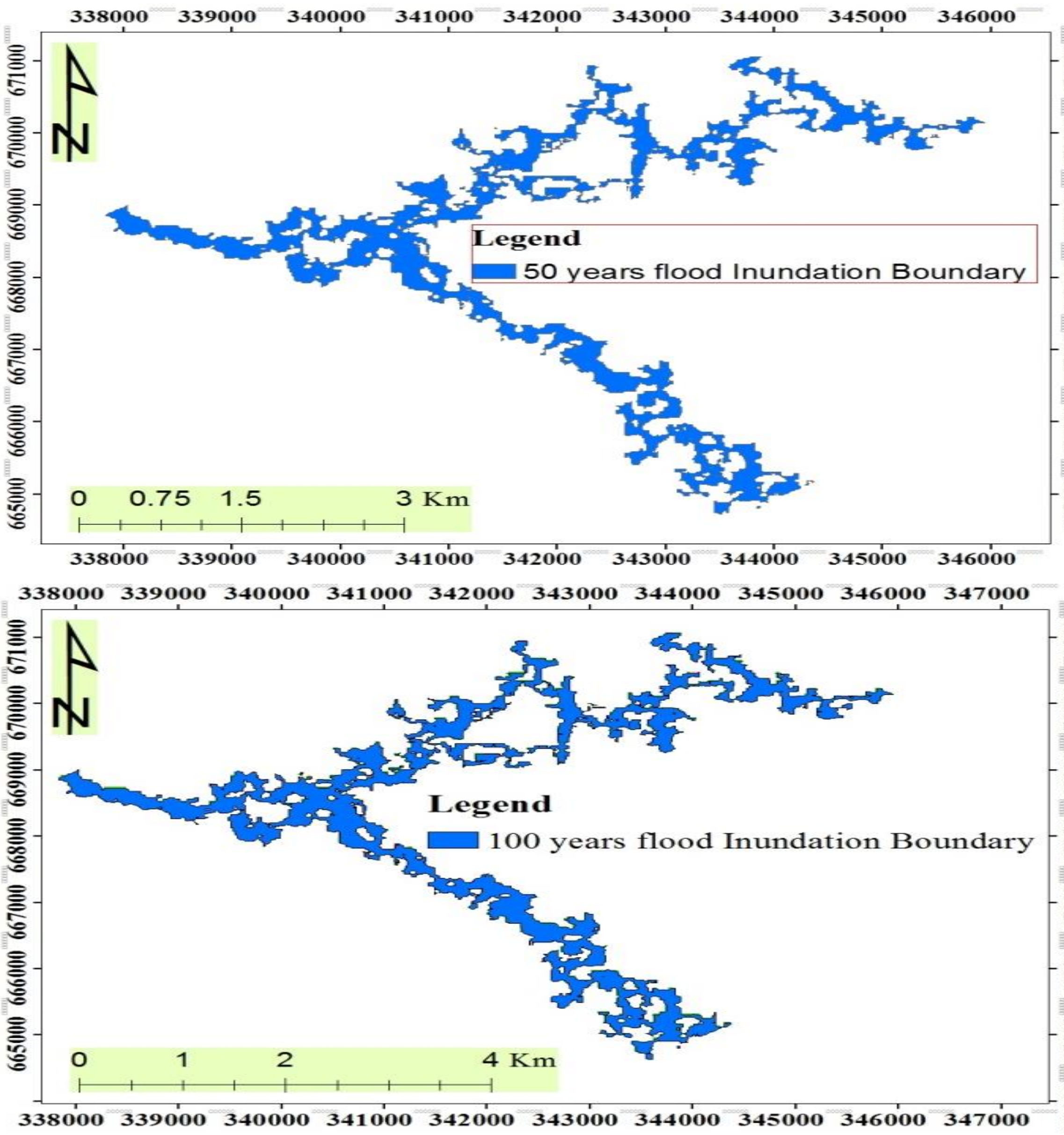

Figure 4.2: Floods areal extents of Kulifo River for different return period

4.2. Flood depth

The flood depth analysis reveals that two main areas along the Kulifo River experience high flood depths: the upstream part of the floodplain and a downstream area far away from the river, where irrigation land is located. For a 100-year return period, the analysis indicates that maximum flood depths of up to 15.2 meters are recorded. These depth values serve as indicators of the expected floodwater levels at different locations along the river. Figure 4.3, the flood depth map, visually represents the spatial distribution of flood depths in the floodplain. It is evident from the map that the maximum flood depth occurs near the Limat areas of Arba Minch city, situated upstream of the river channel. As we move downstream, the flood depths gradually decrease along the river course. This information is of significant value to emergency responders as it enables them to assess the severity of flooding and devise appropriate response strategies. By understanding the depth of flooding, responders can gauge the potential impact on infrastructure, communities, and overall safety in the affected area. This knowledge allows for better planning and allocation of resources during emergency situations, aiding in the mitigation of the adverse effects of flooding. Emergency responders can utilize the flood depth maps to identify areas where flood depths are most severe and prioritize their efforts accordingly. For instance, areas with higher flood depths may require immediate evacuation or additional emergency measures to ensure the safety of residents. Furthermore, the maps can assist in evaluating the potential damage to infrastructure, such as roads, bridges, and buildings, and support decision-making for implementing protective measures in vulnerable areas.

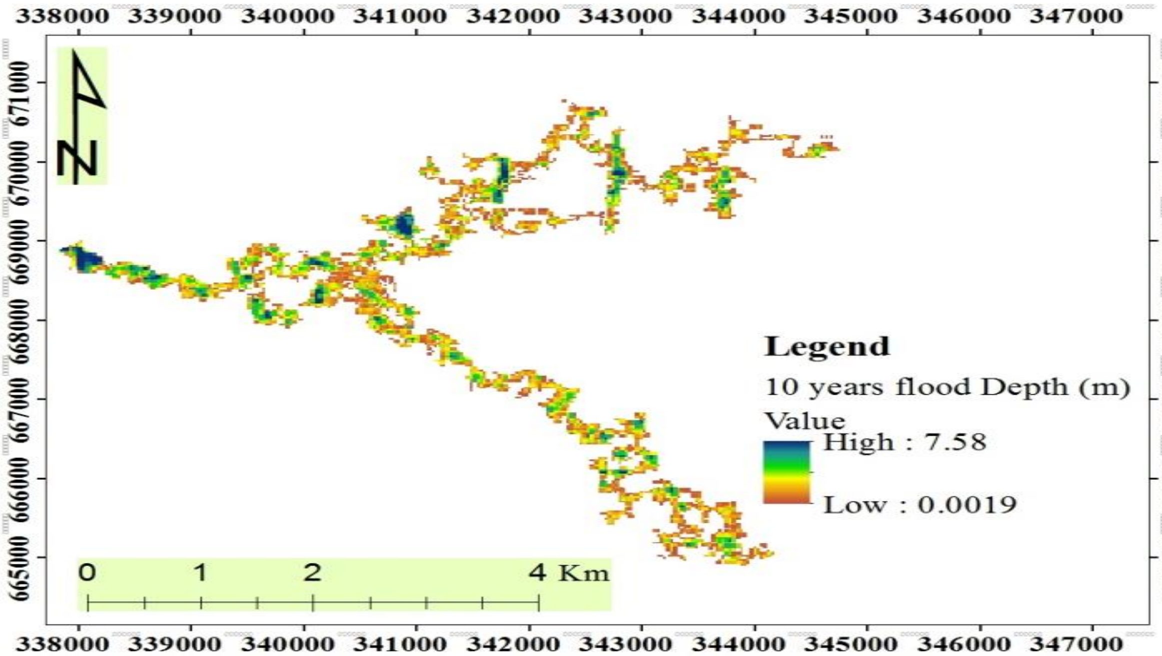
338000 339000 340000 341000 342000 343000 344000 345000 346000 347000
665000 666000 667000 668000 669000 670000 671000
N
Legend
10 years flood Depth (m)
Value
High : 7.58
Low : 0.0019
0 1 2 4 Km

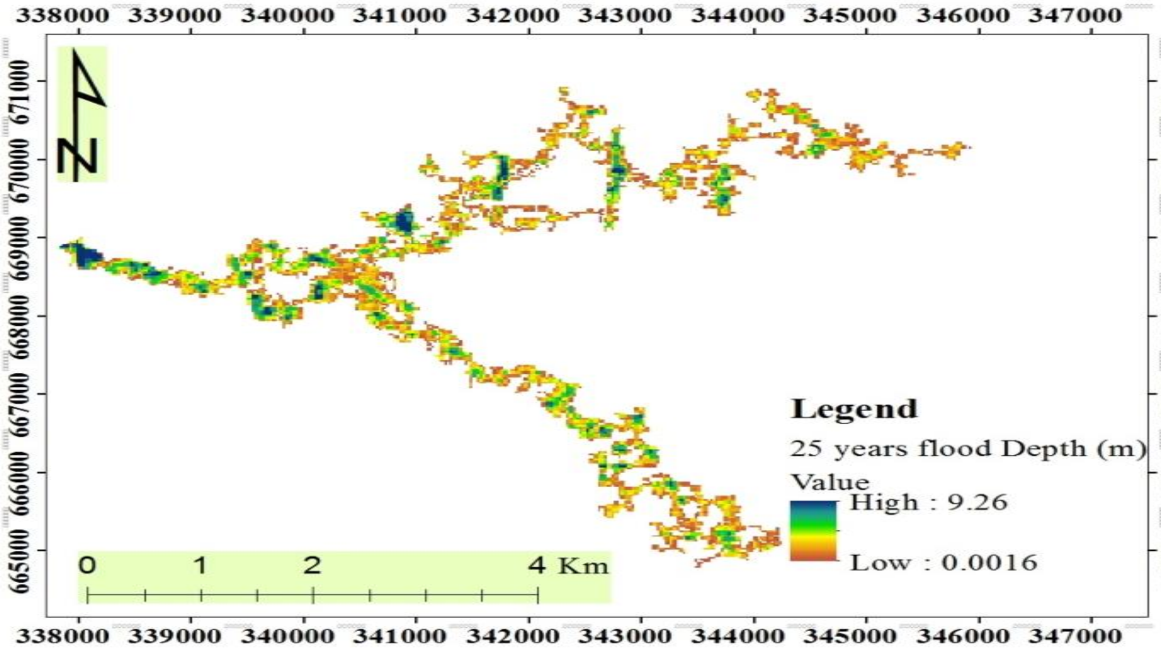
338000 339000 340000 341000 342000 343000 344000 345000 346000 347000
665000 666000 667000 668000 669000 670000 671000
N
Legend
25 years flood Depth (m)
Value
High : 9.26
Low : 0.0016
0 1 2 4 Km

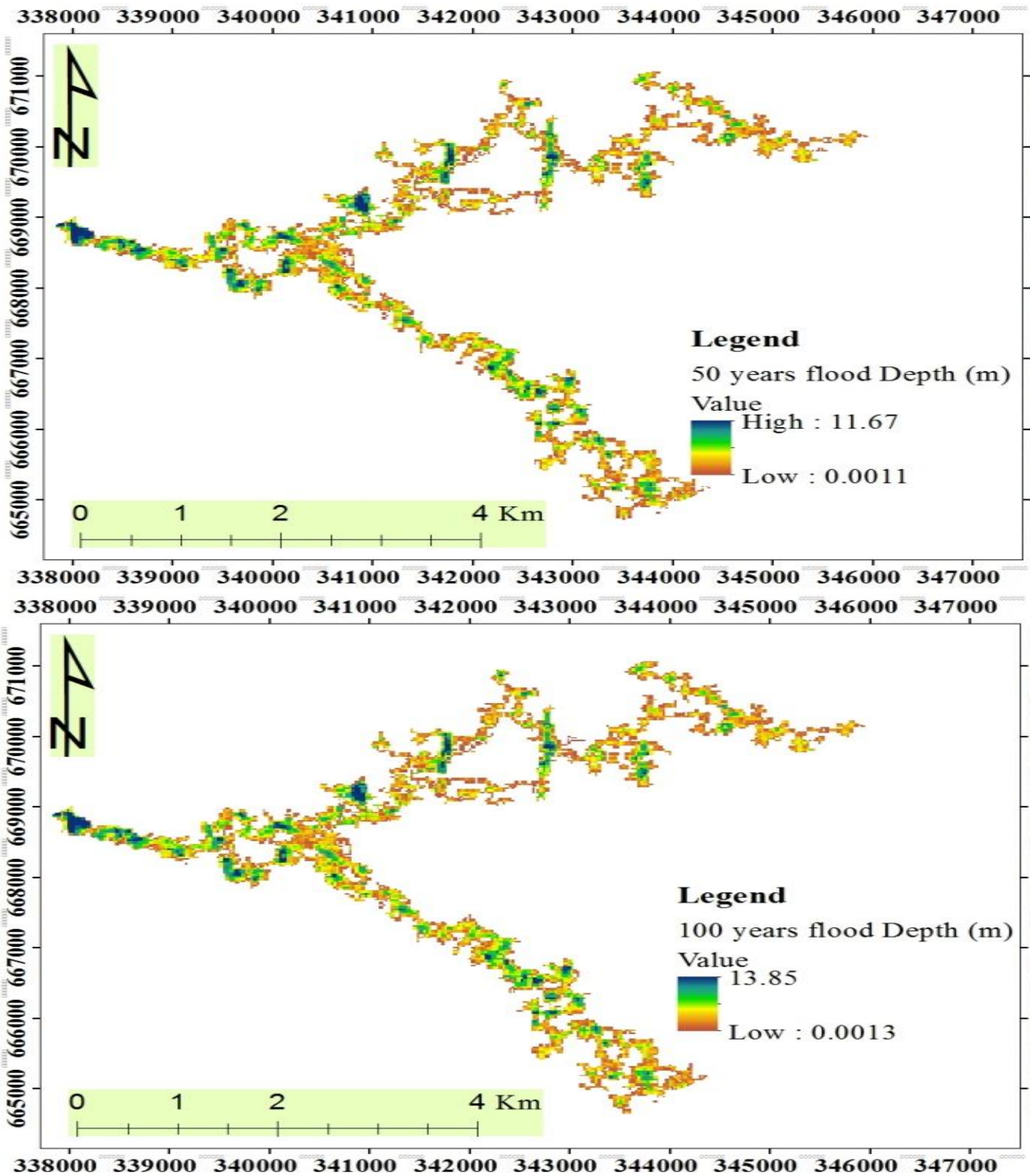

Figure 4.3: flood depth map of Kulifo River for different return periods

4.3. Flood Velocity

The velocities in the floodplain and river channels along the Kulifo River are generally moderate in most locations. However, in certain steeper areas of the floodplain, velocities exceed 2m/s, which may result in some erosion in those regions. It is important to note that during the 100-year flood event, velocities in the river channel can reach over 5.7 m/s. A typical cross-section of the Kulifo River is depicted in Figure 6-30, providing insights into the river's morphology and flow characteristics. Velocity maps play a crucial role in emergency response and engineering tasks. During rescue operations, emergency workers rely on velocity information to determine the speed at which water flows in specific areas. This assists them in assessing the risks and challenges they may encounter while performing rescue operations.

Furthermore, in the construction of flood defense structures, understanding the velocity of water is essential. By knowing the velocity, engineers can design and dimension flood defense structures appropriately, ensuring they can withstand the forces exerted by fast-flowing water. The velocity maps enable engineers to identify areas with high velocity and plan for the implementation of suitable measures to mitigate erosional effects and potential damage to infrastructure.

The knowledge of velocities is also valuable for assessing the potential impacts of flooding on the surrounding environment. High velocities can result in sediment transport, erosion of riverbanks, and changes in the river's course. By understanding the velocity patterns, environmental impacts can be evaluated, and appropriate measures can be taken to minimize adverse effects on the ecosystem and habitats.

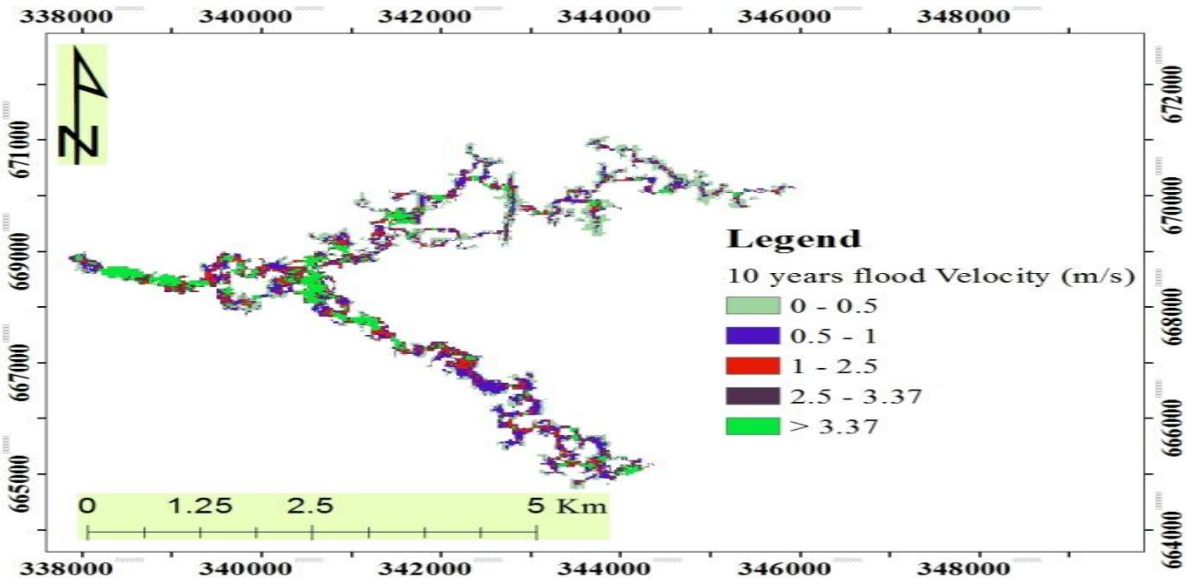
338000
340000
342000
344000
346000
348000
671000
669000
667000
665000
672000
670000
668000
666000
664000
Legend
10 years flood Velocity (m/s)
0 - 0.5
0.5 - 1
1 - 2.5
2.5 - 3.37
> 3.37
0
1.25
2.5
5 Km

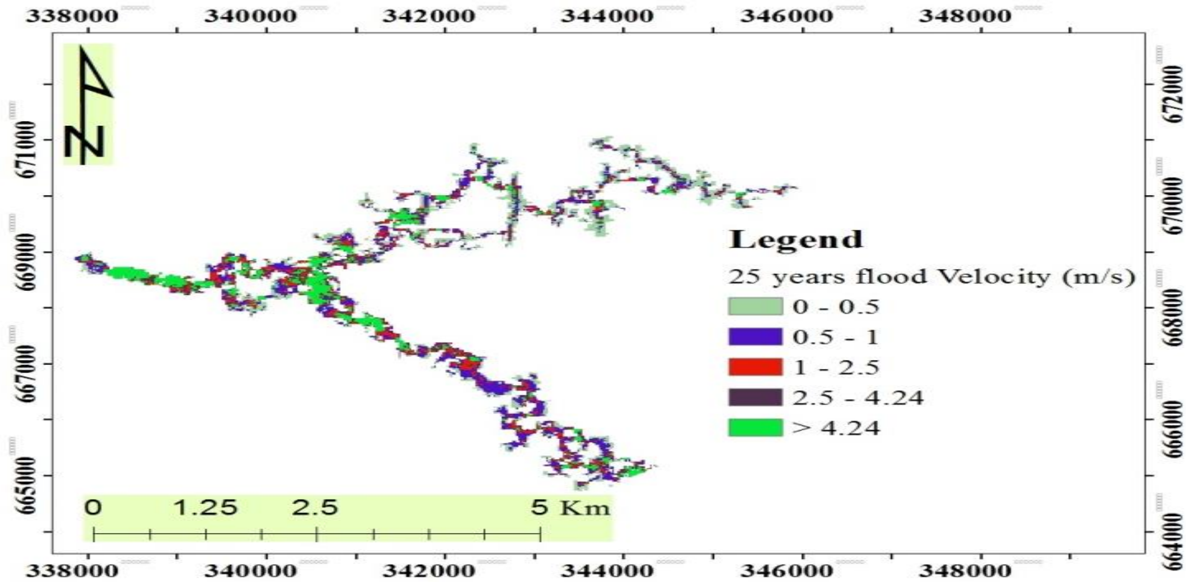
338000
340000
342000
344000
346000
348000
671000
669000
667000
665000
672000
670000
668000
666000
664000
Legend
25 years flood Velocity (m/s)
0 - 0.5
0.5 - 1
1 - 2.5
2.5 - 4.24
> 4.24
0
1.25
2.5
5 Km

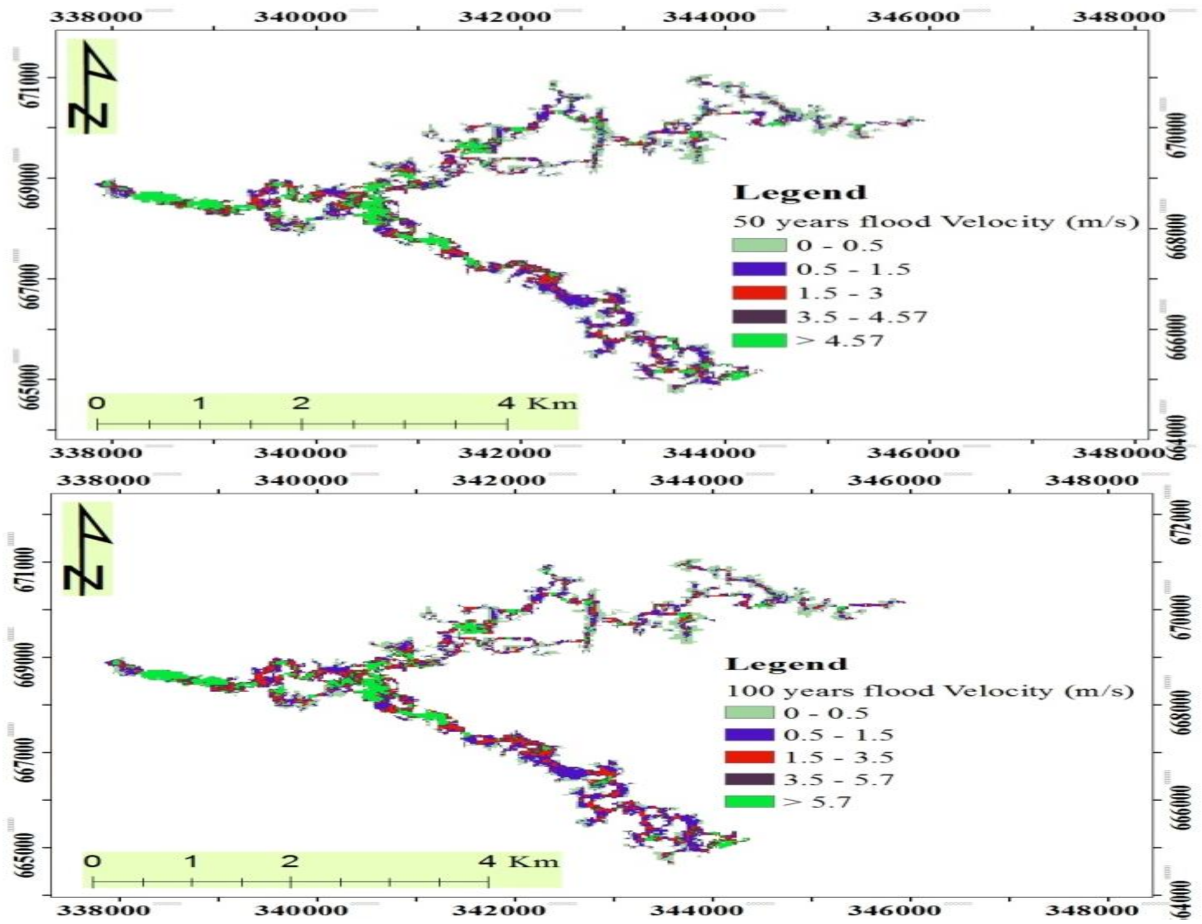

Figure 4.4: flood Velocity map of Kulifo River for different return periods

4.4. Flood Hazard Map

A flood hazard refers to the potential danger that arises from the occurrence of a flood event. The severity and impact of this hazard can vary depending on factors such as the intensity and duration of the flood, the characteristics of the affected area, and the vulnerability of the exposed population and infrastructure. In the context of the study, the depth-velocity hazard classification diagram used is based on the guidelines provided by the Federal Emergency Management Agency FEMA (2018). FEMA's guidelines serve as a framework for assessing flood hazards and categorizing them based on the parameters of flood depth and velocity. By considering the combined effects of these two factors, the depth-velocity product is determined, which helps in understanding the potential risks associated with floods. The study adopts the upper limits of the depth-velocity product for each hazard level as provided by FEMA's flood severity grid. The flood severity grid, depicted in Figure 4.5, visually represents the different hazard levels associated with specific combinations of flood depth and velocity. This grid serves as a reference tool for classifying flood hazards into different categories, such as low, moderate, high, and extreme. Each category represents a different level of risk and potential impact.

By utilizing the depth-velocity hazard classification diagram and referring to FEMA's flood severity grid, the study can assess and communicate the level of hazard associated with different flood scenarios. This information is valuable for emergency management and planning purposes. It helps stakeholders understand the potential risks and consequences of floods in specific areas, allowing them to make informed decisions regarding preparedness, response, and mitigation measures.

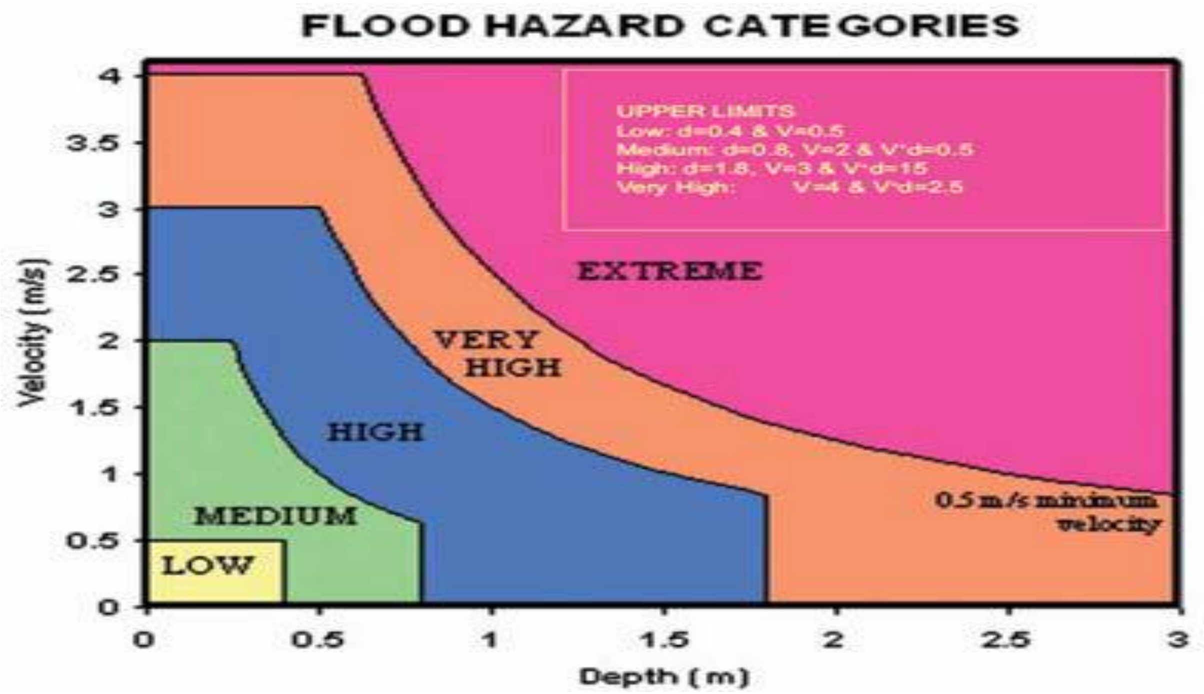

Figure 4.5: Flood hazard category according to FEMA Classification

The hazard classification scheme used in the study employs a scale ranging from 1 to 5 to assign a hazard index to different flood scenarios. This index represents the level of hazard associated with specific combinations of flood depth and velocity. A lower hazard index indicates a lower level of risk and potential impact, while a higher index signifies a greater hazard and potential for severe consequences. Table 4.2, presented in the study, outlines the hazard classification scheme in detail. The table specifies the criteria for flood depth and velocity ranges and assigns corresponding hazard levels. By comparing the observed flood depth and velocity values with the criteria in the table, the hazard level of a particular flood event can be determined. The specific criteria in Table 4.2 may vary depending on the study and the guidelines used.

However, it generally includes ranges of flood depth and velocity, as well as corresponding hazard levels. For instance, the criteria for the low hazard level may involve relatively shallow flood depths and lower velocity ranges. In contrast, the extreme hazard level would encompass higher flood depths and significantly greater velocities.

Table 4.2: Flood Depth and Velocity Severity Grid Categories source: FEMA (2018)

Flood index	Flood severity category	Depth *velocity range (m^2 /sec)	Description
1	Low hazard	≤ 0.2	Generally safe for vehicles, people and buildings.
2	Medium hazard	0.2 - 0.5	Unsafe for small vehicles.
3	High hazard	0.5 - 1.5	Unsafe for vehicles, children and elderly.
4	Very high hazard	1.5 - 2.5	Unsafe for vehicles and peoples
5	Extreme hazard	> 2.5	Unsafe for all vehicles, peoples, and buildings

Table 4.3 below, provides information on the area and percentage coverage of different hazard classes within the floodplain. The findings indicate that approximately 59% of the total flooded area falls under the extreme, very high, and high hazard categories. This implies that these areas are deemed unsafe for all individuals, including children, elderly people, vehicles, and structures vulnerable to flooding. The extreme and very high hazard areas are predominantly located in the upstream portion of the floodplain of Limat area. This region is characterized by a high population density, contributing to the increased hazard levels. These areas require particular attention and immediate action due to the significant risks associated with flooding. On the other hand, the high, medium, and low hazard areas are relatively distributed across the middle and downstream regions of the floodplain. These areas are characterized by varying slope gradients, with the middle section exhibiting steep gradients and the downstream section transitioning from steep to gentle gradients.

Table 4.3: Areal and percentage coverage of different hazard class

Hazard class	Area(ha)	% coverage's
Low	81	18%
Medium	106	23%
High	156	34%
Very high	91	20%
Extreme	25	5%

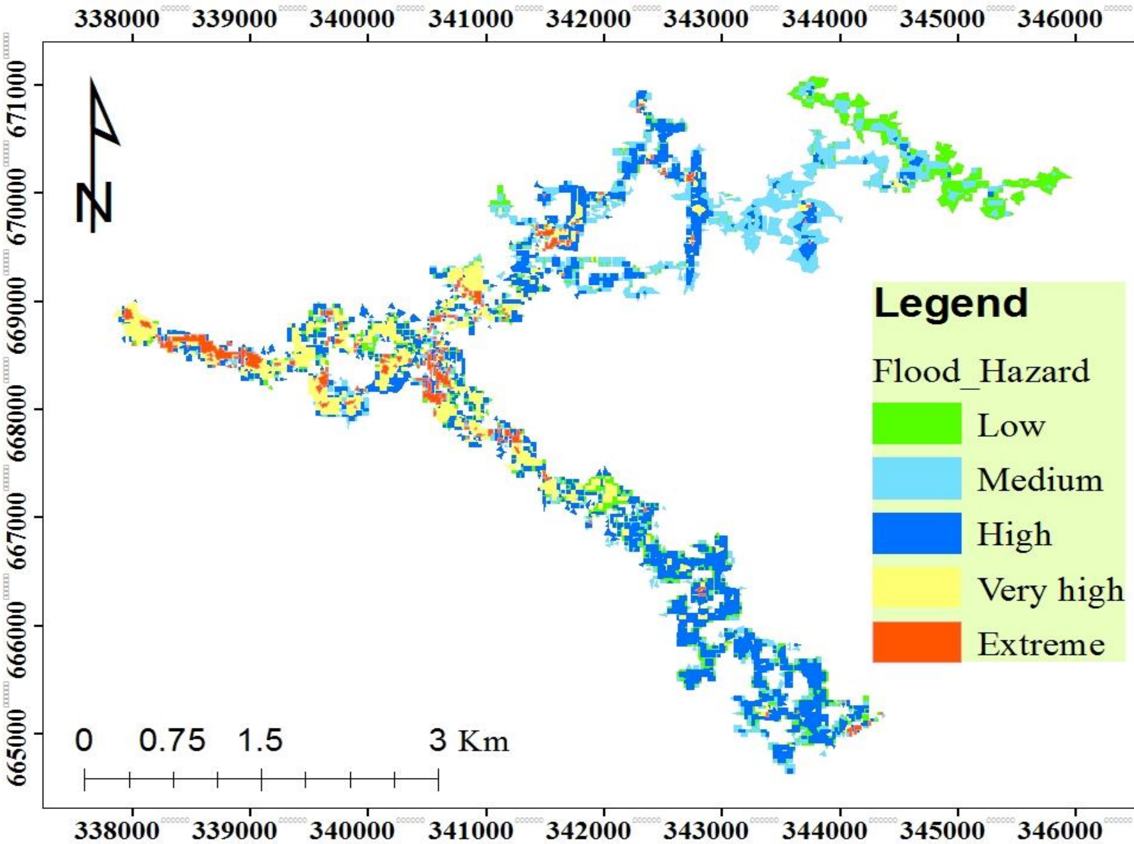

Figure 4.6: Flood hazard of Kulifo River for 100 years flood frequency

4.5. Flood Vulnerability map

In the study area, a flood vulnerability map provides an overview of the different vulnerability levels. The vulnerability levels are categorized into five distinct categories: very low, low, moderate, high, and very high. The map highlights areas that are classified as having a very low vulnerability level, indicating a relatively low risk of harm or damage from flooding. These areas typically possess favorable physical characteristics, such as higher elevation or natural barriers, and have well-developed infrastructure and effective flood mitigation measures in place. The low vulnerability areas are also at a relatively low risk of harm or damage, but they may have slightly fewer protective measures or face minor challenges related to flood management. Moderate vulnerability areas are characterized by a moderate level of risk and may experience some adverse impacts during flooding. These areas may have varying levels of preparedness and infrastructure development.

The high vulnerability areas face a higher risk of harm or damage during flood events. They may have significant physical vulnerabilities, such as being located in low-lying areas or near water bodies with a high flood risk. Additionally, these areas may have limited or inadequate flood protection measures, making them more susceptible to flood-related impacts. The very high vulnerability areas are at the highest risk of harm or damage during floods. These areas often have multiple vulnerabilities, including a combination of physical, socioeconomic, and infrastructure-related factors that increase their susceptibility. They may be located in flood-prone zones with limited capacity for flood control or have populations with limited resources and inadequate access to early warning systems or emergency services.

The flood vulnerability map presented in Figure 4.6 is crucial for understanding and prioritizing areas that require targeted interventions and investments in flood risk reduction and resilience-building measures. It helps decision-makers, emergency management agencies, and other stakeholders identify areas that need immediate attention and allocate resources effectively to enhance preparedness, response, and recovery efforts.

Table 4.4: Areal and percentage coverage for different flood vulnerability levels

Vulnerability Levels	Area (ha)	% coverage
Very low	128.8	28%
Low	118.8	27%
Moderate	93.8	20%
High	74.8	16%
Very high	42.8	9%

Table 4.4 and Figure 4.7 provide important insights into the distribution of vulnerability levels across the flooded area. The very high and high vulnerability levels cover approximately 25% of the flooded area and are primarily characterized by urban regions within the Limat area. These urban regions exhibit several factors that contribute to their heightened vulnerability to flooding. These factors include high population density, gentle slopes, high flood depths, and high flood velocities. The combination of these factors amplifies the potential for harm and damage during flood events. High population density increases the number of people and properties at risk, while gentle slopes allow floodwaters to spread over a larger area. The presence of high flood depths and velocities further exacerbates the potential impacts, as deeper and faster-moving water can cause more extensive damage to infrastructure and pose a greater threat to human lives. The moderate vulnerability level covers approximately 20% of the flooded area. These areas exhibit characteristics such as medium-density urban dwellings, scattered rural populations, and intensive agriculture. The moderate vulnerability level suggests a moderate level of risk and potential impacts during floods. While these areas may have some level of vulnerability, they typically have a mix of urban and rural characteristics, and the level of preparedness and infrastructure development may vary. The low and very low vulnerability classes encompass approximately 55% of the flooded area. These areas are characterized by agricultural lands, vegetation, lower rural population densities, and gentle to flat slopes. The low vulnerability class indicates a relatively lower risk of harm or damage during floods. These areas may have natural features that provide some level of protection, such as vegetation or flatter terrain, and they may have fewer built structures or less densely populated areas.

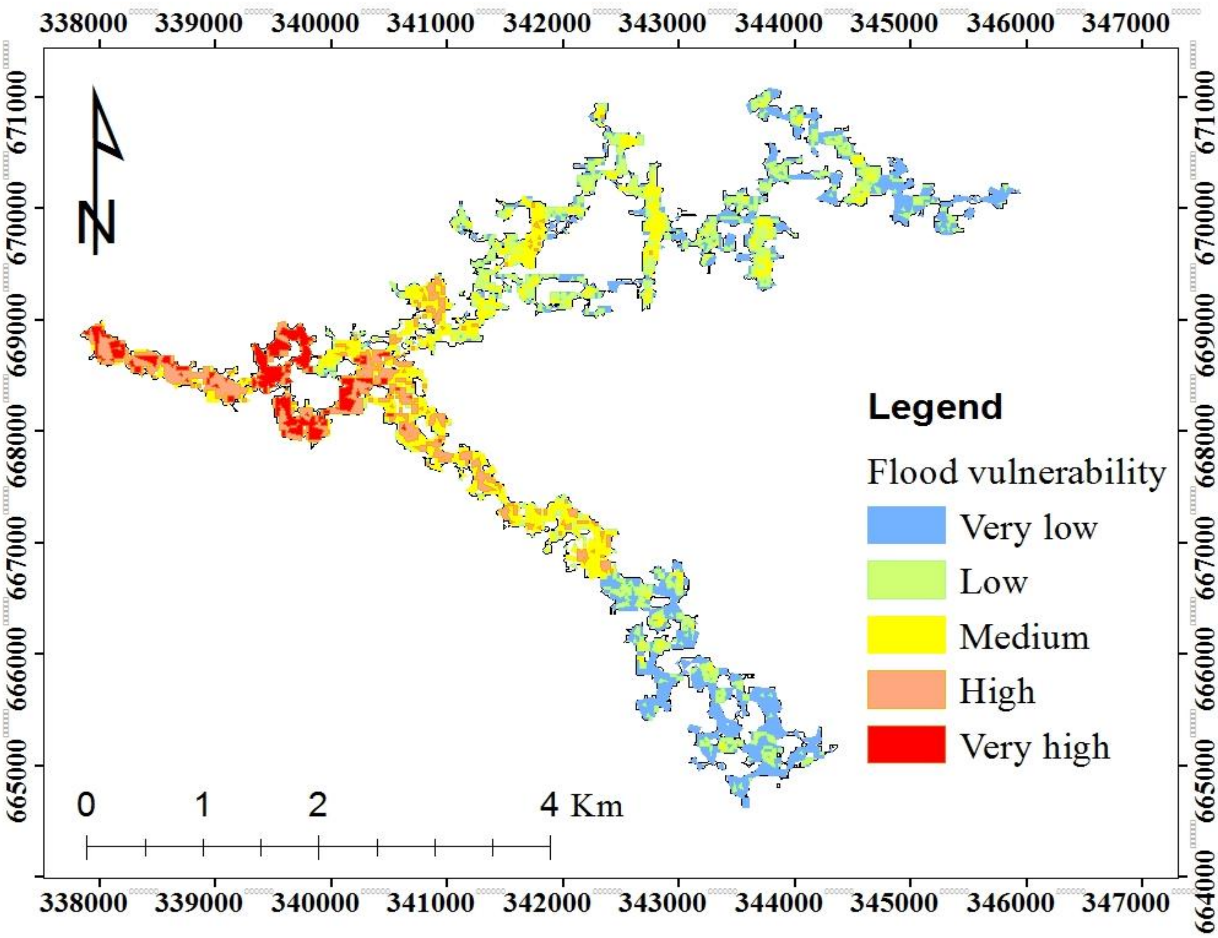

Figure 4.7: Flood Vulnerability of Kulifo River for 100 years flood frequency

4.6. Flood Risk map

In the context of the Kulifo River floodplain, the flood risk map provides a comprehensive understanding of the flood risk levels across the region. The map classifies the flood risk into five distinct levels, ranging from very low to very high risk. The flood risk map is developed by considering multiple factors. Firstly, hazards are evaluated, which involve analyzing flood-related parameters such as flood depth, velocity, and duration. These parameters provide insights into the likelihood and intensity of flood events. Secondly, vulnerability is assessed, taking into account the susceptibility and potential impacts of flooding on individuals, communities, infrastructure, and the environment. Vulnerability factors may include population density, urbanization, infrastructure quality, and socio-economic conditions. Areas with higher vulnerability are likely to experience more severe consequences during a flood event.

Lastly, exposure is considered, which refers to the presence of valuable assets or elements at risk within the floodplain. These assets may include residential and commercial buildings, critical infrastructure, agricultural lands, and environmentally sensitive areas. The degree of exposure contributes to the level of potential damage and impacts that may occur during a flood event. By integrating these factors, the flood risk map provides a spatial representation of the varying levels of flood risk across the Kulifo River floodplain. The map highlights areas with very low risk, indicating a minimal likelihood of flooding and limited potential consequences. Conversely, areas with very high risk are characterized by a high probability of flooding and significant potential for adverse impacts.

The flood risk map serves as a valuable tool for decision-makers, urban planners, emergency management agencies, and other stakeholders. It helps them identify areas that require specific attention and prioritize actions for flood risk reduction and management. For example, areas with high or very high flood risk may necessitate the implementation of structural measures like levees or flood barriers, along with non-structural measures such as land-use planning and early warning systems. In contrast, areas with lower flood risk levels may focus on strategies to maintain their resilience and preparedness.

Table 4.5: Areal and percentage coverage for different flood risk levels

Risk Level	Area (ha)	% coverage
Very low	99	22%
Low	140	31%
Moderate	71	15%
High	94	20%
Very high	55	12%

Figure 4.8, the flood risk map, provides important insights into the distribution of flood risk within the flooded area. Approximately 32% of the flooded area is categorized as very high and high risk, primarily concentrated in the densely populated Limat area. The presence of these high-risk zones in urban settlements underscores the vulnerability of these areas to flooding.

Around 53% of the flooded area is classified as low and very low risk. These regions are situated downstream of the floodplain and consist of agricultural lands, sparse rural populations and natural vegetation. While these areas are less susceptible to flooding compared to the high-risk zones, it is important to maintain awareness and preparedness. Even low-risk zones can be affected by extreme flood events, and it is necessary to have measures in place to handle such situations and minimize potential impacts. Approximately 15% of the flooded area is categorized as moderate risk. These areas include parts of the upstream region, the middle and downstream where flat slopes contribute to increased flood risk, as well as urban settlers within Arba Minch city. The moderate-risk zones require attention and targeted interventions to reduce the potential impacts of flooding on the affected communities and infrastructure. This may involve implementing flood protection measures, improving drainage systems, and raising awareness among residents about flood risks and appropriate actions to take during flood events.

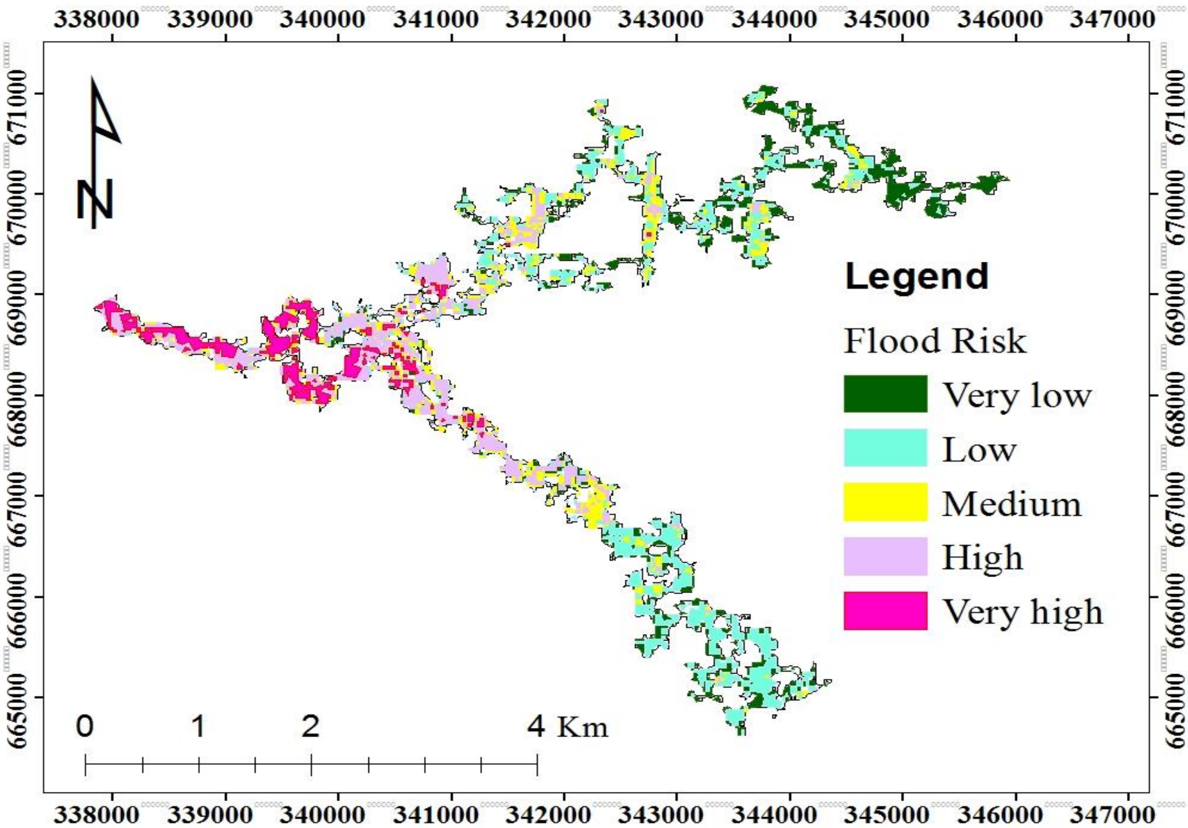

Figure 4.8: Flood Risk of Kulifo River for 100 years flood frequency

5. CONCLUSIONS AND RECOMMENDATIONS

5.1. Conclusions

The study focused on the evaluation of potential flood hazards, vulnerability levels, and flood risk across the Kulifo River floodplain. To achieve this, advanced hydrological and hydraulic modeling techniques was used, aiming to provide valuable information for effective flood management, land-use planning, and disaster risk reduction strategies.

Data collection was a crucial initial step in the study. Rainfall data was obtained from the National Meteorological Agency (NMA), while stream flow data was collected from the Ministry of Water & Energy, Ethiopia (MoWE). The Digital Elevation Model (DEM) used in the study was acquired from the Alaska Satellite Facility (ASF), and land use/land cover data were obtained from USGS. Two key models were utilized in the study: HEC-HMS (Hydrologic Engineering Center's Hydrologic Modeling System) and HEC-RAS (Hydrologic Engineering Center's River Analysis System). The HEC-HMS model was employed to generate inflow design floods for different return periods. Historical rainfall and stream flow data were analyzed to determine the magnitude and frequency of floods in the Kulifo River basin. The model was calibrated and validated using observed stream flow data to ensure accuracy and reliability in simulating flood hydrographs. The calibration and validation process yielded very good performance indicators, including Nash-Sutcliffe Efficiency (NSE), Percent Bias (PBIAS), coefficient of determination (R^2), and Relative Mean Square Error (RMSE).

The flood hydrographs for different return periods were generated after model calibration and validation in HEC-HMS model and then used as inputs for the HEC-RAS model. HEC-RAS is a widely used hydraulic model that considers 2D flow areas and roughness coefficients to simulate the hydraulic behavior of the Kulifo River during flood events. The outputs of the HEC-RAS model were integrated with Geographic Information System (GIS) software to map flood inundation areas. By overlaying the simulated flood extents on topographic maps, a detailed flood inundation map was generated, visually representing the areas prone to flooding along the Kulifo River. The flood inundation maps provided valuable information about the spatial extent and severity of flooding for different return periods. Notably, they revealed significant flood-prone areas along the Kulifo River, with the size of the inundated area increasing significantly with higher return periods. The maximum recorded flood depth and velocities during the 100-year return period indicated the potential for catastrophic flooding.

Based on the flood inundation maps, a flood hazard map was developed. This map classified the flood-prone areas into hazard categories, ranging from extreme to low. The map highlighted that approximately 59% of the flooded area fell under extreme, very high, and high hazard categories, indicating areas unsafe for individuals, vehicles, and vulnerable structures. The upstream portion of the floodplain, particularly the Limat area, exhibited the highest hazard levels due to its gentle slope gradient and high population density.

To assess flood vulnerability, various indicators contributing to susceptibility were considered, including flood depth, velocity, duration, slope, land use/land cover, and population density. By analyzing these factors, vulnerability levels were classified into five classes: very low, low, moderate, high, and very high. The study found that approximately 20% of the flooded area had very high and high vulnerability, primarily consisting of urban regions with high population density, gentle slopes, high flood depths, and velocities. Moderate vulnerability covered around 25% of the flooded area, including medium-density urban dwellings, scattered rural populations, and intensive agriculture. The remaining 55% of the flooded area had low and very low vulnerability, characterized by agricultural lands, vegetation, lower rural population densities, and flat to gentle sloping terrain.

Finally, the flood hazard and vulnerability information were combined to develop a comprehensive flood risk map. This map provided a clear understanding of the different risk levels across the Kulifo River floodplain, classified into five categories: very low, low, moderate, high, and very high. Approximately 32% of the flooded area fell under the very high and high-risk categories, primarily concentrated in the densely populated Limat area of Arba Minch city. These high-risk zones emphasized the vulnerability of urban settlements to flooding, necessitating the implementation of effective mitigation measures and the development of robust emergency response plans. Approximately 53% of the flooded area was classified as low and very low risk, consisting of downstream agricultural lands, sparse rural populations, and natural vegetation. While these areas are at lower risk, it is still essential to maintain preparedness measures to minimize potential impacts. Around 15% of the flooded area fell under the moderate risk category, requiring targeted interventions to reduce flood impacts on communities and infrastructure.

The flood risk map served as a valuable tool for decision-making and planning processes. It provided policymakers, urban planners, and disaster management agencies with crucial information to prioritize and allocate resources for flood risk reduction measures. By identifying high-risk areas, the map guided the implementation of structural and non-structural measures such as the construction of flood protection infrastructure, land-use planning regulations, early warning systems, and community-based disaster preparedness initiatives. The map also facilitated the identification of areas suitable for floodplain zoning and the relocation of vulnerable populations to safer areas. Overall, the study's findings and the comprehensive flood risk map provided a foundation for informed decision-making, enabling stakeholders to develop effective strategies for flood management, land-use planning, and disaster risk reduction in the Kulifo River floodplain.

5.2. Recommendations

Based on the findings of the study, several recommendations can be made to address the risks and vulnerabilities associated with flooding in the Kulifo River floodplain:

Implement flood protection infrastructure: Constructing and maintaining flood protection infrastructure such as levees, flood walls, and embankments can help mitigate the impacts of flooding. These structures can redirect floodwaters, reduce the extent of inundation, and protect vulnerable areas, particularly in high-risk zones identified in the flood risk map.

Land-use planning and zoning regulations: Develop and enforce land-use planning and zoning regulations that restrict or prohibit construction in high-risk flood areas. This can help prevent further development in flood-prone regions and protect lives and properties from potential flood damage. Encourage the relocation of vulnerable populations and critical infrastructure to safer areas.

Improve early warning systems: Enhance early warning systems to provide timely and accurate flood forecasts and warnings to at-risk communities. This can include installing real-time monitoring stations, improving communication networks, and implementing efficient dissemination mechanisms to ensure that people receive timely evacuation notices and can take necessary precautions.

Develop community-based disaster preparedness initiatives: Engage with local communities and empower them to be more resilient in the face of flooding. This can involve conducting awareness campaigns, training community members in emergency response and evacuation procedures, and establishing community-driven initiatives such as local flood response teams and community evacuation centers.

Strengthen emergency response and coordination: Enhance coordination among relevant government agencies, emergency services, and stakeholders involved in flood response and recovery. Develop comprehensive emergency response plans that outline roles, responsibilities, and procedures for different agencies and organizations. Conduct regular drills and exercises to test the effectiveness of response mechanisms.

Enhance drainage and storm water management: Improve the drainage infrastructure and storm water management systems to effectively handle excessive rainfall and reduce the risk of urban flooding. This can include constructing and maintaining storm water channels, improving culverts and bridges, and implementing sustainable drainage systems (such as rainwater harvesting and permeable pavements) to manage surface water runoff.

Promote ecosystem-based approaches: Encourage the conservation and restoration of natural ecosystems such as wetlands and floodplains. These ecosystems can act as natural buffers, absorbing floodwaters, reducing flood velocities, and providing valuable ecological services. Incorporate ecosystem-based approaches into flood management strategies to enhance resilience and reduce the impacts of flooding.

Conduct regular monitoring and updates: Continuously monitor and update flood hazard and vulnerability maps to reflect changes in land use, climate patterns, and population dynamics. Regular monitoring allows for the identification of emerging risks and vulnerabilities, enabling timely adjustments and improvements in flood risk reduction strategies.

Foster regional cooperation and knowledge exchange: Collaborate with neighboring regions, national institutions, and international organizations to share experiences, best practices, and technical expertise in flood management. Establish regional cooperation frameworks for coordinated flood risk reduction efforts, information sharing, and capacity building initiatives.

Promote insurance and financial mechanisms: Encourage the adoption of flood insurance schemes and financial mechanisms that provide compensation and support for individuals, businesses, and communities affected by floods. This can help reduce the economic burden and facilitate recovery efforts after flood events.

REFERENCE

A.I. Krylova, E. A. (2017). Num. Model. In Atmosphere, The derivation of the Saint– Venant equations. Bull. Nov. Comp. Center: NCC Publisher.

Alcántara, M. A. (2014). Channel Adjustment and Channel-Floodplain Sediment Exchange in the Root River, Southeastern Minnesota. Utah State University: Graduate Thesis Studies.

Ali, M. M. (2015). Fundamentals of Computational Hydraulics. BUET, Dhaka, Bangladesh. Bangladesh University of Engineering Technology.

Aliy, T. (2018). Flood Inundation Mapping with Integration of GIS and Hydraulic Model (HEC- RAS) for Early Warning in Dechatu Catchment, Dire Dawa City, Eastern Ethiopia. Adama, Ethiopia: Adama Science and Technology University.

ARORA, K. (2009). Irrigation, Water Power and Water Resources Engineering. KOTA (Raj): A.K. Jain.

Arora, K. R. (2003). Soil Mechanics and Foundation Engineering. KOTA (Raj): A, K.Jain.

Ayele Elias Gebeyehu, Z. C. (2019). Assessment and Mapping of Land Use Change by Remote Sensing and GIS: A Case Study of Abaya Chamo Sub-basin, Ethiopia. Nature Environment and Pollution Technology an International Quarterly Scientific Journal, 500-501.

Ayka, A. (2008). Hydrological Models Comparison for Estimation of Floods in the Abaya-Chamo Sub-Basin. Addis Ababa University: M.Sc. Thesis.

Bravard, J. P., & Petit, F. (2009). Geomorphology of Streams and Rivers. In Encyclopedia of Inland Waters (pp. 387–395). Elsevier. https://doi.org/10.1016/B978- 012370626-3.00043-

Chanson, H. (2004). The hydraulics of open channel flow (2nd ed). Butterworth- Heinemann.

CHOW, V. T. (1959). Open-Channel Hydraulics. New York: McGraw-Hill Book Company,

Dadi, M. (2023). Applied Hydrology Course Materials. Hawassa University.

Dahl, T., Heath, R., Gibson, S., & Nygaard, C. (2019). HEC-RAS unsteady flow and sediment model of the Mississippi River: Tarbert Landing to the Gulf. Engineer Research and Development Center (U.S.). https://doi.org/10.21079/11681/31782

David L. Rosgen, P. (1996). A Stream Channel Stability Assessment Methodology. Wildland Hydrology Pagosa Springs. CO 81147.

Davidian, J. (1984). Computation of Water-Surface Profiles in Open Channels. Applications of Hydraulics.

Genet Markos (2020). Application of Hydro system Models for Flood Extent Mapping Including Levee and Weir Breach Analysis for Kulfo River Flood plain in Arba Minch Town, Ethiopia, Arba Minch University: M.Sc. Thesis.

Girma, N. T., & Horlacher, H.-B. (2004). Investigation of Performance of Sediment Transport Formulas in Natural Rivers Based on Measured Data in Kulfo River Southern Ethiopia. 4, 8.

Janicke, S. (2002). Stream Channel and Floodplain Erosion. Report No. RR18.

Kalikidan Mekon, Fikadu Berisha, Daraje Baye, Ergo Fentaw, & Debebe Ernamo and Mustariya Jemal. (2016). Flood Modeling and Frequency Analysis in the Case of Kulfo Watershed Abaya-Chamo Basin. Arba Minch University.

Leopold, L. B. (1970). An Improved Method for Size Distribution of Stream Bed Gravel. U. S. Geological Survey.

LIANG, C. (2015). Spatial Simulation Based Riverbank Slope Instability and Susceptibility Assessment in the Lower River Murray. The University of Adelaide.

Mengesha, F. (2008). Channel Stability Analysis-The Case of Borkena River (Ethiopia). Addis Ababa University. M.Sc. Thesis.

Merwade, S. D. (2018). 1D HEC-RAS Simulation and Flood Inundation Mapping in HEC-RAS. Purdue University: Lyles School of Civil Engineering.

Mesekerem Tsegaye (2015). Kulfo River Channel Stability Analysis, Southern Ethiopia. Arba Minch University: MSc. Thesis.

Olsen, D. S. (1993). Assessing stream channel stability thresholds. The University of Montana.
125 rokaj, S., Corti, B., Giovannini, A., Cancelliere, G., Biotto, D., & Radice, A. (2021). Flood Mitigation Measure and Water Storage in East Africa: An Analysis for the Rio Muaguide, Mozambique. Hydrology, 8(2), 92.https://doi.org/10.3390/hydrology 802009

Sewnetu, G. (2020). Channel Stability Assessment and Stabilization Measure of Mersa River, Ethiopia. Addis Ababa University: M.Sc. Thesis.

Shen, H. W., Schumm, S. A., & Collins, F. (n.d.-a). Stability of Stream Channel Patterns7

Subramanian, K. (2008). Engineering Hydrology. Indian Institute of Technology Kanpur: Tate Mc Graw-Hill.

Tamiru, B. (2006). Flood Mapping and Mitigation Measures for Lower Kulfo Reach. Arba Minch University: M.SC. Thesis.

U.S Army Corps of Engineers. (2000). Design and Construction of Levees Manual. Washington: Department of the Army U.S.

U.S, F. H. (2013). Urban Drainage Design Manual. U.S: Hydraulic Engineering Circular No.22.

U.S. Army Corps of Engineers. Hydrologic Engineering Center (2021). HEC-RAS River Analysis System. User's Manual. USACE: Hydrologic Engineering Center.

US Army Corps of Engineers. Hydrologic Engineering Center (2016). HEC-RAS River Analysis System User's Manual. US: Institute for Water Resource's Hydrologic Engineering Center (HEC).

Wankie, T. (2015). Assessment of Hydrological Impact of Land-Use Change in Kulfo River Watershed Using SWAT. Arba Minch University: M.SC. Thesis.

Yirgu, T., Yihunie, Y., Assele, A., & Wogayehu, T. (2020). Land Use/Land Cover Dynamics and its Environmental Impacts in Kulfo Watershed, Gamo Highlands, Southwestern Ethiopia. Journal of Geography, Environment and Earth Science International, 1–11. https://doi.org/10.9734/jgeesi/2020/v24i230197

APPENDIX

Apendix A: Maximum Annual Rainfall of Kulifo Catchment

S.No	**Year**	**Max Areal RF (mm)**
1	1988	56.45
2	1989	86.78
3	1990	47.3
4	1991	64.99
5	1992	85.7
6	1993	84.25
7	1994	45.74
8	1995	48.99
9	1996	46.58
10	1997	82.09
11	1998	56.09
12	1999	90.63
13	2000	65.36
14	2001	57.77
15	2002	48.87
16	2003	46.8
17	2004	38.8
18	2005	102.4
19	2006	66
20	2007	67.9
21	2008	80.8
22	2009	48.8
23	2010	71.5
24	2011	64.5
25	2012	59.9
26	2013	86.2
27	2014	37.8
28	2015	60.7
29	2016	57.7
30	2017	61.3
31	2018	49.74
32	2019	48
33	2020	68

Apendix B: Flood hydrographs for different return period

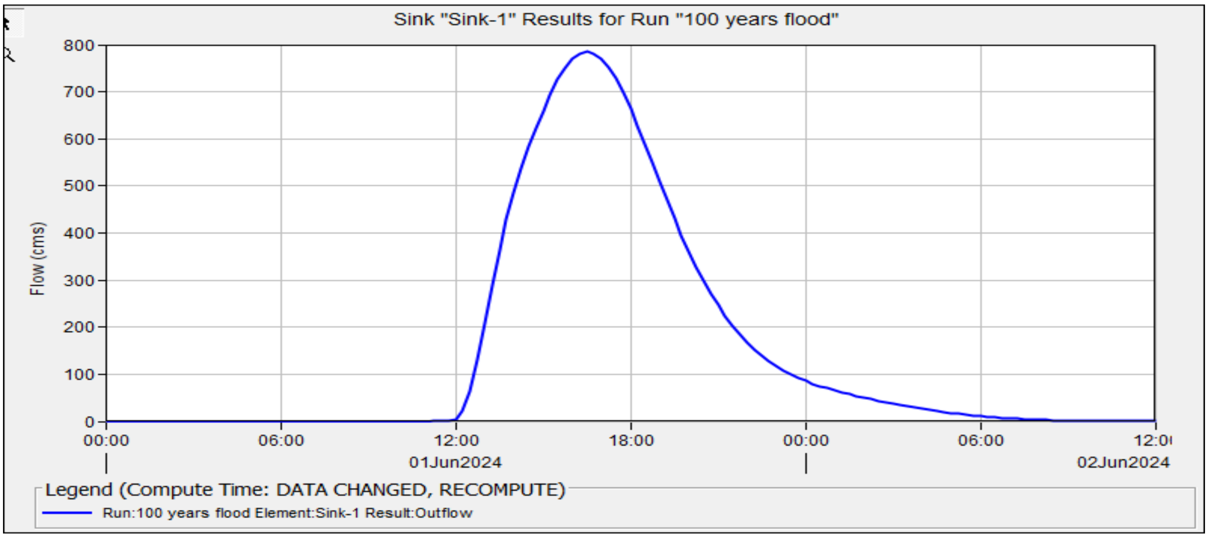

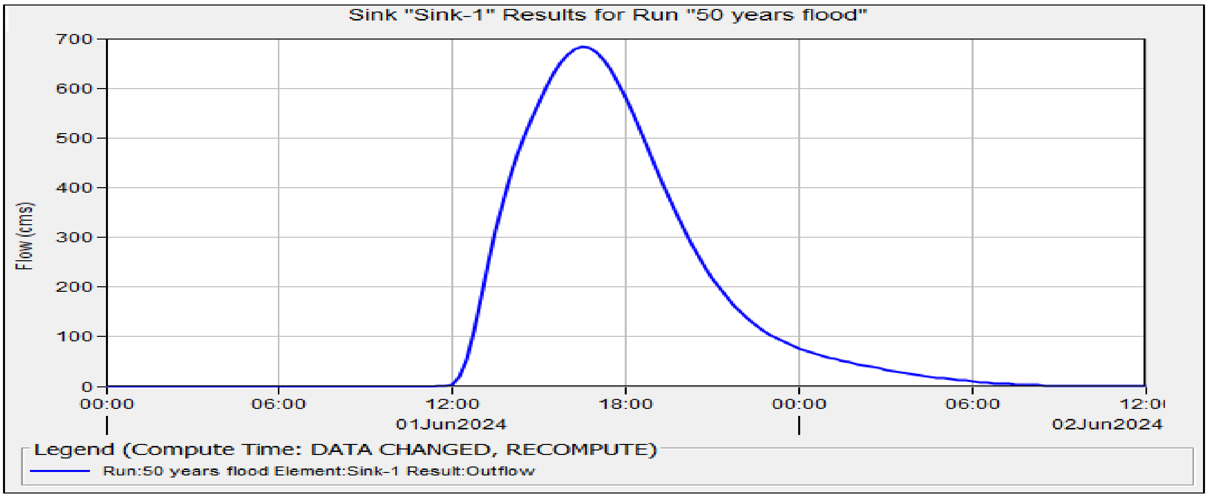

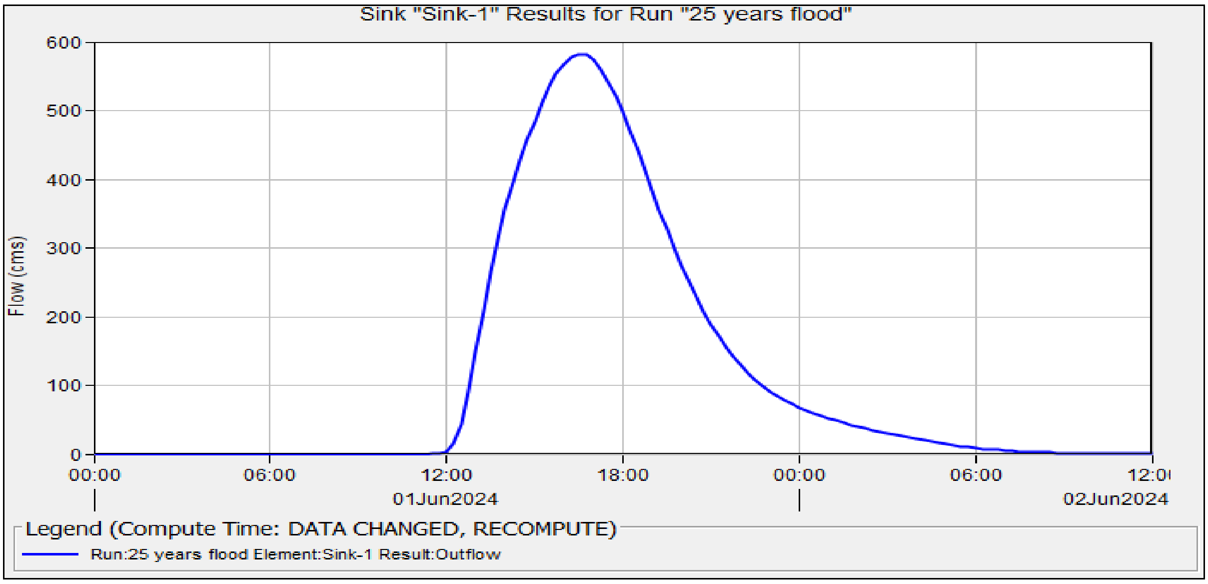

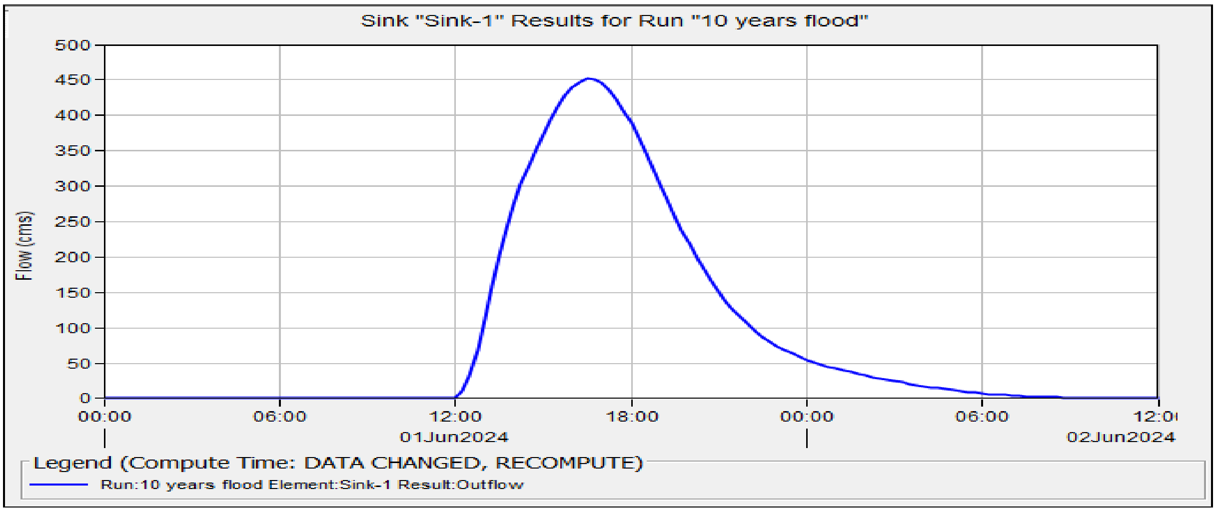
Sink "Sink-1" Results for Run "10 years flood"
Flow (cms)
500
450
400
350
300
250
200
150
100
50
0
00:00
06:00
12:00
18:00
00:00
06:00
12:00
01Jun2024
02Jun2024
Legend (Compute Time: DATA CHANGED, RECOMPUTE)
Run:10 years flood Element:Sink-1 Result:Outflow

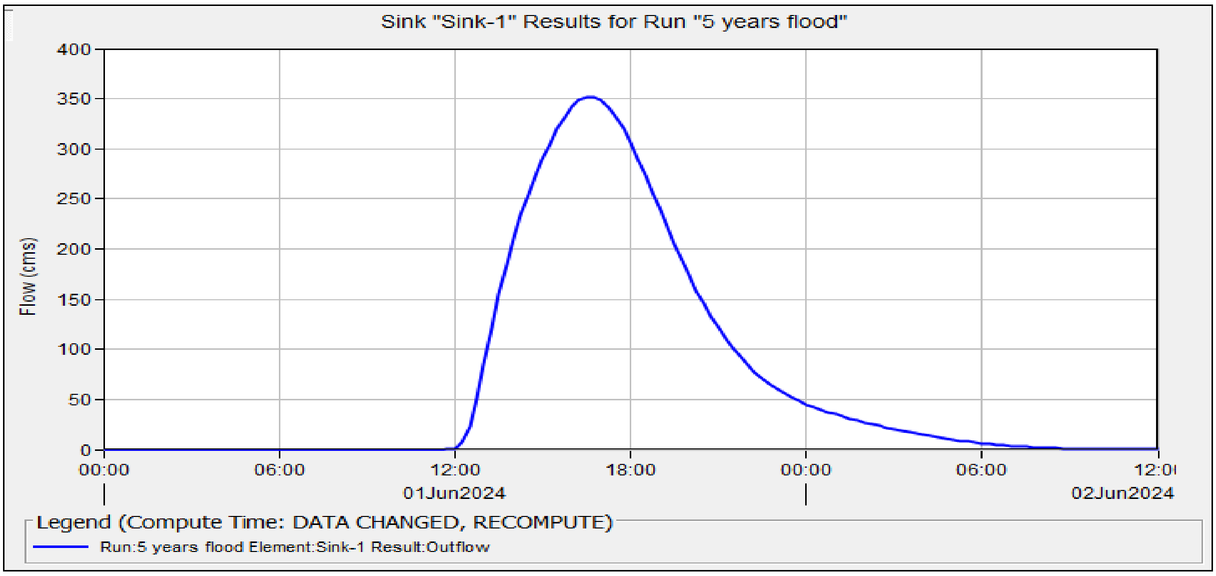
Sink "Sink-1" Results for Run "5 years flood"
Flow (cms)
400
350
300
250
200
150
100
50
0
00:00
06:00
12:00
18:00
00:00
06:00
12:00
01Jun2024
02Jun2024
Legend (Compute Time: DATA CHANGED, RECOMPUTE)
Run:5 years flood Element:Sink-1 Result:Outflow

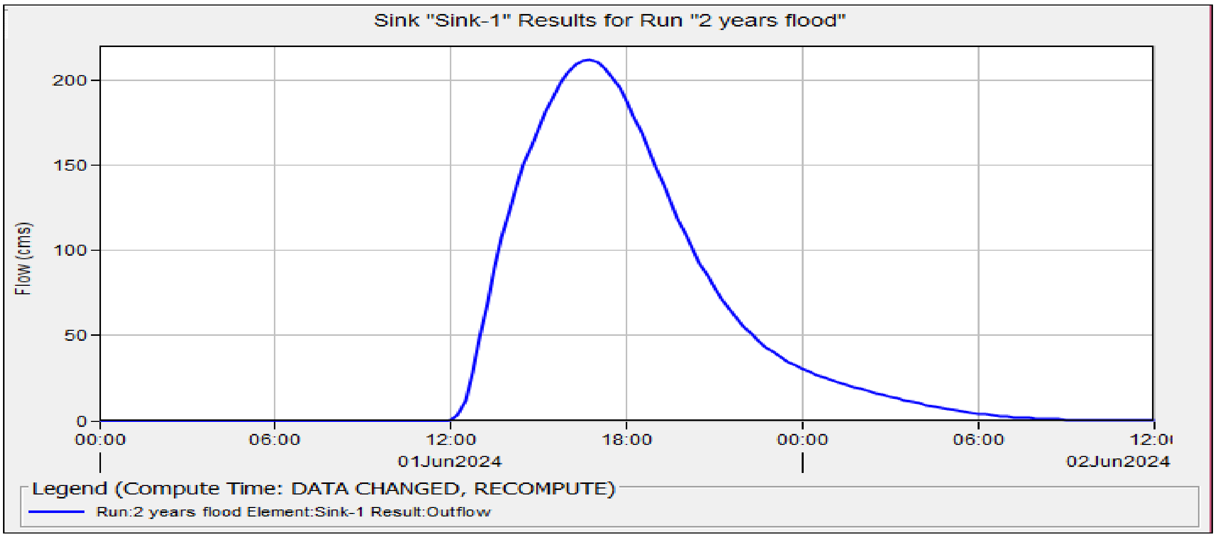
Sink "Sink-1" Results for Run "2 years flood"
Flow (cms)
200
150
100
50
0
00:00
06:00
12:00
18:00
00:00
06:00
12:00
01Jun2024
02Jun2024
Legend (Compute Time: DATA CHANGED, RECOMPUTE)
Run:2 years flood Element:Sink-1 Result:Outflow

Appendix C: Vulnerability parameters

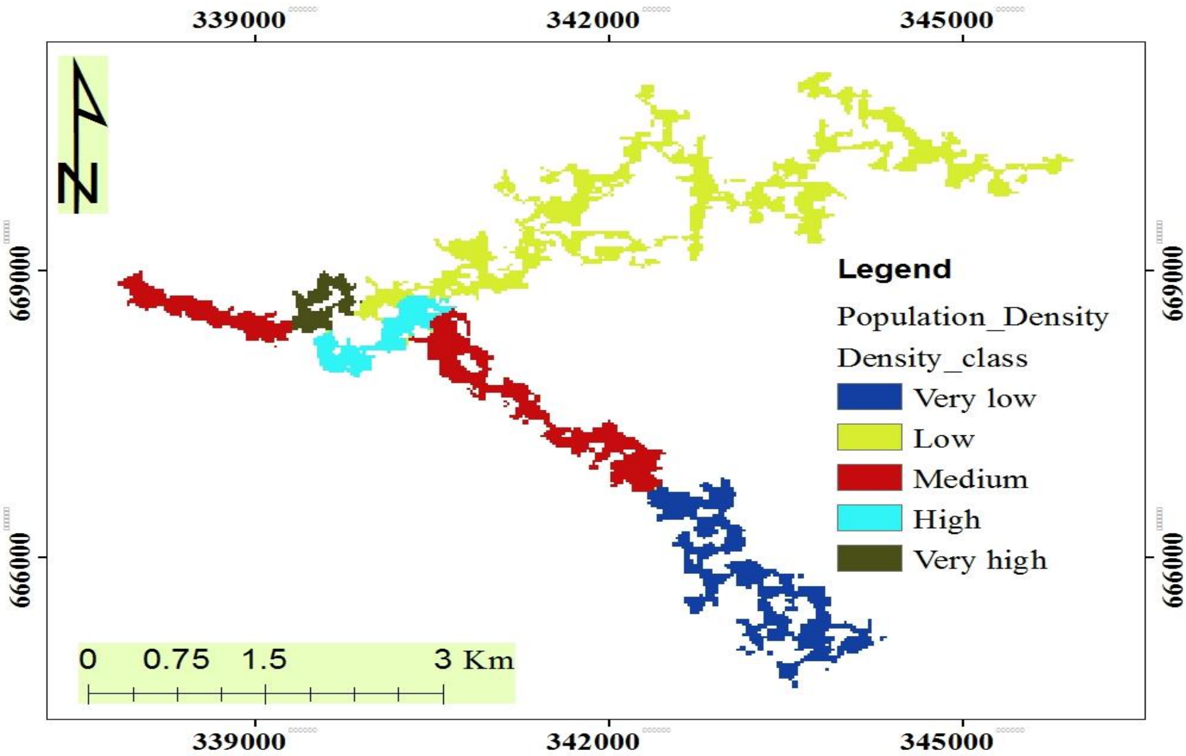

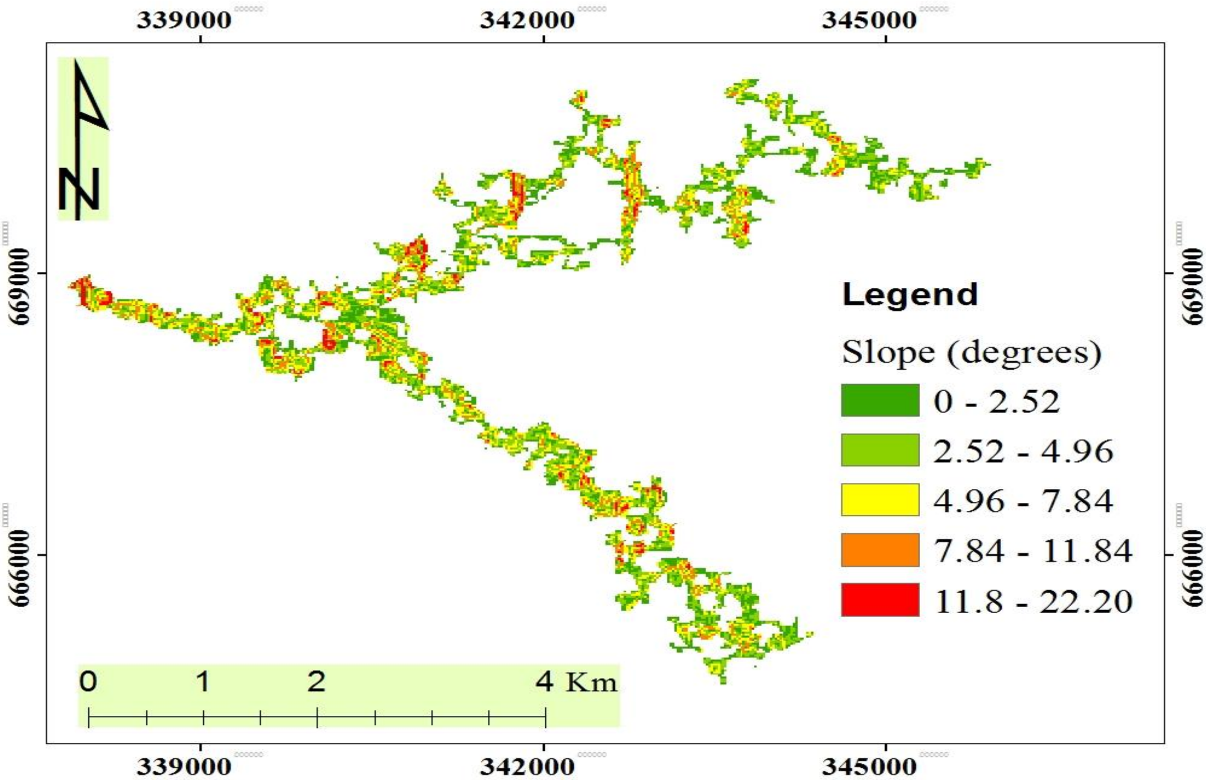

Appendix D: Stream order and Hill-shade of Kulifo Watershed

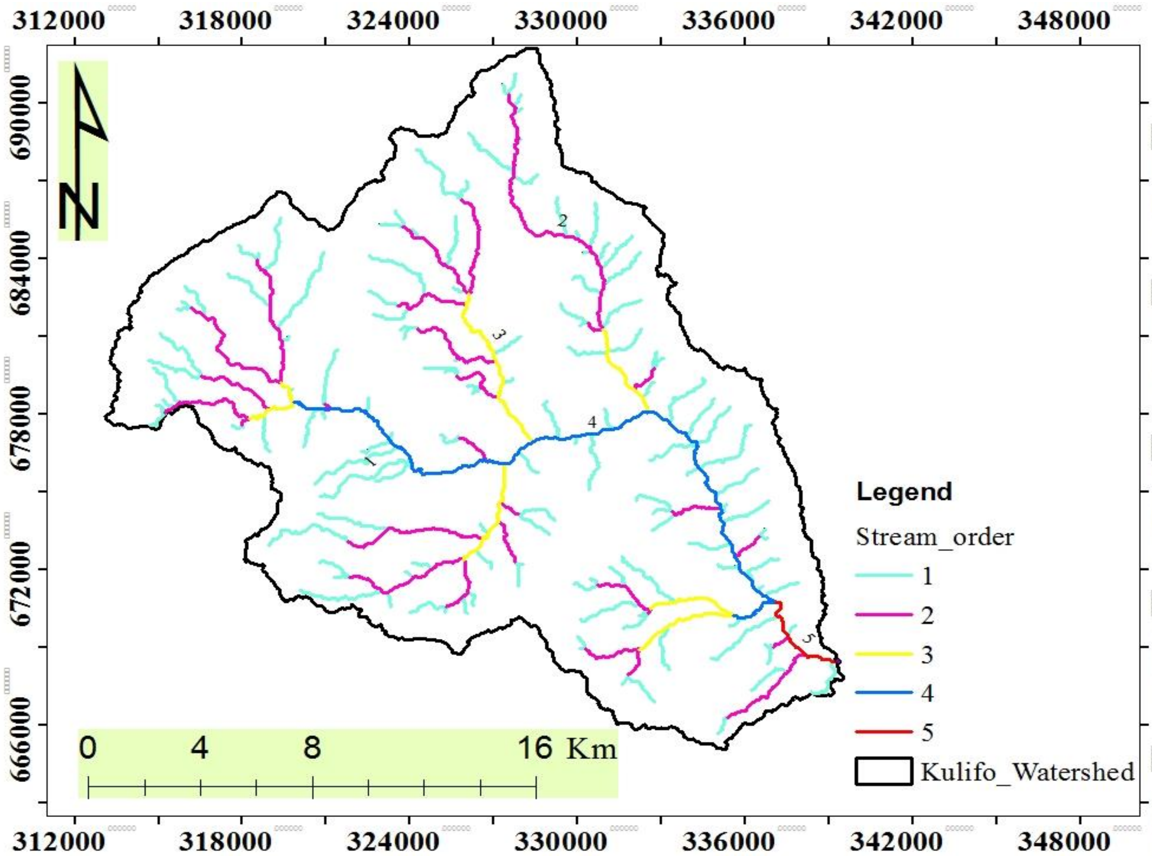

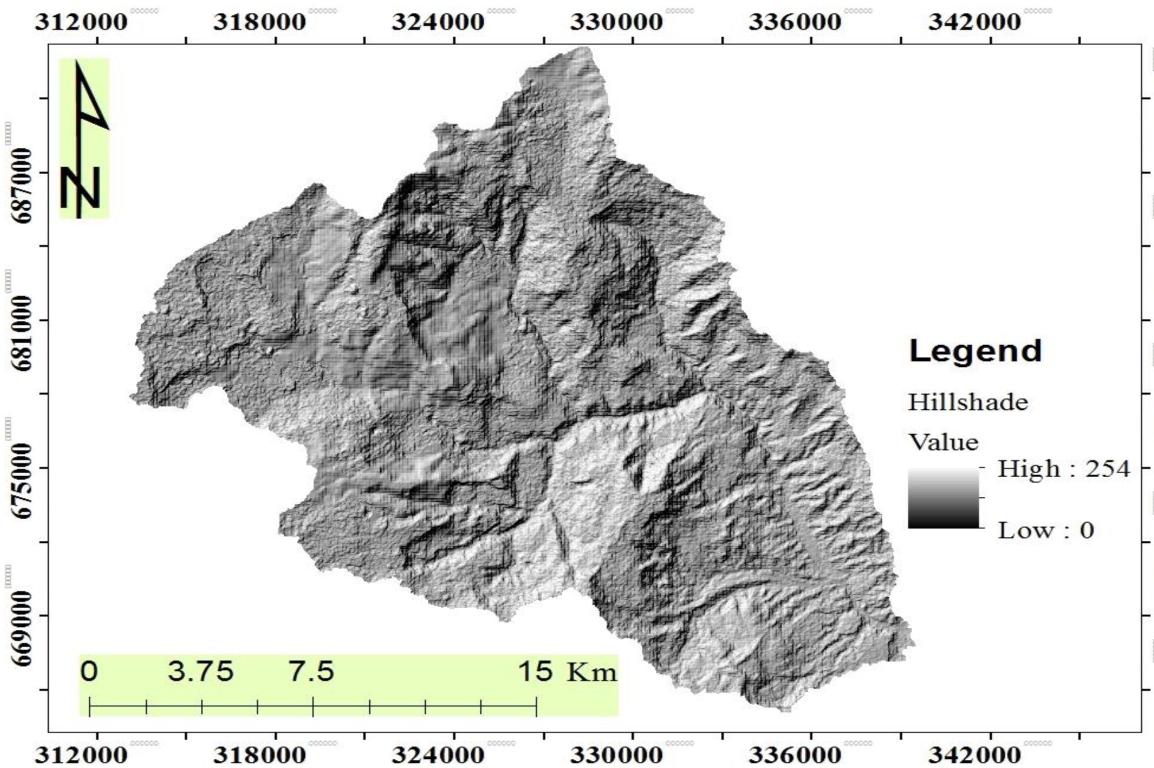

Appendix E: 100 years flood inundation area

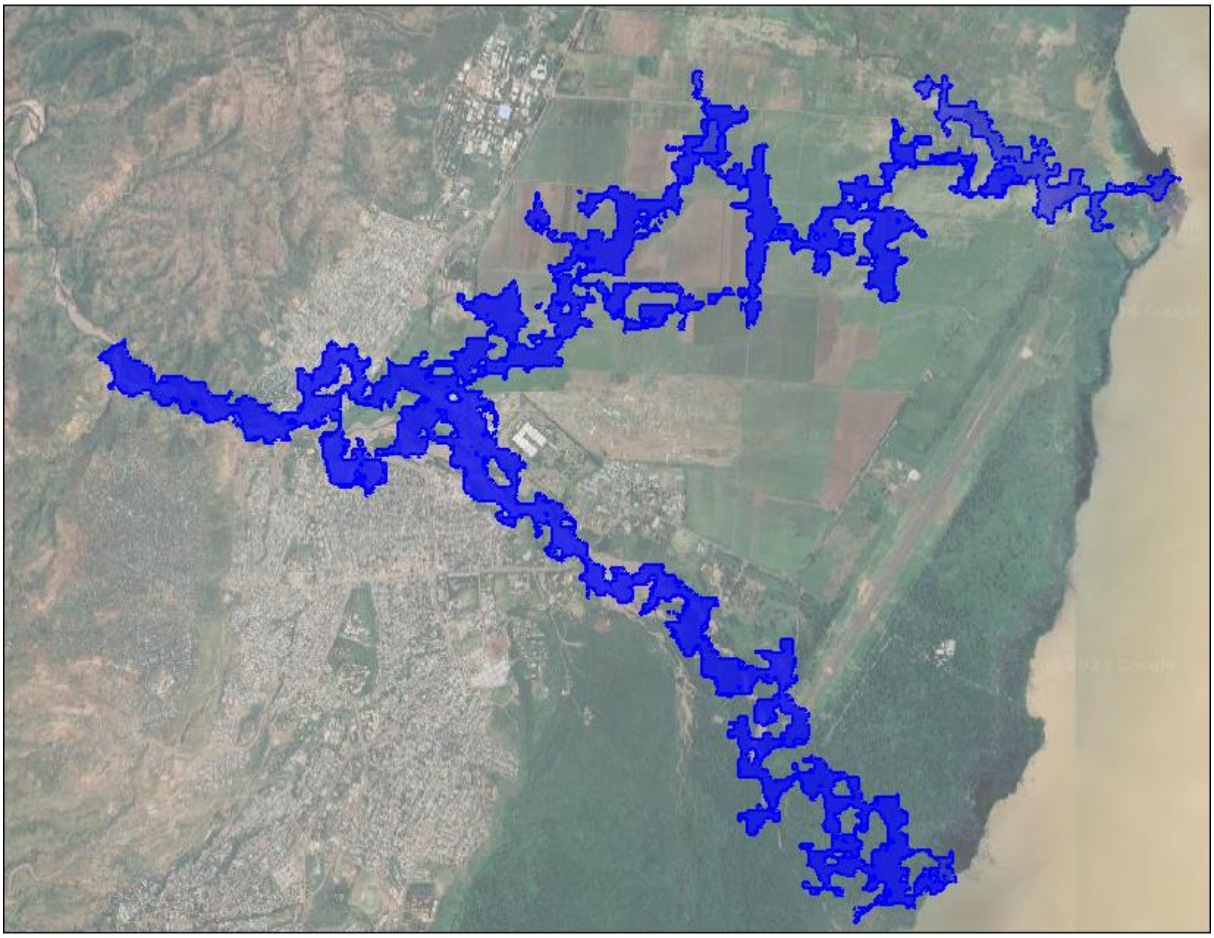

Appendix F: flood inundation at Limat area

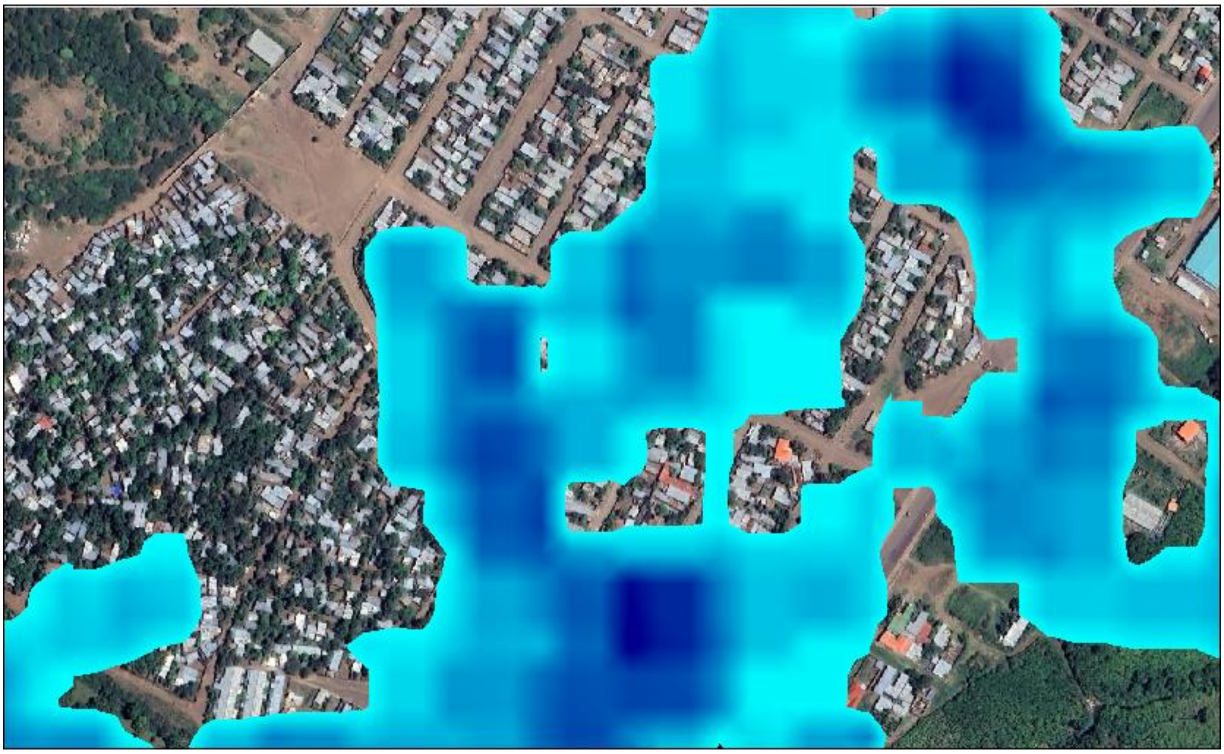

Appendix G: Various Pictures